Plant-specific glutaredoxin ROXY9 regulates hyponastic growth by inhibiting TGA1 function

Dissertation

for the award of the degree

"Doctor of Philosophy" (Ph.D.)

Division of Mathematics and Natural Sciences

of the Georg-August-Universität Göttingen

within the doctoral program Biology

of the Georg-August University School of Science (GAUSS)

Submitted by

Ning Li

from Shandong, China

Göttingen 2017

Thesis Committee

Prof. Dr. Christiane Gatz

(Department of Plant Molecular Biology and Physiology)

Prof. Dr. Volker Lipka

(Department of Plant Cell Biology)

Dr. Corinna Thurow

(Department of Plant Molecular Biology and Physiology)

Members of the Examination Board

Reviewer: **Prof. Dr. Christiane Gatz**

(Department of Plant Molecular Biology and Physiology)

Second reviewer: **Prof. Dr. Volker Lipka**

(Department of Plant Cell Biology)

Further members of the Examination Board:

Prof. Dr. Ivo Feussner

(Department of Plant Biochemistry)

PD Dr. Thomas Teichmann

(Department of Plant Cell Biology)

Dr. Marcel Wiermer

(Department of Plant Cell Biology)

PD. Dr. Martin Fulda

(Department of Plant Biochemistry)

Date of the oral examination: 30.03.2017

1 Introduction

1.1 Hyponastic growth

Being confined to a fixed location, plants have to re-orient their growth directions when it comes to getting access to limiting resources like light or water. Hyponasty, also called hyponastic growth, puts leaves and petioles into a more vertical position to escape from unfavorable conditions, such as submergence (Cox et al., 2003; Pierik et al., 2005), root waterlogging (Rauf et al., 2013), decreased light intensities (Vandenbussche et al., 2003; Pierik et al., 2005), increased far-red (FR) to red light (R) ratios (Whitelam and Johnson, et al., 1982; Vandenbussche et al., 2003; Pierik et al., 2005; Millenaar et al., 2009), and elevated temperatures (Koini et al., 2009; van Zanten et al., 2009). Upward bending of the leaves is due to differential growth rates between the adaxial and the abaxial sides of the petioles (Kang et al., 1979; Polko et al., 2012b; Cox et al., 2004). This requires the reorientation of cortical microtubules (Polko et al., 2012b) and expression of cell wall-loosening enzymes like e.g expansins (Vreeburg et al., 2005, Rauf et al., 2013) and members of the *XYLOGLUCAN ENDOTRANSGLYCOSYLASE*/*HYDROLASE* (*XTH*) gene family (Lee et al., 2011). It is hypothesized that hyponastic growth is induced by an asymmetrical distribution of growth-regulating factors. Candidates are ethylene (ET) and auxin or an increased sensitivity of the abaxial site to growth promoting cues. The significance of asymmetrical distribution of auxin in tropic responses is well established (Went and Thimann, et al., 1937; Friml and Palme, et al., 2002), but the contribution of such a mechanism in nastic responses seems unlikely (Cox et al., 2003). ET can play a role in differential growth processes like petiole epinasty (Kang et al., 1979), shoot gravitropism (Kaufman et al., 1995; Friedman et al., 2003), apical hook formation (Ecker et al., 1995), but the molecular mechanisms leading to differential ET production/sensitivity during hyponasic growth are unknown.

1.1.1 Ethylene and hyponastic growth in *Arabidopsis thaliana*

Application of ET triggers hyponastic growth in the several ecotypes of Arabidopsis, including Columbia, but not in Landsberg (Millenaar et al., 2005). Thus, a plausible hypothesis was that environmental cues would lead to the synthesis or accumulation of ET as a common signaling molecule. This concept is well established for Arabidopsis plants subjected to root waterlogging (Rauf et al., 2013) or complete submergence (Millenaar et al., 2005). However, ET is a negative regulator of hyponastic growth at high temperature (van Zanten et al., 2009). Conflicting data are available concerning the role of ET in the hyponastic growth of plants subjected to low light intensities. Vandenbussche et al. (2003) found that two-week-old Arabidopsis seedlings, which were grown on the ET precursor 1-aminocyclopropane-1-carboxylic acid (ACC), produced ET upon transfer to low light conditions (35 µmol photons m^{-2} s^{-1}). Mutants deficient in ET signal transduction (*ein2, etr1-3*) showed no increased leaf angle when continuously grown under 45 µmol photons m^{-2} s^{-1} as opposed to 125 µmol photons m^{-2} s^{-1}. In contrast, Millenaar et al. (2009) found that *ein2*, *etr1-4* and *ein4* plants responded like wild-type when plants were transferred from 200 to 20 µmol photons m^{-2} s^{-1} for 0 to 24 hours. No increase in ET production was observed. These studies indicate that growth conditions, ecotype and developmental stage of the plant might influence the underlying signaling cascades.

Moreover, Polko et al. (2015) found that overexpression of the mitotic cyclin CYCLINA2;1(CYCA2;1) shows exaggerated hyponasty, indicating a role for cell divisions in regulating hyponastic growth. According to experimental results and mathematical modeling, it was assumed that ET can attenuate the amplitude of hyponasty by decreasing the cell proliferation rate at the proximal abaxial side of the petiole relative to the adaxial side (Polko et al., 2015).

1.1.2 Photoreceptors and hyponastic growth

A similar complex picture arises with respect to the involvement of photoreceptors in hyponastic growth. Hyponastic growth is a part of the shade avoidance syndrome (Franklin et al., 2008), which is efficiently induced when the ratio of red (R) to far red (FR) light is reduced (Whitelam & Johnson et al., 1982). Elongation of petioles, hyponastic growth and reduction of leaf blade area occur when the amount of R is reduced due to the absorption of R but not FR by chlorophyll from shading plants or when the amount of FR is enriched due to the reflection by neighboring plants. These conditions are perceived by phytochromes A and B, which are activated by FR or R, respectively (reviewed in Franklin et al., 2008; Ballaré, et al., 2009; Keuskampet et al., 2010a). Under control light conditions, the R photoreceptor PhyB interferes with hyponastic growth as revealed by the constitutively high petiole angles in the *phyB-5* mutant (Millenaar et al., 2009). Under low R/FR, most of PhyB is in the inactive Pr form allowing the shade avoidance response (Robson et al., 1993). If light intensities are high but R/FR ratios low, PhyA is activated by FR and represses the shade avoidance response. This antagonistic interaction of both photoreceptors allows adjusting growth to the R/FR ratios and the light intensities at the same time. Hyponastic growth initiated by decreased R/FR ratios does not involve the ET pathway (Vandenbussche et al., 2003)

Different mechanisms have to be considered when decreased light intensities serve as the signal for hyponastic growth. Decreasing the light intensity but adding R did not reduce hyponastic growth at 6 h, 24 h and 48 h. Thus, PhyB is not able to repress hyponastic growth under low light conditions. However, addition of blue light interfered with hyponastic growth at least at 6 hours. Apparently, blue-light-activated photoreceptors can interfere with hyponastic growth under low light. Candidates are PhyA, which can be activated by blue light, cryptochromes and phototropins (Millenaar et al., 2009).

The *phot1 phot2* mutant behaved like wild-type when plants were shifted from control light to low light. However, photoreceptors PhyA and cryptochromes Cry1 and Cry2 were required for hyponastic growth (Millenaar et al., 2009). Taken together, it seems that hyponastic growth can be inhibited if photoreceptors are activated by either R or B, but that residual activation is important to sustain hyponastic growth. The control of hyponastic growth by photoreceptors plays a role only during the first 6 hours. When plants are subjected to low light for longer periods other signals resulting from reduced photosynthesis control the response (Millenaar et al., 2009).

1.1.3 Auxin and other plant hormones and hyponastic growth

As mentioned above, upward bending of the leaves is due to differential growth rates between the adaxial and the abaxial sides of the petioles (Cox et al., 2004; Polko et al., 2012b; Polko et al., 2015). As already described early in the last century, the phytohormone auxin is transported through the plant in a polar manner and is essential for differential growth (Went and Thimann et al., 1937). Auxin acts through the activation of cell wall-loosening enzymes, allowing water uptake and cell expansion (Ordin et al., 1956; Taiz et al., 1984; Catalá et al., 2000). The direction of cell expansion is determined by cortical microtubules that are reoriented during this process (Polko et al., 2012b). Several studies have shown that inhibition of polar auxin transport or mutants in auxin signaling show impaired hyponastic growth in response to low light (Millenaar et al., 2009). However, the defect was mainly observed after 12 hours indicating the hormone is required for maintenance of the elevated leaf angle and that other growth promoting factors have to act early. Auxin does not play a role when hyponasty is triggered by ET (van Zanten et al., 2009).

Abscisic acid (ABA) antagonizes ET-induced hyponastic growth (Benschop et al., 2007). Like-wise, methyl jasmonate (MeJA) is a negative regulator of low light-induced hyponastic growth (Ritsema et al., 2010); in contrast, it promotes

ET-induced hyponasty (van Zanten et al., 2012). SA suppresses both ET and low light-induced hyponasty (Ritsema et al., 2010; van Zanten et al., 2012).

1.1.4 Transcription factors and hyponastic growth

A few transcription factors have been involved in hyponastic growth. Hyponasty in response to root waterlogging is regulated by NAC (NAM, ATAF1/2, CUC2) transcription factor SPEEDY HYPONASTIC GROWTH (SHYG) in *Arabidopsis thaliana*. Ectopic expression of *SHYG* in *Arabidopsis* enhances waterlogging-triggered hyponastic leaf movement, while *shyg* knockout mutants show reduced hyponastic leaf movement. Several genes related to cell wall–loosening like *EXPANSINs* and *XYLOGLUCAN ENDOTRANSGLYCOSYLASE/HYDROLASEs* are up-regulated in *SHYG* overexpressing lines and down-regulated in *shyg* mutants. Moreover, *ACC OXIDASE5 (ACO5)*, which encodes for a key enzyme of ET biosynthesis, is a direct target gene of SHYG (Rauf et al., 2013).

Phytochrome Interacting Factor 4 is a basic-loop-helix (bHLH)-type transcription factor that is required for hyponastic growth at elevated temperatures. This transcription factor is stabilized when active phytochrome levels are reduced under low light or reduced R/FR ratios. However, at least PIF4-dependent hypocotyls length can be stimulated in plants lacking phytochromes, pointing at a mechanism of heat sensing that involves other molecular components (Koini et al., 2009).

1.2 TGA transcription factors

TGA transcription factors belong to the basic region/leucine zipper motif (bZIP) transcription factor (TF) superfamily (Jakoby et al., 2002). TGA factors can specifically recognize the DNA sequence TGACGTCA and were named according to the first three letters of the sequence (Katagiri et al., 1989; Lam et al., 1989). The ten genes of the

TGA family fall into five clades (Clade I: TGA1 and TGA4, clade II: TGA2, TGA5 and TGA6, clade III: TGA3 and TGA7, clade IV: TGA9 and TGA10, clade V: TGA8 (PAN)). The first three clades are mainly related to pathogen defense processes (Zhang et al., 2003; Kesarwani et al., 2007) and the other two clades are mainly related to flower development (Running et al., 1996; Murmu et al., 2010).

Clade II TGA TFs (TGA2, TGA5, TGA6) regulate the plant defense response systemic acquired resistance (Zhang et al., 2003) and the expression of detoxification genes (Fode et al., 2008; Mueller et al., 2008). Clade II TGA TFs directly interact with NONEXPRESSOR OF PR GENES 1 (NPR1) (Zhang et al., 1999) and the *tga2 tga5 tga6* triple mutant plants show a similar phenotype like the *npr1-1* mutant in terms of *pathogenesis-related 1* (*PR1)* expression and systemic acquired resistance (Zhang et al., 2003). Activation of detoxification genes, which is independent of NPR1, requires the interaction between clade II TGA TFs and the GRAS protein SCL14. *scl14* and *tga2 tga5 tga6* mutants show susceptibility to the SA structural analog 2,6-dichloroisonicotinic acid (INA) or to 2,4,6-triiodobenzoic acid (TIBA) (Fode et al., 2008).

Clade I TGA transcription factors (TGA1, TGA4) are involved in defense responses against biotrophic pathogens (Kersawani et al., 2007, Shearer et al., 2012). They have two conserved cysteines (Cys-260 and Cys-266) which can form an intramolecular disulfide bridge (Despres et al., 2003). In the absence of SA, 50% of the TGA1 protein is in the oxidized form and 50% is in the reduced form. After exogenous application of SA, only the reduced form exists. The interaction with NPR1 takes place in yeast and *Arabidopsis* after a change of the conserved cysteine residues into a serine and aspartic acid, respectively (Despres et al., 2003), which prevents formation of the disulfide bridge. It was concluded that reduction of the protein allows the interaction with NPR1. Besides forming an internal disulfide bridge, TGA1 is S-nitrosylated or glutathionylated in vitro after treatment with S-nitrosoglutathione, a physiological nitric oxide donor (Lindermayr et al., 2010).

Still, the function of TGA1 is more likely independent of NPR1 as revealed by the triple mutant *tga1 tga4 npr1-1*, which is more susceptible to *Pseudomonas syringae* pv *maculicola* (*Psm ES4326*) than *npr1-1* mutants and *tga1 tga4* double mutants. Moreover, a number of defense genes that are positively regulated by NPR1 are negatively regulated by TGA1 and TGA4. However, the enhanced expression of these genes in the *tga1 tga4* double mutant does not fit to the observed higher susceptibility of the mutant (Shearer et al., 2012). Further studies found that apoplastic defense responses such as oxidative burst and callose deposition after treatment of plants with Pathogen Asscociated Molecular Patterns (PAMPs) are reduced in the *tga1 tga4* double mutant plants. Total and apoplastic PR1 protein accumulation was reduced in in *tga1 tga4* double mutant as well. Moreover, *tga1 tga4* plants showed increased sensitivity to tunicamycin, an inhibitor of N-linked glycosylation that can trigger ER stress, suggesting that the reduced defense responses are associated with aberrant protein secretion. It was concluded that clade I TGA factors act as positive regulators of ER-related secretion pathways (Wang et al., 2013).

1.3 Glutaredoxins

Glutaredoxins (GRXs) are small, ubiquitous oxidoreductases that are important for the regulation of the redox status of target proteins by using glutathione (GSH) as a cofactor. All GRXs contain a conserved active site (CxxC/S) and a GSH binding site (Lillig et al., 2008). Based on the active site, GRXs are divided into three classes (Lemaire et al., 2004). Class I dithiol CxxC type (usually CPYC) and class II monothiol CGFS type are common to all prokaryotes and eukaryotes. Class III CCMC/S type GRXs (also called ROXYs) are only found in the genomes of land plants (Lemaire et al., 2004). For the monothiol mechanism, the CGFS-type GRXs reduce glutathionylated proteins by forming an GRX-GSH complex. The complex is further reduced by a GSH.

For the dithiol mechanism, the CxxC-type GRX reacts with a disulfide bridge of a target protein, resulting in a GRX-protein-mixed disulfide complex. The complex is further reduced by the second resolving cysteine of the active site, yielding a reduced target protein and an oxidized GRX. Subsequently, the oxidized GRX is reduced by GSH, resulting in a reduced GRX and an oxidized GSH. The oxidized GSH can be reduced by glutathione reductase in the presence of NADPH (Fernandes and Holmgren et al., 2004).

It is known that GRXs are involved in assembly of iron sulfur [Fe-S] clusters as well. [Fe-S] clusters are important for fundamental life processes such as electron transfer, substrate binding/activation, enzyme activity, iron-sulfur storage, and regulation of gene expression (Glaser et al., 2000; Johnson et al., 2005). Iron-sulfur [Fe-S] clusters are common in all prokaryotes and eukaryotes, including bacteria, plants and animals. There are more than 120 different types of enzymes and proteins known to contain [Fe-S] clusters.

In *Arabidopsis*, AtGrxC5, a class I glutaredoxin possessing a WCSYC active site, incorporates a [2Fe-2S] cluster when it is in its dimeric holoprotein conformation. Here, the second active site cysteine (Cys32) is required for cluster binding (Couturier et al., 2011). Plant chloroplast class II CGFS-type glutaredoxins, GrxS14 and GrxS16, are able to complement a yeast *grx5* mutant defective in [Fe-S] cluster assembly and GrxS14 can transfer [2Fe–2S] clusters to apo ferredoxin in vitro (Bandyopadhyay et al., 2008).

In yeast, GRX-3 (class II, CGFS) and the BolA-like protein Fe repressor of activation-2 can form a [2Fe-2S]-bridged heterodimer. The heterodimer can transfer [Fe-S] clusters (or Fe^{2+}) to Aft2 (activators of ferrous transport) that facilitates Aft2 dimerization, which leads to decrease the DNA-binding affinity and down-regulation of the expression of iron-uptake genes (Poor et al., 2014).

1.3.1 CC-type glutaredoxins (ROXYs)

The land plant-specific CC-type GRXs (named ROXYs in *Arabidopsis*) are characterized by carrying a conserved CC motif in their active site. The biochemical activities of these proteins are poorly understood. Couturier et al. (2010) reported that the in vitro purified poplar class III glutaredoxin protein GrxS7.2 possesses two absorption bands at 322 and 415 nm in the UV/Visible spectrum which is a typical feature of proteins incorporating an [Fe-S] cluster. Yet, the oxidoreductase activity of GrxS7.2 was very weak as compared to the other two class I GRXs, GrxC1 and GrxC4.

The *Arabidopsis thaliana* genome encodes 21 *ROXY* gens. Besides the conserved CC motif, these proteins contain a L**LL motif and the ALWL motif at the C-terminal end (Figure 2.1). CC-type GRXs can interact with TGA TFs physically and genetically. In *Arabidopsis*, the best studied ROXYs are ROXY1, ROXY2, ROXY18 and ROXY19 (Gutsche et al., 2015).

The mutant *roxy1* was isolated on the basis of aberrant petals with reduced number and abnormal shape. In contrast to wild-type *Arabidopsis*, which has four petals with almost equal size, the petal number of the *roxy1* mutant varies between 0 and 4 with an average of 2.5 (Xing et al., 2005). TGA transcription factors (TGA2, TGA3, TGA7, PAN) were identified as proteins interacting with ROXY1 by yeast two-hybrid screening (Li et al., 2009). Since the petal number of *pan* (PAN is a clade IV TGA transcription factor) is five, it was hypothesized that PAN and ROXY1 interact genetically. Indeed, the *roxy1 pan* double mutant has five petals. This indicates that ROXY1 represses the function of PAN. Furthermore, the residue Cys340 in PAN is important for the phenotype as concluded from the observation that PAN encoding the point mutation C340S cannot complement the phenotype. Therefore, it was speculated that PAN activity is regulated through a redox modification at C340 which is catalyzed by ROXY1. However, experimental evidence for such a mechanism is still

		active center	L**LL motif	ALWL motif
ROXY1	At3g02000	CCMC	VMASHINGS**LVPLL**KDAG	ALWL
ROXY2	At5g14070	CCMC	VMASHINGS**LVPLL**KDAG	ALWL
ROXY3	At3g21460	CCMS	VMTLHLNGS**LKILL**KEAG	ALWL
ROXY4	At3g62950	CCMC	IISFHVDGS**LKQML**KDAK	AIWL
ROXY5	At2g47870	CCMC	VISFHVDGS**LKQML**KASN	AIWL
ROXY10	At5g18600	CCMS	VMSLHLNGS**LIPML**KRAG	ALWV
ROXY11	At4g15700	CCMS	VMSLHLNRS**LVPML**KRAG	ALWL
ROXY12	At4g15690	CCMS	VMSLHLNRS**LVPML**KRAG	ALWL
ROXY13	At4g15680	CCMS	VMSLHLNRS**LVPML**KRVG	ALWL
ROXY14	At4g15670	CCMS	VMSLHLNRS**LIPML**KRVG	ALWL
ROXY15	At4g15660	CCMS	VMSLHLNRS**LIPML**KRFG	ALWL
ROXY17	At3g62930	CCMS	VMTLQVKNQ**LAAML**RRAG	AIWV
ROXY18	At1g03850	CCLG	LMAAHINGD**LVPTL**RQAG	ALWL
ROXY19	At1g28480	CCMC	VMATHISGE**LVPIL**KEVG	ALWL
ROXY21	At4g33040	CCMC	LVALHLSGQ**LVPKL**VQVG	ALWV
ROXY6	At1g06830	CCLC	VMSMHLSSS**LVPLV**KPY---LC	
ROXY7	At2g30540	CCMS	VMSLHLSGS**LVPLV**KPFQANLC	
ROXY8	At3g62960	CCLC	VMSLHLSGS**LVPLI**KPYQSFHN	
ROXY9	At2g47880	CCLC	VMSLHLSGS**LVPLI**KPYQSILY	
ROXY16	At1g03020	CCMS	LMSLQVRNQ**LASLL**RRAGAIWI	
ROXY20	At5g11930	CCMC	LVALHLSGQ**LIPRL**VEVGALWA	

Figure 2.1: Alignment of the C-terminal sequences of CC-type glutaredoxins (Zander et al., 2012).

The L**LL motif is shown in bold letters with the critical leucine residues in blue. The C-terminal ALWL motif is shown in red.

missing. The single mutant of the closest homolog of ROXY1, *roxy2*, does not cause any obvious phenotype but the *roxy1 roxy2* double mutant was did not produce pollen, similar to the *tga9 tga10* double mutant (Xing et al., 2008; Murmu et al., 2010). Since ROXY1 and ROXY2 can interact with TGA9 and TGA10 (Murmu et al., 2010), it was concluded that ROXY1 and ROXY2 regulate anther development by regulating the activity of TGA9 and TGA10.

ROXY19 (GRX480) was isolated as a TGA2-interacting protein through a modified yeast one-hybrid screening. The expression of *ROXY19* is induced by SA and requires TGA factors and NPR1 (Ndamukong et al., 2007). Ectopic expression of *ROXY19* represses the activation of the jasmonic acid/ET (JA/ET) defense pathway. It acts very early in this singalling cascade by repressing the promoter of the *ORA59* gene. ORA59 is a regulator of JA/ET-inducible defense genes, including plant defensin gene *PDF1.2*. Consistently, plants ectopically expressing ROXY19 are more susceptible to necrotrophic pathogens (Lai et al., 2014). ROXY19-mediated suppression of gene expression depends on clade II TGA TFs. Since SA represses the JA/ET pathway in a TGA2/5/6-dependent manner, it was postulated that SA-induced ROXY19 mediates the SA-imposed antagonism over the JA/ET pathway (Ndamukong et al., 2007; Zander et al., 2012). However, this hypothesis was not yet confirmed in the *roxy19* mutant. Moreover, ectopically expressed ROXY19 represses detoxification genes which depend on clade II TGA factors (Huang, et al., 2016).

ROXY18, the closest homolog of ROXY19, was studied by La Camera et al. (2011). The *roxy18* mutant plants are less susceptible to *B. cinerea* as compared to wild-type plants and constitutive expression of *ROXY18* leads to an increased susceptibility to *B. cinerea,* indicating a negative role in regulating defense responses against *B. cinerea*. However, the expression of classical TGA-dependent defense genes like *PR1* and *PDF1.2* are not influenced after infection of the mutant by *B. cinerea*. Therefore, the mechanism how ROXY18 enhances the susceptibility to *B. cinerea* has remained unknown (La Camera et al., 2011).

The ALWL motif, which is present at the C-terminal end of many ROXYs, is required for the functions of ROXY1 and ROXY18: Complementation analysis of *roxy1-2* mutant with other ROXYs under the control of *ROXY1* native promoter revealed that only the *ROXYs* containing the ALWL motif are capable of rescuing the abnormal petal phenotype of the *roxy1* mutant (Li et al., 2009). In addition, only ROXYs with the C-terminal ALWL motif suppress *ORA59* promoter activity in *Arabidopsis* protoplasts

(Zander et al., 2012). Recent analysis has shown that the transcriptional co-repressor TOPLESS binds to the ALWL motif (Uhrig et al., 2017). The repressive function of ALWL-containing ROXYs can therefore be explained by the recruitment of TOPLESS to TGA-regulated promoters.

The L**LL motif at the C-terminal end of ROXY1 was found to be required for the interaction with PAN and TGA3 in yeast (Li et al., 2011). The interaction is disrupted by substitutions of any leucine in L**LL to alanine. Consistently, transgenic plants expressing leucine-mutagenized ROXY1 proteins under the control of the *ROXY1* native promoter fail to complement the abnormal petal development of the *roxy1* mutant. Likewise, the repressive function of ROXY19 on the *ORA59* promoter requires this motif (Zander et al., 2012). Whether this motif is required for directly contacting TGA factors or whether it is required for a correct tertiary structure of the protein has not been further investigated.

The CC-active center was found to be required for the biological function of some ectopically expressed *ROXYs*. For example, the *roxy1* phenotype can be complemented by ectopic expression of *ROXY1* under the control of the *CaMV 35S* promoter, whereas the mutation in the first cysteine (SCMC) of the active site leads to a protein that is unable to complement. In contrast, the mutation in the last cysteine (CCMS) restores the phenotype of over 50% of the T1 *roxy1-3* mutants (Xing et al., 2005). In contrast, when expressed under the endogenous *ROXY1* promoter, the protein was functional (Ziemann et al., 2010). Even mutating the active site into SSMS did not abolish its function. Thus, the importance of the active site for ROXY1 function is still controversial. *ROXY19* containing a SSMS sequence in the active site was not functional in planta (Huang et al., 2016).

1.4 Aim of the study

Since the transcription factors TGA1 and TGA4 have redox-active cysteines and since they interact with ROXYs, the question arose whether ROXYs are involved in the redox modification of TGA1 and TGA4. In the course of this thesis, it was discovered that the *tga1 tga4* mutant shows compromised hyponastic growth. This observation led to the following questions.

- Which signaling cascades activate TGA1/TGA4-depenent hyponastic growth?
- Which genes are regulated by TGA1/TGA4 during hyponastic growth?
- Are the redox-active cysteines important for TGA1 to regulate hyponastic growth?
- Which ROXYs can regulate hyponastic growth and is the catalytic center important for their *in vivo* activities?

2 Materials and Methods

2.1 Materials

2.1.1 Organisms

2.1.1.1 Bacteria

strain	Description (Genotype)	Usage	Reference
Escherichia coli DH5α	F^- Φ80*lac*ZΔM15 Δ(*lac*ZYA-*arg*F) U169 *rec*A1 *end*A1 *hsd*R17(r_k^-, m_k^+) *pho*A *sup*E44 *thi*-1 *gyr*A96 *rel*A1 $λ^-$	Plasmid construction	Thermo Fisher Scientific
Escherichia coli DB3.1	F– *gyr*A462 *end*A1 Δ(sr1-*rec*A) *mcr*B *mrr* *hsd*S20(rB–, mB–) *sup*E44 *ara*-14 *gal*K2 *lac*Y1 *pro*A2 *rps*L20(SmR) *xyl*-5 λ– *leu* *mtl*1	Plasmid construction	Thermo Fisher Scientific
Agrobacterium tumefaciens GV3101 (pMP90RK)	C58; Rif^R; $Gent^R$	Plant transformation	(Koncz and Schell, 1986)

2.1.1.3 Plants

Genotype	Description	Reference
Col-0	*Arabidopsis thaliana* Columbia-0 (Col-0)	TAIR
tga1 tga4	*tga1* and *tga4* double mutant in Col-0 background	Prof. Dr. Yuelin Zhang, (Kesarwani et al., 2007)
tga2 tga5 tga6	*tga2*, *tga5* and *tga6* triple mutant in Col-0	(Zhang et al.,

	background	2003)
npr1-1	Knock out line lacking functional NPR1	(Cao et al., 1994)
ein2-1	a strong allele of *ein2* generated by ethylmethane sulfonate (EMS) mutagenesis	(Roman et al., 1995)
phyB-9	a strong allele of *phyB* generated by ethylmethane sulfonate (EMS) mutagenesis	Professor Dr. Gregg A. Howe (Campos et al., 2006)
cry1 cry2	*cry1 (hy4-B104)* and *cry2-1* double mutant in col-0 background	Professor Dr. Alfred Batschauer (Mockler et al., 1999)
phot1 phot2	*phot1-5* and *phot2-1* double mutant in col-0 background	Professor Dr. Alfred Batschauer (Lariguet et al., 2006)
shyg-1	homozygous T-DNA insertion line SALK-066615	Prof. Dr. Bernd Mueller-Roeber (Rauf et al., 2013)
shyg-2	homozygous T-DNA insertion line GK-343D11	Prof. Dr. Bernd Mueller-Roeber (Rauf et al., 2013)
35S:SHYG	*SHYG* overexpression line in Col-0	Prof. Dr. Bernd Mueller-Roeber (Rauf et al., 2013)
HA-gTGA1	*tga1 tga4* mutant complemented with genomic *TGA1* with 1xHA fused to the N-terminus of TGA1	Prof. Dr. Yuelin Zhang (Shearer et al.,

		2012)
HA-gTGA1cys	*tga1 tga4* mutant complemented with genomic *TGA1* conserved cysteine (CNLKQSC) mutated to NNLKQSS with 1xHA fused to the N-terminus of TGA1	Prof. Dr. Yuelin Zhang The University of British Columbia, Vancouver
35S:HA-ROXY19	*ROXY19* overexpression line in Col-0 with 3xHA fused to the N-terminus of ROXY19	(Li-Jun Huang et al., 2016)
35S:HA-ROXY9	*ROXY9* overexpression line in Col-0 with 3xHA fused to the N-terminus of ROXY9	Dr. Martin Muthreich and this work
35S:HA-ROXY9SCLC	*ROXY9* overexpression line with the active site (CCLC) replaced by SCLC in Col-0 with 3xHA fused to the N-terminus of ROXY9	This work
35S:HA-ROXY9CSLC	*ROXY9* overexpression line with the active site (CCLC) replaced by CSLC in Col-0 with 3xHA fused to the N-terminus of ROXY9	This work
35S:HA-ROXY9CCLS	*ROXY9* overexpression line with the active site (CCLC) replaced by CCLS in Col-0 with 3xHA fused to the N-terminus of ROXY9	This work
35S:HA-ROXY9AALA	*ROXY9* overexpression line with the active site (CCLC) replaced by AALA in Col-0 with 3xHA fused to the N-terminus of ROXY9	This work
35S:HA-ROXY9⊿SILY	*ROXY9* overexpression line with the C-terminal SILY motif deleted in Col-0 with 3xHA fused to the N-terminus of ROXY9	This work
35S:HA-ROXY9rALWL	*ROXY9* overexpression line with the C-terminal SILY motif replaced by ALWL motif in Col-0 with 3xHA fused to the	This work

	N-terminus of ROXY9	
35S:HA-ROXY8	*ROXY8* overexpression line in Col-0 with 3xHA fused to the N-terminus of ROXY8	This work

2.1.2 Plasmids

Plasmid	**Description**	**Reference**
pB2GW7.0-HA	Gateway destination vector for gateway cloning with N-terminal 3xHA tag and Basta resistance gene for plant selection	(Weiste et al., 2007)
pB2GW7.0-HA-ROXY9	LR reaction result of pB2GW7.0-HA with pDonor-ROXY9	Dr. Martin Muthreich
pB2GW7.0-HA-ROXY9SCLC	LR reaction result of pB2GW7.0-HA with pDonor-ROXY9SCLC	This work
pB2GW7.0-HA-ROXY9CSLC	LR reaction result of pB2GW7.0-HA with pDonor-ROXY9CSLC	This work
pB2GW7.0-HA-ROXY9CCLS	LR reaction result of pB2GW7.0-HA with pDonor-ROXY9CCLS	This work
pB2GW7.0-HA-ROXY9 Δ SILY	LR reaction result of pB2GW7.0-HA with DNA fragment ROXY9 Δ SILY which the ROXY9 C-terminal SILY motif was deleted	This work
pB2GW7.0-HA-ROXY9rALWL	LR reaction result of pB2GW7.0-HA with DNA fragment ROXY9 rALWL in which the ROXY9 C-terminal SILY motif was replaced by ALWL motif	This work
pB2GW7.0-HA-ROXY9AALA	LR reaction result of pB2GW7.0-HA with DNA fragment ROXY9AALA	Dr. Martin Muthreich

pB2GW7.0-HA-ROXY8	LR reaction result of pB2GW7.0-HA with pDonor-ROXY8	This work
pDONR207	Gateway entry vector with Gentamicin resistance	Invitrogen
pDONR207-ROXY9	BP reaction result of pDonor207 with DNA fragment ROXY9	Dr. Martin Muthreich
pDONR207-ROXY9SCLC	BP reaction result of pDonor207 with DNA fragment ROXY9SCLC which the ROXY9 active site (CCLC) was replaced by SCLC	Moritz Willmer
pDONR207-ROXY9CSLC	BP reaction result of pDonor207 with DNA fragment ROXY9CSLC which the ROXY9 active site (CCLC) was replaced by CSLC	Moritz Willmer
pDONR207-ROXY9CCLS	BP reaction result of pDonor207 with DNA fragment ROXY9CCLS which the ROXY9 active site (CCLC) was replaced by CCLS	Moritz Willmer
pDONR207-ROXY8	BP reaction result of pDonor207 with DNA fragment ROXY8	This work

2.1.3 Primers

2.1.3.1 Primers for real-time PCR

Abr.	**Primer**	**Sequences (5'-3')**
126	SHYG qRT For	GCATGAATATCGTCTTGCCGATTC
127	SHYG qRT Rev	GGCAAAGAACCCAATCATCCAGTC
128	EXPA8 qRT For	CCTCTCCAACGATAATGGAGGTTG
129	EXPA8 qRT Rev	TGGTACTCTTCGGAAAGAGACAGG

130	EXPA11 qRT For	GCTTCTGGAACAATGGGTGGAG
131	EXPA11 qRT Rev	TTAACGCCGCCGTCATTGTC
332	GH3.6 qRT For	TCACCACCTATGCTGGGCTTTAC
333	GH3.6 qRT Rev	TGAAACCAGCCACGCTTAGGAC
342	IAA19 qRT For	TGACGTCGTCGGGTAGTAATAGTG
343	IAA19 qRT Rev	AGCGTCACCACCAGATGAAACG
352	XTH8 qRT For	TCTATCGCAGCAACACCGACAC
353	XTH8 qRT Rev	TGCTTTGTCTGAAATCCACATCCG
318	XTH33 qRT For	AGCTGGGTTGGTGTCAAAGAAC
319	XTH33 qRT Rev	AATCCAGCGGGAAGCTTGAGTC
	ROXY1 qRT For	AGCTTAGGATTCGGCGGTTTGG
	ROXY1 qRT Rev	AGCCAGGGACTCTATACGAAGCAG
	ROXY2	QuantiTect QT00829031
	ROXY3 qRT For	TTAGGCTGTAGCCCTACGGTTC
	ROXY3 qRT Rev	TGGCCGTTCCTACGAATTTCCC
	ROXY4	QuantiTect QT00797622
	ROXY5	QuantiTect QT00725788
	ROXY6	QuantiTect QT00852516
	ROXY7	QuantiTect QT00760144
	ROXY8	QuantiTect QT00797629
102	ROXY9 qRT For	CTAGCCATCATCAGATCTTCAGAC
106	ROXY9 qRT Rev	TGGGACAAGAGAGCCACTAAGGTG
	ROXY10 qRT For	AGCCAACGAGGTCATGAGTCTAC
	ROXY10 qRT Rev	AGCCCGCTTAAGCATGGGAATC
	ROXY11 qRT For	GCGTGAACCCGACGATCTATGAAC
	ROXY11 qRT Rev	CCTATGAACACCACTGGCACTGTC
	ROXY12 qRT For	ACTTTGGCGTGAACCCGACTATC
	ROXY12 qRT Rev	CCAATGCTTGCTCTATCTCCCTTC

377	ROXY13 qRT For	TCCATCTCAATCGCTCTCTGGTTC
378	ROXY13 qRT Rev	ATCAAAGCCATAGTGCTCCAACCC
	ROXY14 qRT For	TTCATAGGAGGGCAGCTTGTCG
	ROXY14 qRT Rev	AGCATTGGAATGAGAGAACGGTTG
	ROXY15 qRT For	TTGGCGTGAACCCGACAATC
	ROXY15 qRT Rev	GCCAAGCTGAGCCAATGCATAC
	ROXY16	QuantiTect QT00868077
	ROXY17	QuantiTect QT00797608
	ROXY18	QuantiTect QT00867314
	ROXY19	QuantiTect QT00869715
388	ROXY20 qRT For	CGTTGGAGTTCACCCAACAGTG
389	ROXY20 qRT Rev	ACGGCGAGGTAAGCAATTTCTCC
	ROXY21	QuantiTect QT00820407

2.1.3.2 Primers for cloning

Abr.	**Primer**	**Sequences (5'-3')**
153	ROXY9 SILY removed For	CATTGATCAAACCCTATCAGTAGTCCCTTCCGACCCAGC
154	ROXY9 SILY removed Rev	GCTGGGTCGGAAGGGACTACTGATAGGGTTTGATCAATG
155	ROXY9 SILY replaced by ALWL For	CATTGATCAAACCCTATCAGgctctctggctcTAGTCCCTTCCGACCCAGC
156	ROXY9 SILY replaced by ALWL Rev	GCTGGGTCGGAAGGGACTAGAGCCAGAGAGCCTGATAGGGTTTGATCAATG
	Seq-L1	TCGCGTTAACGCTAGCATGGATCTC
	Seq-L2	GTAACATCAGAGATTTTGAGACAC

2.1.4 Chemicals, kits and antibodies

2.1.4.1 Chemicals

Chemical	Source
1-Aminocyclopropane-carboxylic acid (ACC)	Calbiochem
Acrylamide/Bisacrylamide	Sigma-Aldrich
2-Mercaptoethanol	Carl Roth
Agarose	Biozym
Ammonium persulfate (APS)	Biometra
Ammonium thiocyanate	Sigma-Aldrich
Bromophenol blue	Roth
Bovine serum albumin (BSA)	Serva
Dimethylsulfoxid (DMSO)	Carl Roth
Ethylenediaminetetraacetic acid (EDTA)	Applichem
Ethidiumbromide	Roth
Fat-free milk powder	commercial
Fluoresceine	BioRad
Glycerine	Roth
Glycerol	Sigma
Guanidinium thiocyanate	Sigma
luminol	Sigma Aldrich
2-(N-morpholino) ethanesulfonic acid (MES)	Roth
Murashige and Skoog medium (MS medium)	Duchefa
Sodium acetate	Roth
Orange G	Sigma
Peptone BD	Biosciences
Phenol	Sigma
Select Agar	Life Technologies
Select yeast extract	Gibco BRL

Sodium salicylate	Sigma-Aldrich
Sodium lauryl sulfate (SDS)	Roth
Sucrose	Roth
SYBR Green I	Cambrex
Tryptone	Oxoid
Tween20	Roth
Tris	Roth
Urea	Sigma

2.1.4.2 Kits and Enzymes

Kit and Enzyme	**Source**
Nucleo Spin® Gel and PCR Clean-up	Macherey-Nagel
Nucleo Spin® Plasmid	Macherey-Nagel
Phusion High-Fidelity DNA Polymerase	Thermo Scientific
RevertAid Reverse Transcriptase	Thermo Scientific
BIOTAQ™ PCR Kit	Bioline
Advantage® 2 Polymerase Mix	Clontech
Gateway® Technology kit	Invitrogen
Pierce 660nm Protein Assay Reagent	Thermo Scientific
SuperSignal™ West Femto kit	Thermo Scientific

2.1.4.3 Antibodies

Antibody	**Description**	**Source**
anti-HA (ChIP grade)	Monoclonal antibody against HA tag from rabbit	Abcam
Anti-rabbit	HRP-conjugated anti rabbit IgG from goat	Life Technologies

2.1.4.4 Standards

Standard	**Source**
GeneRuler DNA Ladder Mix	MBI Fermentas
Prestained Protein Ladder	MBI Fermentas

2.1.4.5 Devices

Device	**Source**
arium® pro DI Ultrapure Water deionization device	Sartorius
Chemocam	Intas
Gene Pulser® II	BioRad
MyCyclert™ thermocycler	BioRad
Pico17 microcentrifuge	Thermo Scientific
pH –Meter HI2212	Hanna Instruments
Photometer Libra S11	Biochrom
Real-time PCR iCycler	BioRad
NanoDrop 2000	Thermo Scientific
Vacuum pump Cyclo 1	Roth

2.2 Methods

2.2.1 Plant growth and treatments

All lines used were in the Columbia-0 (Col-0) background. Seeds were surface-sterilized by gas (Cl_2, generated by mixing of 100 ml sodium hypochlorite and 5 ml hydrochloric acid) for two hours before sowing on soil (steamed and supplied with 0,5 ml/L Wuxal as fertilizer). After keeping at 4°C for 2 days for stratification, they were shifted to climate chambers.

For testing hyponastic growth (the study of petiole angles or gene expression), plants were grown at 22°C in short-day (60% relative humidity, 12-h-light/12-h-dark, fluence rate of 100-120 µmol $m^{-2}s^{-1}$). Absolute petiole angles were measured using Image J analysis of photographs. Straight lines were drawn between the adaxial surface of the petiole of leaf number 7 or 8 and the horizontal plane.

For propagating seeds, plants were grown at 22°C in long-day (60% relative humidity, 16-h-light/8-h-dark, fluence rate of 100-120 µmol $m^{-2}s^{-1}$).

2.2.1.1 Low light treatment

Low light was performed by reducing the light intensity from 100~ 120 to 15 ~ 20 µmol m^{-2} s^{-1} and it was always initiated 1.5 hours after photoperiod the started to minimize circadian clock effects.

2.2.1.2 Light shifting treatment

Light shifting assay was conducted in two steps: low light pretreatment and afterwards control light treatment. For low light pretreatment, it was initiated 1.5 hours after the beginning of the light period with reduction of the light intensity from 100~ 120 to 15 ~ 20 µmol m^{-2} s^{-1} until nearly end of the photoperiod in the climate chamber. For afterwards control light treatment, the low light pretreatment plants were shifting back to control light directly before the lights went off and photographs were taken or petioles were harvested 7.5 hours after the beginning of the second light period.

2.2.1.3 ACC treatment

Four-week-old soil-grown plants grown under SD (12-h-light/12-h-dark) conditions were sprayed with 1 mM ACC until the surfaces were equally moistened. Control plants were sprayed with water.

2.2.1.4 SA treatment

Four-week-old soil-grown plants grown under SD (12-h-light/12-h-dark) conditions were sprayed with 1 mM SA until the surfaces were equally moistened. SA treatment was initiated 1 hour after low light treatment. Control plants were sprayed with water.

2.2.2 Molecular biology methods

2.2.2.1 Overlap extension PCR cloning

Overlap extension PCR cloning was performed for making mutations of different sites of ROXY9 using pDONOR 207-ROXY9 as a template. The first two PCRs were performed using chimeric primers combined with vector specific primers to create an overlapping part at both ends (namely PCR fragment 1 and fragment 2) so that the final PCR products have overlapping regions. PCR products were subsequently purified using the Nucleospin Extract II Gel Extraction kit (Macherey-Naggel, Germany). After determining the concentration of each DNA fragments using NanoDrop 2000, equimolar amounts of purified two fragments were used as template in a new PCR reaction. The new DNA fragments containing hybridized insert mutation sites were amplified using vector specific primers. PCR reactions were performed using Phusion High-Fidelity DNA Polymerase (Thermo scientific) with a MyCycler™ Bio-Rad thermocycler. LR reactions were performed to clone the products into Gateway destination vector.

Overlap extension PCR reaction

PCR1

Component	**Amount**
Plasmid DNA	100 ng
Phusion DNA Polymerase	0.5 µl
5x PCR buffer	10 µl
10 mM dNTPs	1 µl
10 µM pDONOR For	1 µl
10 µM Gene Rev	1 µl
H2O	35.5 µl

Total 50 µl

PCR2

Component	**Amount**
Plasmid DNA	100 ng
Phusion DNA Polymerase	0.5 µl
5x PCR buffer	10 µl
10 mM dNTPs	1 µl
10 µM Gene For	1 µl
10 µM pDONOR Rev	1 µl
H2O	35.5 µl

Total 50 µl

PCR3

Component	**Amount**
PCR1 product	100 ng
PCR2 product	100 ng
Phusion DNA Polymerase	10 µl
5x PCR buffer	1 µl
10 mM dNTPs	1 µl
10 µM pDONOR For	1 µl
10 µM pDONOR Rev	
H2O	

Total 50 µl

Cycle steps	**Temperature and duration**	**Cycles**
Initial denaturation	98°C, 2 min	1
Denaturation	98°C 30 sec	
Annealing	55°C, 30 sec	30
Extension	72°C, 1 min	
Final extension	72°C, 10 min	1
Hold	4°C, ∞	1

2.2.2.2 Plasmid extraction

E.coli cells were collected by centrifuge for 15 sec and plamids were isolated using the Nucleospin Mini kit (Macherey and Nagel).

2.2.2.3 Measurement of DNA and RNA concentrations

Thermo Scientific™ NanoDrop 2000 was used to quantify and assess the purity of nucleic acids. 1 µl of DNA (plasmid) or RNA was used for measurement at a wave length of 260 nm. The sample purity was calculated by the ratio 260/280 nm. The optimal ratio for DNA is OD260/OD280≈1.8 and for RNA is 1.9~2.0.

2.2.2.4 Gateway cloning

The Invitrogen GATEWAY® Technology was used for constructing the entry vectors and destination vectors. The vectors were made by following the steps described in the Invitrogen manual.

2.2.2.5 Gene transfer into *E. coli*

The transformation was performed with the heat shock method according to Hanahan (1983). *E. coli* competent cells (DH5α, 200 µl) were thawed on ice for a few minutes. BP or LR reaction results were added and the mixtures were incubated on ice for 30 min. Heat shock was performed at 42°C for 90 sec after which the cells were immediately placed on ice for 2 min. 1 ml dYT was added to the ice-cold cells. After 1 hour recovery at 37°C, the cells were streaked on dYT plates supplemented with required antibiotics. Plates were incubated overnight at 37°C.

2.2.2.6 Gene transfer into *A. tumefaciens*

The transformation was performed with electroporation method according to Mattanovich (1989). Cells of *A. tumefaciens* GV3101 strain (40 µl) were thawed on ice for a few minutes before adding 100 ng of plasmid. The mixtures were then transferred to an electroporation cuvette following by a single electric pulse (2.5 kV, 25 µF, 400 W) using GenePulser II equipment. The cells were immediately washed out with 1 ml YEB into a new e-tube and incubated for 2 hours at 29°C. The cells were then streaked on YEB plates supplemented with required antibiotics. Plates were incubated at 29°C for 2 days.

2.2.2.7 Arabidopsis transformation

Floral dip method was used for Agrobacterium-mediated Arabidopsis transformation (Clough and Bent, 1998). Agrobacterium cells, transformed with plasmid of interest, were pre-cultured overnight in 5 ml YEB media supplemented with required antibiotics at 29°C with constant shaking. The pre-cultured YEB media was then mixed in a new 400 ml large culture with required antibiotics in the following day and shacked at 29°C overnight until OD600 $\approx$ 0.8. Cells were harvested by centrifugation (4000 rpm, 10 min, RT). After discarding the supernatant, cells were re-suspended in 5% sucrose solution mixed with 0.05% Silwet-L77. Arabidopsis inflorescences were dipped into the solution for a few seconds. Plants were then covered with hood and placed in a climate chamber overnight. Positive T1 candidates were selected by Basta selection and protein expressions were analyzed by western blot analysis.

2.2.3 Transcript analysis

2.2.3.1 RNA extraction

TRIZOL method (Chomczynski 1993) was used for plant RNA isolation. Plant powders which were ground in liquid nitrogen were mixed with 1.3 ml of Trizol solution (380 ml/L phenol saturated with 0.1 M citrate buffer pH 4.3, 0.8 M guanidinthiocyanate, 0.4 M ammoniumthiocyanate, 33.4 ml 3 M Na-acetate pH 5.2, 5% glycerol). After immediately vortexing for 10 min at room temperature, 260 µl chloroform was added to each sample and the mixtures were vortexed for another 10 min. The samples were then centrifuged for 60 min at 13.000 rpm, 4°C. The supernatants (~ 900 µl) were transferred to new 1.5 ml e-tubes. 325 µl of HSB buffer (HSB, 1.2 M NaCl, 0.8 M Na-citrate) and 325 µl of 2-propanol were then added. After mixed well by inverting for several times, the samples were centrifuged again for 30 min at 13.000 rpm, 4°C. The supernatants were discarded and the pellets were washed 2 times with 200 µl of 70% EtOH. The pellets were dissolved in 20-60 µl de-ionized water after they were completely dried at room temperature and the concentration was measured as described before.

TRIzol buffer

Ingredient	Amount per 500 ml
380 ml/l phenol with citrate buffer	190 ml
0.8 M guanidinium thiocyanate	47.264 g
0.4 M ammonium thiocyanate	15.224 g
33.4 ml/l Na-acetate (3 M stock)	16.7 ml
5% glycerine (100%)	25 ml
ddH_20	to 500 ml
Store at 4˚C	

2.2.3.2 cDNA synthesis

1 µg RNA was used for cDNA synthesis. The RNA samples were first incubated with 1 µl DNase together with 1 µl 10x DNase buffer (Fermentas) for 30 min. 1 µl 25 mM EDTA then was added to each sample for denaturing DNase activity. After denaturing at 60°C for 10 min, 20 pmol of oligo dT primer and 200 pmol of random nonamer oligonucleotides were added and annealed at 70°C, 10 min. Finally, 20 nmol dNTPs, 4 µl RT 5x reaction buffer and 60 U reverse transcriptase H (Fermentas) were added and the reaction was incubated at 42°C for 70 min followed by incubation at 70°C for 10 min. The prepared cDNA was stored at -20°C for further analysis.

Reaction mix and program for cDNA synthesis

Stock component	Volume	Temperature and duration
1 mg/ml RNA	1 µl	37°C, 30 min
10x DNase buffer	1 µl	
DNase	1 µl	
ddH_2O	to 10 µl	
25 mM EDTA	1 µl	65°C, 10 min
100 µM oligo-dT	0.2 µl	70°C, 10 min
200 µM random monomer	1 µl	
5x RT-buffer	4 µl	42°C, 70 min then 70°C, 10 min
10 mM dNTPs	2 µl	
Reverse Transcriptase	0.2 µl	
ddH2O	to 20 µl	

2.2.3.3 Quantitative real-time PCR (qRT-PCR)

Quantificative real-time PCR was performed using MyiQ™ Real-Time PCR Detection Systems (Bio-Rad, USA). The primers used in real-time PCR are listed in Table 2.1.3.1. The reaction mixture of real-time PCR was as follows: 1 µl of 1:10 diluted cDNA, 1x NH4-reaction buffer (Bioline), 2 mM $MgCl_2$, 100 µM dNTPs, 0.4 µM primers, 0.25 U BIOTaq DNA polymerase, 10 nM fluoresceine (BioRad), 100,000x diluted SYBR Green I (Cambrex) solution and 17.2 µl de-ionized water water (final volume 25 µl). The conditions of real-time PCR were as follows: 95°C for 6 min, 40 cycles of 95°C for 20 s and 55°C for 20 s, followed by 72°C for 40 s. The obtained Ct values were normalized to housekeeping gene UBQ5 and calculation of relative gene expression was done with the $2^{-[CT(\text{gene of interest})-CT(\text{reference gene})]}$ method (Schmittgen and Livak, 2008).

Reaction mix for qRT-PCR using BIOTAQ DNA Polymerase

Stock component	Volume in a 25 µl reaction
10X NH_4 reaction buffer	2.5 µl
$MgCl_2$ 25 mM	1 µl
dNTPs 10 mM	0.25 µl
For and Rev primers (each 4 mM)	2.5 µl
Sybr Green (1/1000)	0.25 µl
Fluorescein (1 µM / 1:1000)	0.25 µl
BIOTAQ DNA Polymerase	0.05 µl
cDNA template	1 µl

Program of qRT-PCR cycler using BIOTAQ DNA Polymerase

Cycle step and repeat	Temperature and duration	Cycles
Initial denaturation	95°C ,90 sec	1
Denaturation	95°C, 20 sec	
Annealing	55°C, 20 sec	39
Extension	72°C, 40 sec	
Final extension	72°C, 4 min	1
	95°C, 1 min	1
Generation of melting curve	55°C, 1 min	1
	55°C, 10 sec (+0.5°C/cycle)	81

2.2.3.4 Microarray analysis

Four-week soil-grown wild-type, *tga1 tga4* were used for transcriptome analysis. For each type of sample, the petioles of 15 plants were harvested and four independent experiments were performed. Total RNA was extracted by TRIZOL method. RNA samples were sent to the transcriptome lab at Goettingen University where the RNA samples were analyzed with Affymetrix GeneChips® Gene 1.0 ST Arrays.

Robust Multi-array Average (RMA) was used to normalize the arrays. Fold change values, and corresponding p-values derived from moderated t-statistics were obtained from the Affymetrix CEL files using the Robin 1.1.2 software (Lohse et al., 2010) (analyzed by Dr. Corinna Thurow). The AgriGO analysis tool from website (http://bioinfo.cau.edu.cn/agriGO/) was used for the functional classification of differentially expressed genes. The Motif Mapper (version 5.2.4.01) was used to define significant enriched promoter mitifs compared to 1000 randomly composed, equally sized, reference promoter datasets. (Berendzen et al., 2012)

2.2.4 Protein analysis

2.2.4.1 Protein extraction

Proteins of four-week-old soil-grown Arabidopsis plants were harvested for protein extraction. Urea buffer was added to the deep frozen plant powder (~ 200 µl) and the mixture was shaked at 65°C for 10 min. Afterwards the solution was centrifuged for 20 min at 13000rpm at room temperature and the supernatant was used for further protein expression analysis.

Protein extraction buffer

Ingredient	Final concentration
Urea	4 M
Glycerol	16.6% (v/v)
SDS	5% (w/v)
β-mercaptoethanol	0.5% (w/v)

2.2.4.2 Determination of protein concentrations

Protein concentrations were measured with the detection solution which was made by mixing 20 ml of Pierce 660 nm Protein Assay Reagent with 1 g of Ionic Detergent Compatibility Reagent (IDCR) (Thermo Scientific). 1 µl of protein extract was added to the well of a microtitre plate together with 150 µl of detection solution. The reaction was incubated for 5 min at room temperature. OD was measured at 660 nm by using the BioTek plate reader. Protein concentrations were determined with the help of standard curve derived from 0 µl, 1 µl, 3 µl, 6 µl, 9 µl of 1 mM BSA (Bovine serum albumin).

2.2.4.3 SDS-PAGE

SDS-PAGE (sodium dodecyl sulfate-polyacrylamide gel electrophoresis) was performed according to the method described by Weber (1977). 20 µg protein samples were loaded to the stacking gel and the electrophoresis was performed at 70 V for 30 min and at 120 V for 1 hour and 30 min until bromophenol blue band reached the end of the separation gel. A prestained ladder (6 µl) was used for estimating the size of the protein signals.

Stacking gel (12%, 10 ml)

Ingredient	Amount
ddH_2O	4.0 ml
Acrylamide/	3.3 ml
Bisacrylamide (37.5:1)	
Tris-HCl pH 6.8	2.5 ml
10% SDS	0.1 ml
10% APS	0.1 ml
TEMED	4 µl

Separation gel (12%, 10 ml)

Ingredient	Amount
ddH_2O	6.8 ml
Acrylamide/	1.7 ml
Bisacrylamide (37.5:1)	
Tris-HCl pH 6.8	1.25 ml
10% SDS	0.1 ml
10% APS	0.1 ml
TEMED	10 µl

2.2.4.4 Immunoblot Analysis

After separated in 12% SDS-PAGE gels, proteins were transferred to PVDF (Polyvinylidene difluoride, Roti®-PVDF, Roth) membrane using a semi-dry blot method (150 mA, 30 min). The PVDF membrane was then blocked at room temperature for 30 min with 5% (w/v) non-fat milk in TBST. Immunoblot analysis was carried out using rat α-HA antibody. The antigen protein was detected by chemiluminescence using a SuperSignal™ West Femto Maximum Sensitivity Substrate kit (Thermo scientific) according to the manufacturer's protocol and the luminescence was detected in a chemocam (Intas).

3 Results

3.1 The *tga1 tga4* mutant shows reduced hyponastic growth

The two redundant transcription factors TGA1 and TGA4 encode conserved redox-sensitive cysteine residues, which might serve as targets of the TGA-interacting ROXY-type glutaredoxins. Although TGA1 and TGA4 have been studied for many years, the functional significance of the SA-mediated redox-modification on the expression of target genes has remained unclear (Després et al., 2003; Shearer et al., 2012). Interestingly, we found that the *tga1 tga4* mutant displayed reduced hyponastic growth under various conditions, including low light, ethylene or elevated temperature (Figure 3.1). Due to the robustness and easy scoring of this phenotype, we focused on this novel function of TGA1 and TGA4 in our further analysis.

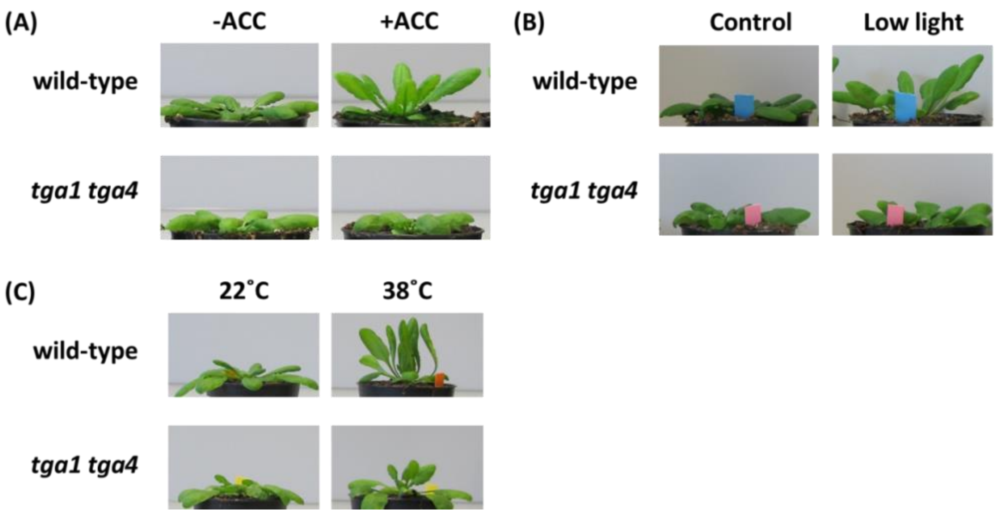

Figure 3.1 The *tga1 tga4* mutant is impaired in hyponastic growth.

(A) Representative photographs of wild-type and *tga1 tga4* plants after 6 h of treatment with the ET precursor ACC (1-aminocyclopropane-1-carboxylic acid, 1mM)

(B) Representative photographs of wild-type and *tga1 tga4* plants after 6 h of low light treatment (15-20 µmol photons m^{-2} s^{-1}).

(C) Representative photographs of wild-type and *tga1 tga4* plants after 6 h of elevated temperature treatment (38˚C).

Before treatments, plants were grown for 4 weeks under short day conditions (12-h-light at 100-120 µmol photons m^{-2} s^{-1}/12-h-dark, 22 ˚C).

3.2 Low light-induced hyponastic growth partially acts through the ethylene and the phototropin pathways

As shown in Figure 3.1, the *tga1 tga4* mutant shows reduced hyponastic growth, independent of whether the response is triggered by low light, ethylene or heat. In order to estimate whether the ethylene pathway plays a role in the light-induced hyponastic growth under our experimental conditions, we analysed the *ethylene-insensitive* (*ein2-1*) mutant (Alonso, et al., 1999). To obtain quantitative data, we measured the angles between leaf petioles and the horizontal plane as shown in Figure 3.2. In the wild-type, petiole angles increased around threefold in response to six hours of low light treatment. This response was diminished in the *ein2* mutant. Apparently, the ethylene pathway contributes to the low light-induced hyponastic growth under our growth conditions.

Next, we tested the influence of photoreceptors on the hyponastic response using the *phyB* (deficient in phytochrome B) (Reed et al., 1993), *cry1 cry2* (deficient in cryptomchromes 1 and 2) (Mockler et al., 1999) and *phot1 phot2* (deficient in phototropins 1 and 2) mutants (Lariguet et al., 2006). All three mutants behaved differently as described (Millenaar et al., 2009). The *phyB* mutant (Landsberg) was reported to have constitutively elevated leaves (Mullen et al., 2006; Millenaar et al., 2009), whereas the *phyB* mutant in the Columbia background had even decreased petiole angles under control light conditions and showed an exaggerated hyponastic response under low light conditions (Figure 3.2C). The *cry1 cry2* double mutant in the Landsberg background showed reduced hyponastic growth (Millenaar et al., 2009), which was not observed in our Columbia-derived mutants (Figure 3.2D). Finally, the *phot1 phot2* (Landsberg/Wassilewklija) was like wild-type in previous experiments (Millenaar et al., 2009), whereas the respective double mutant in the Columbia background showed impaired hyponastic growth (Figure 3.2D). Since our low light treatment (4-week-old plants grown under a 12-h photoperiod at 100-120 µmol photons m^{-2} s^{-1} and subsequent shift to 15-20 µmol photons m^{-2} s^{-1} for six hours) is similar to the treatment of Millenaar et al. (2009) (plant with 15 rosette leaves grown under a 9 h photoperiod at 200 to 20 µmol photons m^{-2} s^{-1}), the use of different ecotypes might explain the discrepancy.

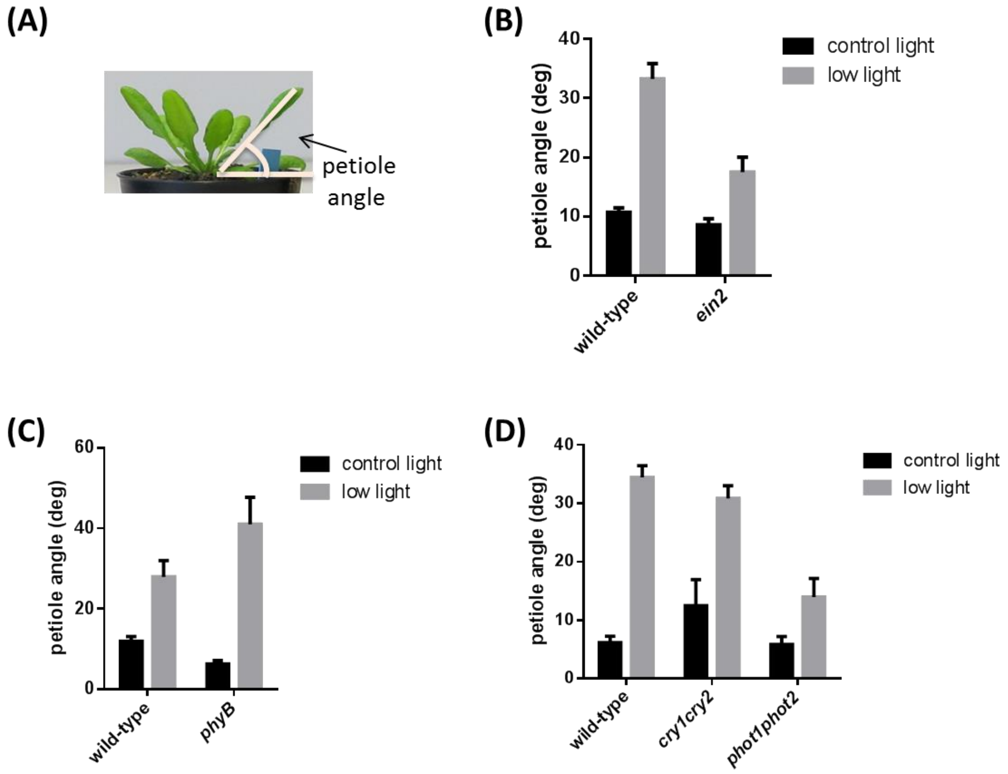

Figure 3.2 Low light-induced hyponastic growth partially acts through the ethylene and the phototropin pathways.

(A) Absolute petiole angles were measured using Image J analysis of photographs. Straight lines were drawn between the adaxial surface of the petiole of leaf number 7 or 8 and the horizontal plane. Plants were grown for 4 weeks under short day conditions (12-h-light at 100-120 µmol photons m^{-2} s^{-1}/12-h-dark). Low light treatment (6 h at 15-20 µmol photons m^{-2} s^{-1}) was initiated 1.5 h after the start of the photoperiod and photographs were taken after 6 h.

(B-D) Leaf angles of the indicated genotypes were measuread as described in (A). Error bars represent the average ± SEM of nine plants. The images for petiole angle measurement are shown in Supplementary Figure S6 and Supplementary Figure S7.

Collectively, our analysis has shown that the reduction of the light intensity is at least partially detected by the blue light receptor phototropin which might trigger ethylene synthesis and signaling. However, both mutations do not diminish the response as strongly as the *tga1 tga4* alleles indicating that TGA1 and TGA4 control responses downstream of these and other signaling cascades.

3.3 Redox-active cysteines of TGA1 are not important for the regulation of hyponastic growth

As revealed by the phenotype of the *tga1 tga4* mutant, TGA1 and TGA4 are required for hyponastic growth and the regulation of their activity might be a means to control the response. Since transcript levels of both proteins did not change upon transfer of plants to low light (Supplementary Figure S1), we explored, whether the activity of these factors might be modulated at the protein level. Previously, it has been reported that two cysteines in the peptide stretch CNLKQSC in TGA1 can form a disulfide bridge which is reduced in SA-treated plants (Despres et al., 2003). Therefore, we asked the question whether these cysteines are important for the function of TGA1. To this end, the *tga1 tga4* mutant was complemented with wild-type and mutant *TGA1* sequences. Since *CaMV35S:TGA1* constructs cannot complement the *tga1 tga4* phenotype (Lindermayr et al., 2010), engineered genomic clones were used. Cysteine residue in position 260 was altered into an asparagine and cysteine residue in position 266 was changed into a serine as described before (Depres et al., 2003). *tga1 tga4* mutants transformed with the wild-type gene are called *gTGA1* plants from here on, plant lines encoding the mutated gene are called *gTGA1cys* plants. Both constructs contain an HA-tag at the N terminus (Figure 3.3A). Seeds containing these constructs were obtained from Prof. Dr. Yuelin Zhang, UBC Vancouver. Two independent lines carrying the *gTGA1* and *gTGA1cys* constructs, respectively, displayed low light-induced leaf re-orientation resembling the wild-type. This analysis shows that the N-terminally tagged TGA1 is functional in this assay, irrespective of whether it contains the redox-regulated cysteines.

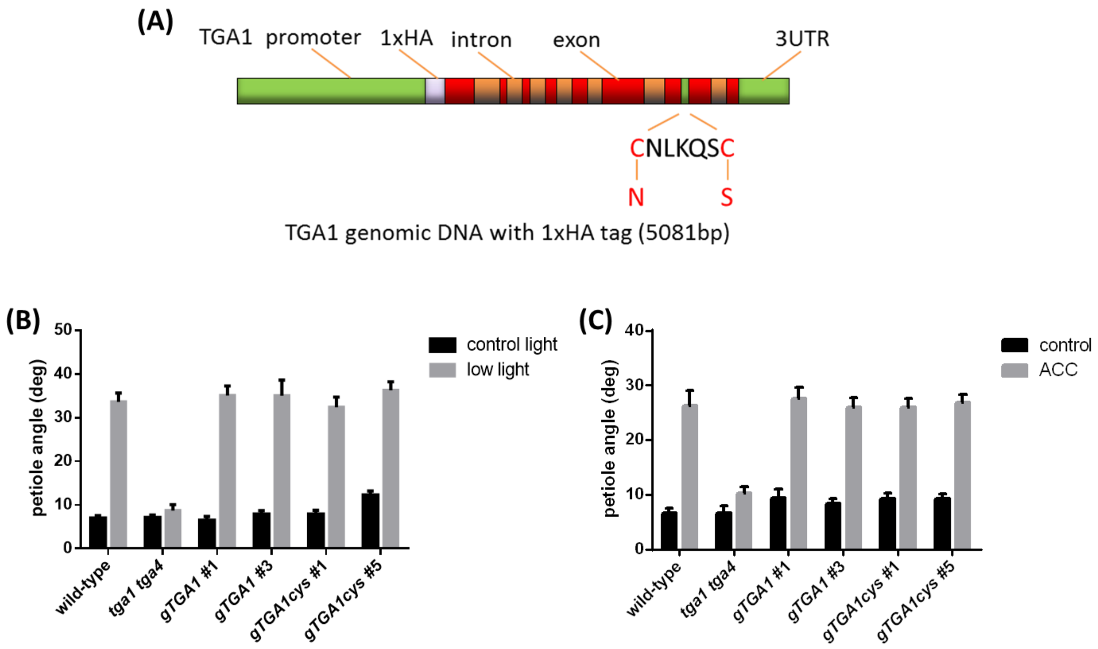

Figure 3.3 Redox-active cysteines of TGA1 are not important for the regulation of hyponastic growth.

(A) Structure of the genomic *TGA1* genes (*gTGA1* and *gTGAcys*) used for complementation assays. The relative position of the redox-active cysteines, which were mutated to asparagine and serine in *gTGAcys*, respectively, is shown.

(B) Effect of low light treatment (reduction in light intensity from 100-120 to 15-20 µmol m^{-2} s^{-1}) on the hyponastic growth of wild-type, *tga1 tga4*, and two independent transgenic *gTGA1* and *gTGA1cys* complementation lines. See Figure legend 3.2 for details of plant growth and leaf angle measurements. Bars represent the average ± SEM of ten plants. The images for petiole angle measurement are shown in Supplementary Figure S9.

(C) Effect of ACC (1-aminocyclopropane-1-carboxylic acid, 1 mM, 6 h) on the hyponastic growth of the indicated plant lines. Plants were grown for 4 weeks under short day conditions (12-h-light/12-h-dark) before treatment. Bars represent the average ± SEM of ten plants. The images for petiole angle measurement are shown in Supplementary Figure S8.

3.4 Redox-active cysteines of TGA1 are not important for salicylic acid-mediated inhibition of hyponastic growth

Since exogenous salicylic acid (SA) leads to the reduction of C260 and C266 of TGA1 *in vivo* (Després et al., 2003) and since it interferes with low light-induced hyponastic growth (Ritsema, et al., 2010), we hypothesized that the redox-active cysteines might play a role in this effect. Therefore, wild-type, *tga1 tga4* and *gTGA1* and *gTGA1cys* complementation lines were transferred to low light. After transfer, half of the plants were sprayed with 1 mM SA, which led to a reduced hyponastic response in wild-type and the complementation lines. This experiment indicates that the SA-mediated redox modulation does not play a role for the negative effect of SA on hyponastic growth

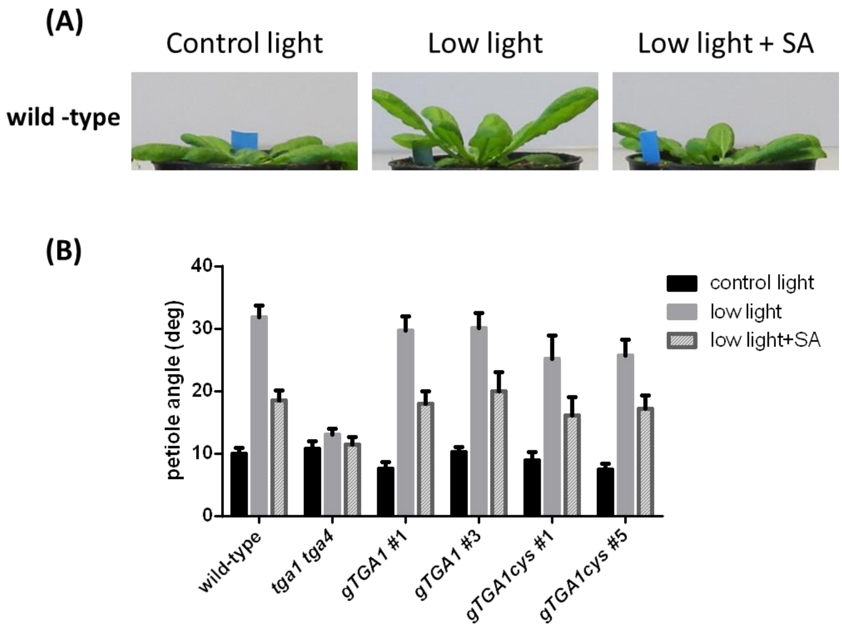

Figure 3.4 Redox-active cysteines of TGA1 are not important for salicylic acid-mediated inhibition of hyponastic growth.

(A) Representative pictures of plants subjected to low light (reduction in light intensity from 100-120 to 15-20 µmol m^{-2} s^{-1}) or low light in combination with 1 mM SA, which was sprayed 1 h after the onset of the low light treatment.

(B) Effect of low light or low light in combination with 1 mM SA on the hyponastic growth of wild-type, *tga1 tga4*, and two independent *gTGA1* and *gTGA1cys* lines. See Figure legend 3.2 for details of plant growth and leaf angle measurements. Bars represent the average ± SEM of 10 plants. The images for petiole angle measurement are shown in Supplementary Figure S10.

3.5 NPR1 and the redundant TGA factors TGA2, TGA5 and TGA6 are required for SA-mediated inhibition of hyponastic growth

SA-mediated suppression of low light-induced hyponasty was further tested in the *npr1-1* mutant, in which SA-activated gene expression and systemic acquired resistance are abolished (Cao et al., 1994). Increased petiole angles can be triggered by low light in the *npr1-1* mutant as well as in wild-type (Figure 3.5). However, the SA-mediated suppression of low light-induced leaf reorientations was almost abolished in *npr1-1*. Since NPR1 and the redundant TGA factors TGA2, TGA5 and TGA6 function together to establish and maintain systemic acquired resistance and in suppressing of the jasmonic acid-induced defense pathway (Cao et al., 1994; Spoel et al., 2003; Zhang et al., 2003; Zander et al., 2009), we asked whether they control SA-mediated suppression of hyponastic growth as well. As shown in Figure 3.5, SA cannot suppress low light-induced leaf movement in the *tga2 tga5 tga6* mutant. It is concluded that TGA2, TGA5, and TGA6 but not TGA1 and TGA4 are required for SA-mediated inhibition of hyponastic growth.

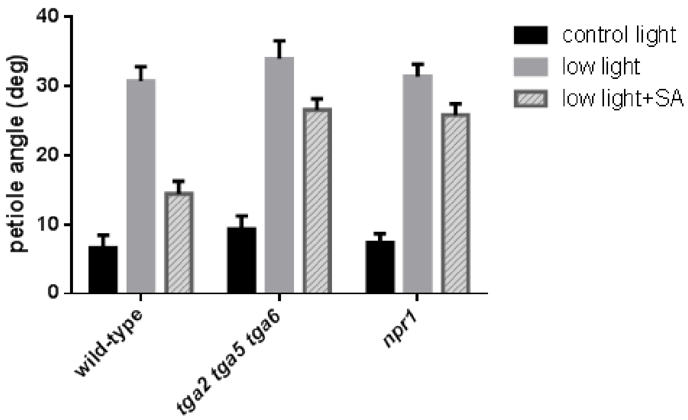

Figure 3.5 NPR1 and TGA2, TGA5 and/or TGA6 are required for SA-mediated inhibition of hyponastic growth.

Four-week-old soil-grown wild-type, *tga2 tga5 tga6*, and *npr1-1* plants were subjected to low light and low light plus 1 mM SA treatment. See Figure legend 3.2 for details of plant growth and leaf angle measurements. Error bars represent the average ± SEM of 6 individual plants. The images for petiole angle measurement are shown in Supplementary Figure S11.

3.6 The redox state of TGA1/TGA4 is not important for the reversal of hyponastic growth after transferring low light-treated plants back to control light intensities

(A)

(B)

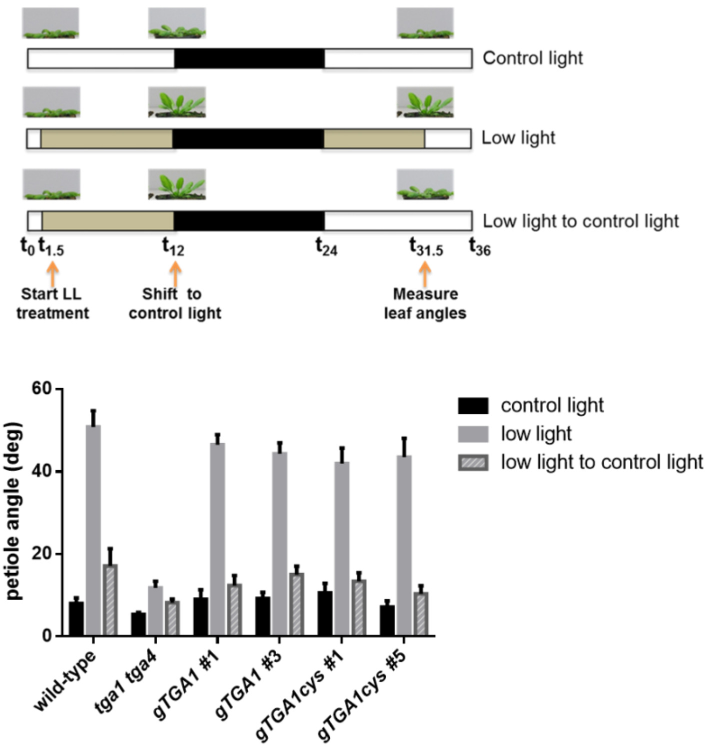

Figure 3.6 The redox state of TGA1/TGA4 is not important for the reversal of hyponastic growth after the transfer of low light-treated plants back to control light conditions.

(A) Scheme of the experimental design. Four-week-old plants were grown under a 12-h-light/12-h-dark regime. Low light (LL) treatment was initiated 1.5 hours after the beginning of the light period ($t_{1.5}$). Plants were transferred back to control light shortly before the lights went off (t_{12}) and plants were analysed after 7.5 h of the second light period ($t_{31.5}$).

(B) Plants of the indicated genotypes were subjected to the light regime displayed in (A). Petiole angles were measured at $t_{31.5}$. Error bars represent the average ± SEM of 8 individual plants. The images for petiole angle measurement are shown in Supplementary Figure S12.

Next, we tested whether the redox state of TGA1 might play a role in the reversal of the hyponastic growth which is observed after transferring low light-treated plants to control light conditions. As described before, low light treatment was initiated 1.5 hours after the start of the photoperiod but was continued in this experiment for 10.5 hours. When the dark period started, half of the plants were transferred to a different growth chamber so that they would face control light conditions in the next morning, whereas half of the plants would face low light conditions after the dark period. Plant leaves of all tested genotypes became more horizontal at 7.5 hours after transfer to control light conditions (Figure 3.6). Collectively, our results suggest that the redox state of TGA1/TGA4 is not important for either initiating or terminating low light-induced hyponastic growth in *Arabidopsis*.

3.7 The expression pattern of CC-type glutaredoxins *ROXY8* and *ROXY9* is consistent with their potential role as repressors of TGA1 and TGA4

Next we searched for other potential mechanisms that might regulate the activity of TGA1 and TGA4. TGA transcription factors interact with CC-type glutaredoxins, which are represented by a 21-membered gene family in *Arabidopsis* (Ziemann et al., 2009). The interaction seems to interfere with TGA factor activity, as demonstrated for ROXY1, which represses the TGA factor PAN. Both factors are co-expressed in floral meristems (Li et al., 2009). Furthermore, ROXY19 is induced by SA and represses genes that are regulated by the SA-responsive NPR1/TGA2, TGA5 and/or TGA6 module (Ndamukong et al., 2007; Zander et al., 2012). In order to test which ROXYs might interfere with the activity of TGA1 and TGA4 during hyponastic growth, expression of all 21 CC-type glutaredoxins was analysed by real-time PCR in response to the light regime described in Figure 3.6 (Figure 3.7). Assuming that ROXYs are negative regulators of TGA1 and TGA4, their expression should be low under low light (when the petioles grow upwards) and high under control light conditions. Whereas several ROXYs were induced by low light (ROXY1, ROXY2, ROXY4, ROXY10, ROXY16, ROXY17), the mRNA levels of ROXY9 and ROXY20 were reduced under low light conditions. After the transfer of low-light treated plants to control light conditions transcript levels were induced or even hyper-induced in the case of ROXY9. This hyper-induction is also observed for ROXY8, which belongs to the same clade as ROXY9. In addition, transcript levels of *ROXY8*, *ROXY9* and *ROXY20* expression are low in *tga1 tga4* (Figure 3.8). This is reminiscent of ROXY19, which controls the activity of TGA2, TGA5 and TGA6 and is regulated by these factors (Ndamukong et al., 2007). In addition, we investigated the expression of *ROXY9* in the *gTGA1* and *gTGA1cys* complementation lines. Consistent with the wild-type-like phenotype of these plants with respect to light-controlled hyponastic growth, the expression of *ROXY9* was repressed by low light and induced after transfer to control light in both lines (Supplementary figure S3). Previously, Dr. Martin Muthreich (Prof. Dr. Christiane Gatz lab, Department of Plant Molecular Biology and Physiology) found that TGA1 and TGA4 interact with ROXY9 in the yeast two hybrid system and in bimolecular fluorescence complementation experiments in Arabidopsis protoplasts. Collectively, our results support a functional relationship between TGA1 and TGA4 and at least ROXY9.

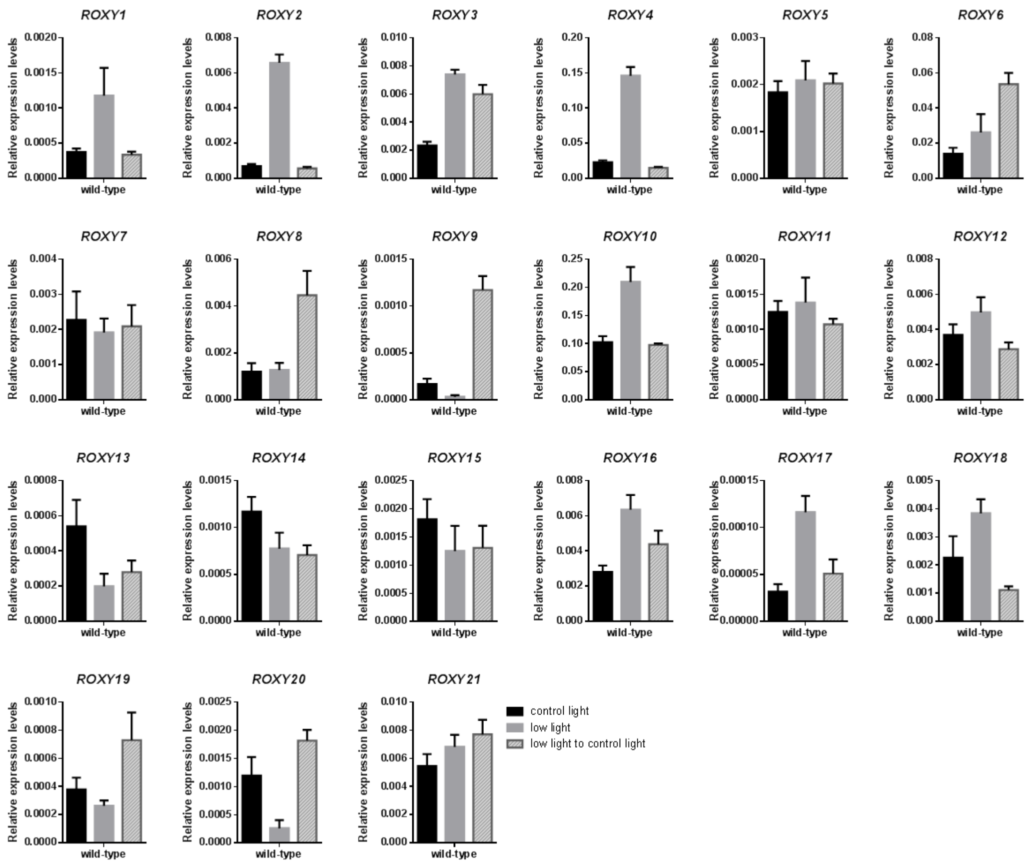

Figure 3.7 Expression of 21 CC-type glutaredoxins

qRT–PCR analysis of 21 ROXYs expression in wild-type. Plants were subjected to the light regime displayed in Figure 3.6A. Transcript levels were normalized to the transcript level of *UBQ5* (ubiquitin 5). Error bars represent the average ± SEM of five biological replicates, each with dissected petioles from five independent plants.

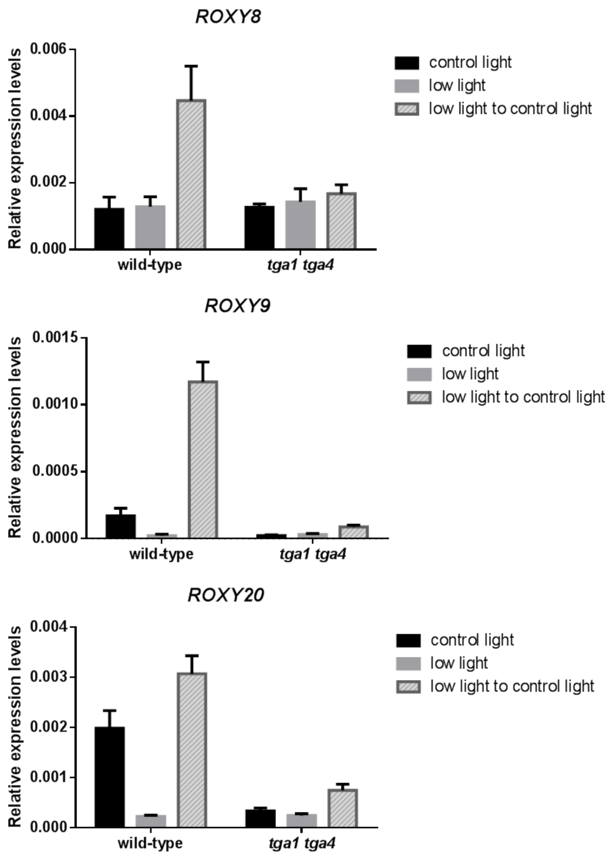

Figure 3.8 Expression of ROXY9 negatively correlates with hyponastic growth and depends on TGA1 and TGA4.

qRT–PCR analysis of *ROXY8*, *ROXY9* and *ROXY20* expression. Plants were subjected to the light regime displayed in Figure 3.6A. Transcript levels were normalized to the transcript level of *UBQ5* (ubiquitin 5). Error bars represent the average ± SEM of five biological replicates, each with dissected petioles from five independent plants.

3.8 Overexpression of ROXY8 or ROXY9 phenocopies the *tga1 tga4* phenotype

Due to the lack of T-DNA insertion mutants in the potentially redundant *ROXY8* and *ROXY9* genes and the potential redundancy with at least *ROXY20*, we asked the question whether ROXY8 and ROXY9 can repress hyponastic growth when ectopically expressed under the control of the *CaMV 35S* promoter. As shown in Figure 3.9, five independent homozygous *35S:HA-ROXY8* and *35S:HA-ROXY9* lines showed reduced degrees of petiole angles in response to low light treatment which is similar to the phenotype of the *tga1 tga4* double mutant. In contrast, *35S:HA-ROXY19* plants responded like wild-type plants, indicating the hyponasty-deficient phenotype of the *35S:HA-ROXY8* and *35S:HA-ROXY9 ROXY8/9* lines requires specific features of the proteins which are not present in ROXY19. Consistent with the concept that ROXY19 represses the function of clade II TGA TFs, *35S:HA-ROXY19* plants did not react to the negative signal SA, as observed before for the *tga2 tga5 tga6* mutant (Figure 3.5)

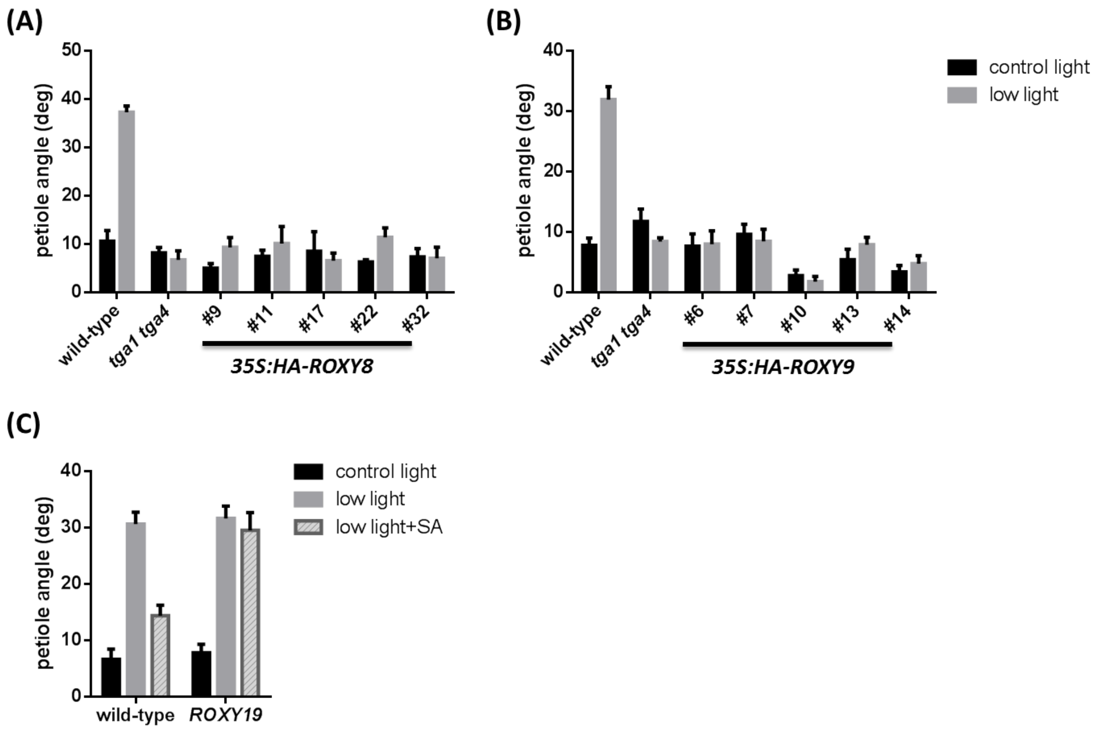

Figure 3.9 Overexpression of ROXY8 or ROXY9 phenocopies the *tga1 tga4* phenotype.
Effect of low light treatment (reduction in light intensity from 100-120 to 15-20 µmol m^{-2} s^{-1}) on the hyponastic growth of wild-type, *tga1 tga4*, and independent transgenic lines expressing either ROXY8 (A), ROXY9 (B) or ROXY19 (C) under the control of the *CaMV 35S* promoter. All proteins were fused to an HA-tag. See Figure legend 3.2 for details of plant growth and leaf angle measurements. Bars represent the average ± SEM of 3 (ROXY8), 9 (ROXY9) or 6 plants (ROXY19). The images for petiole angle measurement are shown in Supplementary Figure S13 and Supplementary Figure S14.

3.9 The sequence of the C-terminal end of ROXY9 is not important for its repressive effect on hyponastic growth

Most of ROXYs contain a functionally important C-terminal ALWL motif, which recruits the transcriptional co-repressor TOPLESS (Uhrig et al., 2017). Only ROXYs possessing this motif complemented the phenotype of *roxy1* (Li et al., 2009). Likewise, only ROXYs with this motif can repress the expression of TGA2-dependent target promoters (Zander et al., 2012). In contrast, ROXY8 and ROXY9 belong to a clade of ROXYs that do not encode the conserved ALWL motif at the very C-terminal end. Instead, ROXY9 contains a SILY motif (Figure 3.10A).

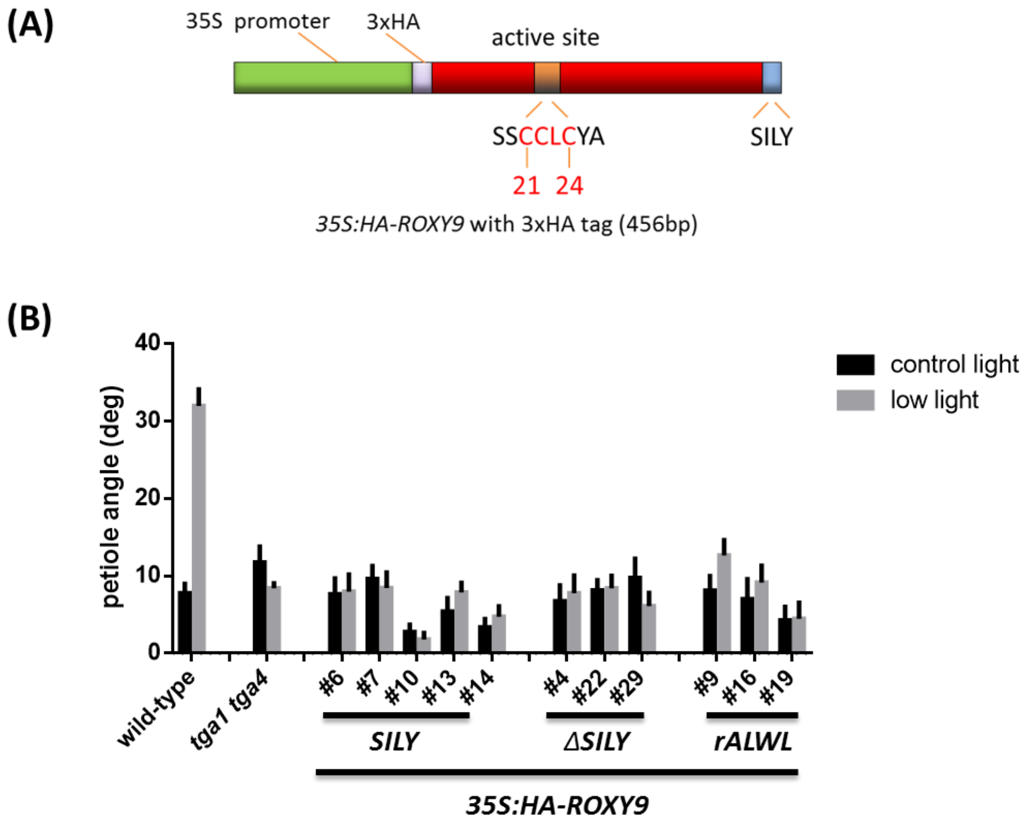

Figure 3.10 The sequence of the C-terminal end of ROXY9 is not important for its repressive effect on hyponastic growth.

Effect of low light treatment (reduction in light intensity from 100-120 to 15-20 µmol m^{-2} s^{-1}) on the hyponastic growth of wild-type, *tga1 tga4*, and independent transgenic lines expressing either ROXY9, ROXY9 lacking the SILY (ROXY9(ΔSILY)) motif and ROXY9 encoding an ALWL motif instead of the SILY motif (ROXY9(rALWL)) under the control of the *CaMV 35S* promoter. All proteins were fused to an HA-tag. See Figure legend 3.2 for details of plant growth and leaf angle measurements. Bars represent the average ± SEM 9 plants of each transgenic line.

In order to analyse the role of the C-terminal end of ROXY9, we either deleted it (*35S:HA-ROXY9ΔSILY*) or replaced it by the ALWL motif (*35S:HA-ROXY9rALWL*). Independent lines carrying these constructs showed impaired hyponastic growth as observed for *35S:HA-ROXY9* lines after transfer to low light intensities. Since the SILY motif is not present in ROXY8, the results obtained with the *35S:HA-ROXY9ΔSILY* were expected. Importantly, we can conclude that the ALWL motif does not interfere with the repressive function of ROXY9 (Figure 3.10B).

3.10 The sequence of CCLC motif in the active center of ROXY9 is important for its repressive effect on hyponastic growth

Next, we characterized the importance of the CCLC motif in the active center (Figure 3.11) which is slightly different from the CCMC/S motif found in most ROXYs. We introduced single point mutations individually for all the three cysteines and expressed these proteins under the *CaMV 35S* promoter in wild-type plants. In addition, a mutant was constructed in which all three cysteines were replaced by alanine residues. Western blot analysis was performed to identify transgenic lines with similar expression levels (Figure 3.11A). For comparison, extracts from plants with functional ROXY9 (ROXY9, ROXY9(ΔSILY), ROXY9(rALWL)) were loaded. Four independent lines of the ROXY9(SCLC) mutant, where the first cysteine was mutated, expressed similar amounts of the protein as transgenic lines expression ROXY9. Comparison of these plants after transfer to low light revealed that the ROXY9(SCLC) mutant protein did not repress hyponastic growth indicating that the first cysteine is important for its function (Figure 3.11B). The same effect was observed for four independent *35S:HA-ROXY9(CSLC)* lines, although protein levels were as high as in those plants that encode the repressive ROXY(ΔSILY) and ROXY(rALWL) mutants. This result underpins the importance of the conserved second cysteine. In contrast, ROXY9(CSLS), in which the third cysteine was mutated, was functional. As expected, ROXY9(AALA) is not functional.

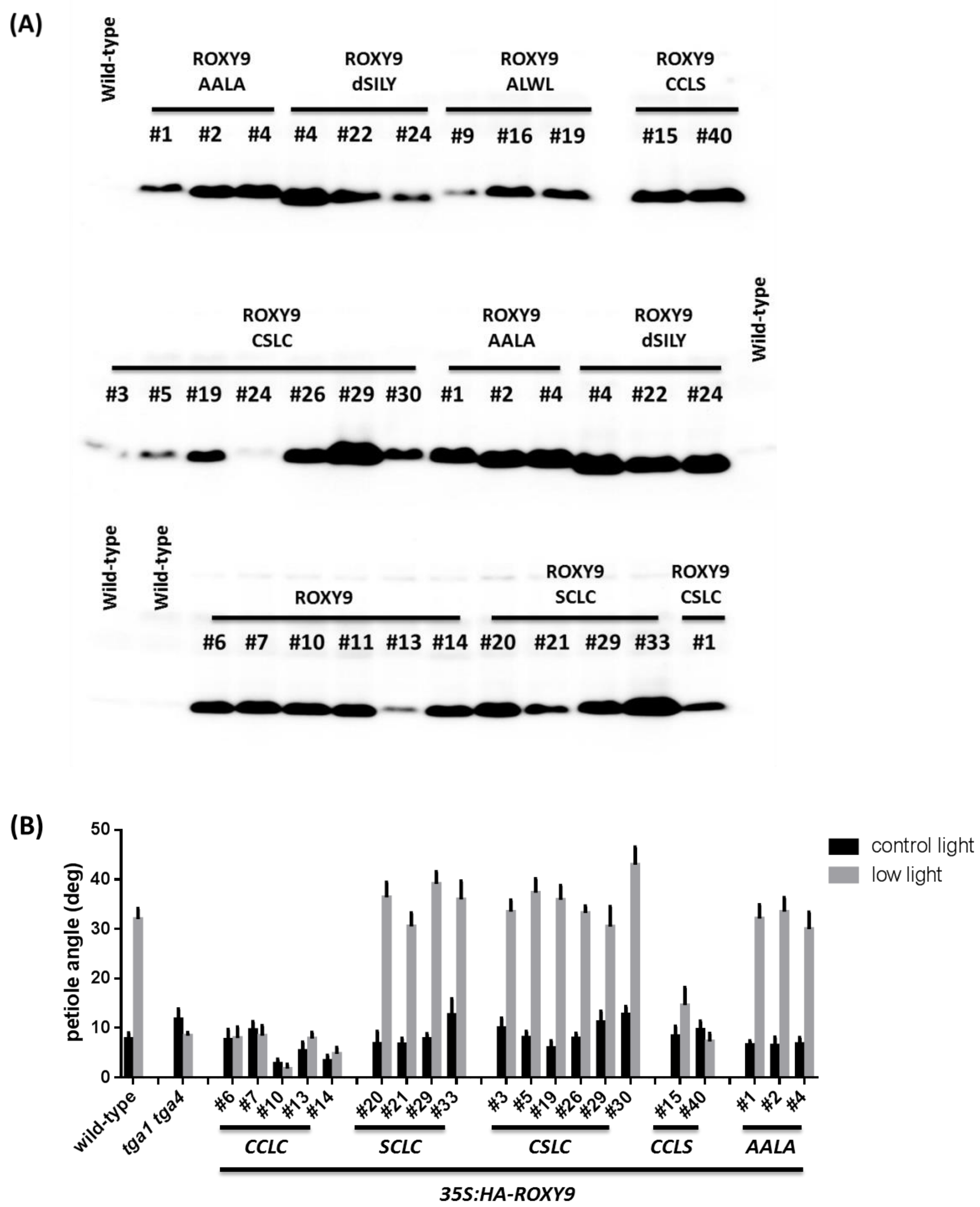

Figure 3.11 The sequence of CCLC motif in the active center of ROXY9 is important for its repressive effect on hyponastic growth.

(A) Western blot analysis of transgenic lines expressing HA-tagged ROXY9 and the indicated mutant versions of ROXY9 under the control of the *CaMV35S* promoter.

(B) Effect of low light treatment (reduction in light intensity from 100-120 to 15-20 µmol m^{-2} s^{-1}) on the hyponastic growth of wild-type, *tga1 tga4*, and independent transgenic lines expressing either ROXY9 or ROXY9 mutants within the active site under the control of the *CaMV 35S* promoter. All proteins were fused to an HA-tag. See Figure legend 3.2 for details of plant growth and leaf angle measurements. Bars represent the average ± SEM 9 plants of each transgenic line.

3.11 The *roxy9* CRISPR-Cas9 mutant is not impaired in hyponastic growth

Due to lack of T-DNA insertion lines, *roxy9* CRISPR-Cas9 mutants were generated by Florian Jung (Master thesis). Seven individual lines containing nucleotide deletions C-terminal to the CCLC active center resulting in frame shift mutations were identified and confirmed by sequence analysis. However, hyponastic growth and reversal of hyponastic growth was not different in these mutants as compared to wild-type.

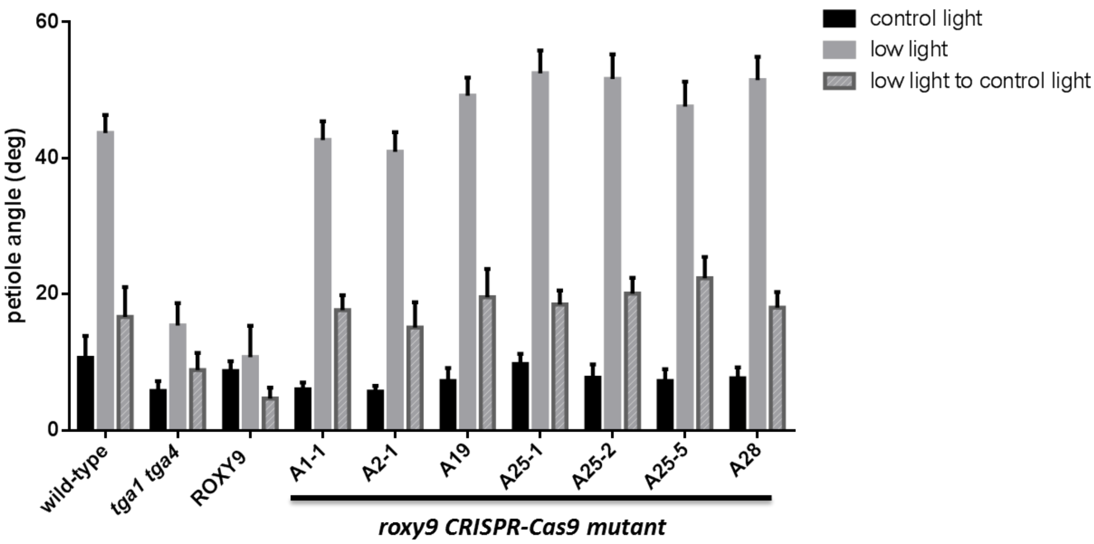

Figure 3.12 The *roxy9* CRISPR-Cas9 mutant is not impaired in hyponastic growth.
Effect of low light treatment (reduction in light intensity from 100-120 to 15-20 µmol m^{-2} s^{-1}) and subsequent transfer to control light) on the hyponastic growth of wild-type, *tga1 tga4*, *35S:HA-ROXY9* and *roxy9* CRISPR-Cas9 mutants. See Figure legend 3.2 and Figure 3.6A for details of plant growth, leaf angle measurements and light regime. Bars represent the average ± SEM of 5 to 6 plants of each genotype.

3.12 The expression of over 150 low-light-induced genes correlates with hyponastic growth in wild-type, *tga1 tga4* and *35S:HA-ROXY9* plants

To identify potential target genes of TGA1 and TGA4, transcriptome analysis was performed with RNA from petioles of wild-type *tga1 tga4* and *35S:HA-ROXY9* plants. Four-week-old plants were treated with low light (reduction in light intensity from 100-120 to 15-20 µmol m^{-2} s^{-1}) for six hours and total RNA was isolated from petioles of 15 plants of each genotype and treatment. The experiment was repeated four times with batches of independently grown plants. Samples were used for ATH1 Affymetrix 1.0 ST gene chip analysis.

In order to get a first impression of the global structure of the dataset, we performed a principal component analysis (PCA) which typically results in clusters of samples with a similar expression pattern (Figure 3.13). The samples from wild-type and *tga1 tga4* plants grown under control light and under low light showed a clear separation indicating that the transcriptomes of both genotypes are different and that they both respond to the low light treatment. In contrast, the clusters representing the *tga1 tga4* mutant and the *35S:HA-ROXY9* plants grown under low light overlapped. These results provide evidence that ROXY9 and TGA1 and TGA4 regulate a similar set of genes.

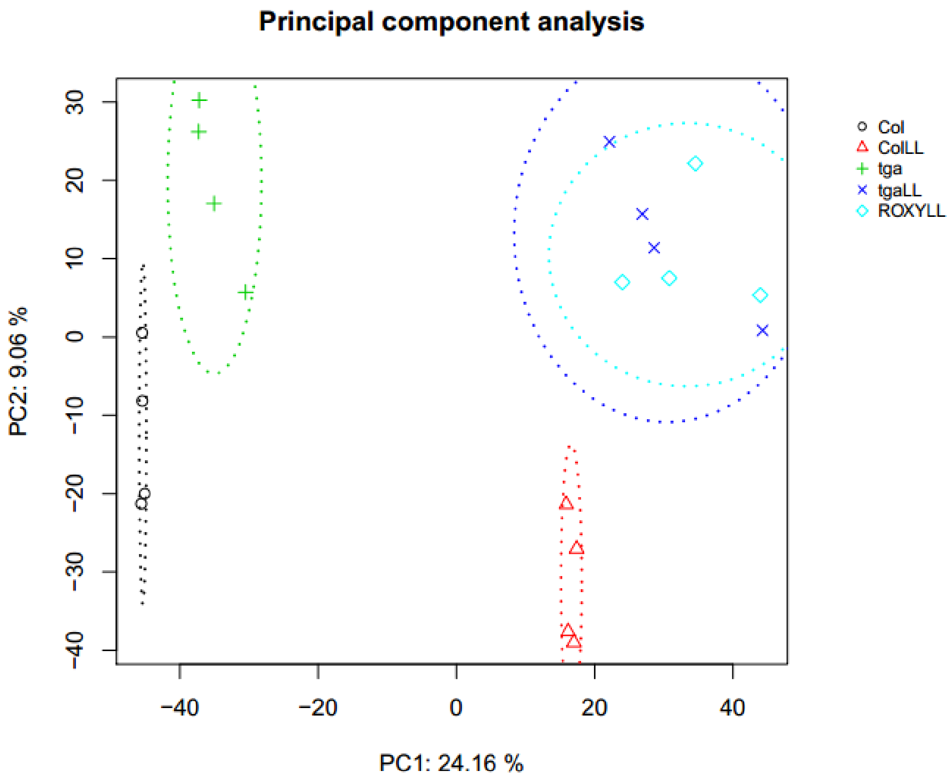

Figure 3.13 TGA1/TGA4 and ROXY9 regulate an overlapping set of genes.
Principal component analysis of the normalized transcriptome data obtained from hybridization of ATH1 Affymetrix 1.0 ST microarrays. Symbols: O, Δ, +, X and ◊, represent four biological replicates of Col-0 grown at 100-120 µmol m^{-2} s^{-1}, Col-0 grown for 6 h at 15-20 µmol m^{-2} s^{-1} (LL), *tga1 tga4* grown at 100-120 µmol m^{-2} s^{-1}, *tga1 tga4* transferred for 6 h to 15-20 µmol m^{-2} s^{-1} (LL) and *35S:HA-ROXY9* plants transferred for 6 h to 15-20 µmol m^{-2} s^{-1} (LL).

To visualize and cluster the relative transcript levels of all those genes that are differentially expressed in wild-type plants depending on the light conditions (fold change (logFC) <-1 or >1, p<0.05) and those that are differentially expressed in at least one the two other genotypes as compared to Col-0 (fold change (logFC) <-0.87 or >0.87, p<0.05), we applied the MarVis software (Kaever et al., 2009) (Figure 3.14). This program groups genes with similar relative expression levels into cluster and color-codes the relative expression levels in the five samples. We first focused on cluster 5, which contains 167 genes that are induced by low light in Col-0 but not in *tga1 tga4* and *35S:HA-ROXY9* plants.

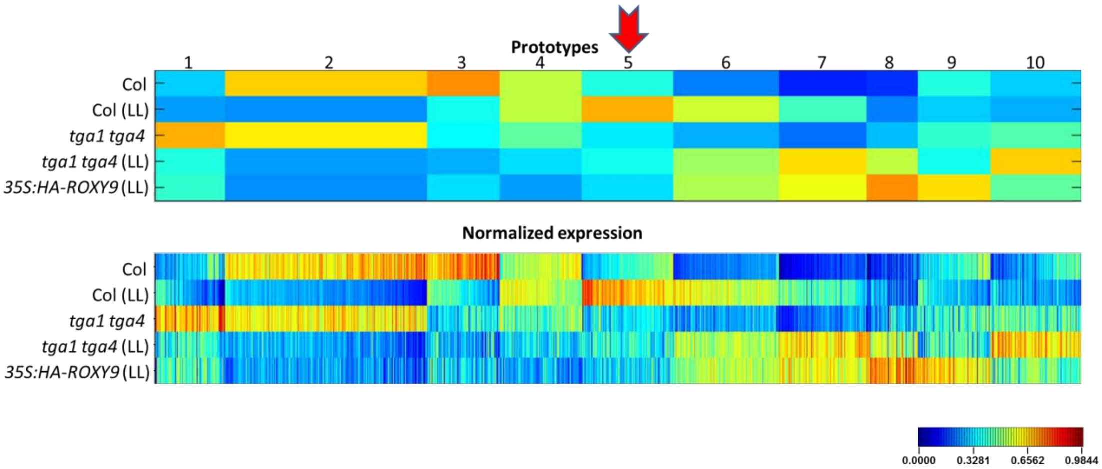

Figure 3.14 MarVis analysis leads to the identification of genes that correlate with hyponastic growth.

Clustering of 1716 genes differentially expressed in at least of the five samples. Genes were clustered into 10 prototypes according to their normalized expression pattern using the MarVis software (upper panel). The width of each prototype column is proportional to the number of genes assigned to this prototype. The lower panel shows the normalized expression profiles of the individual transcripts. The program color codes the relative expression of a given prototype (upper panel) or transcript (lower panel) in the different samples. Red depicts the highest relative expression, blue the lowest (see color scale). Col: Col-0 grown at 100-120 µmol m^{-2} s^{-1}, Col (LL): Col-0 transferred for 6 h to 15-20 µmol m^{-2} s^{-1}; *tga1 tga4*: *tga1 tga4* grown at 100-120 µmol m^{-2} s^{-1}; *tga1 tga4* (LL): *tga1 tga4* transferred for 6 h to 15-20 µmol m^{-2} s^{-1}; *35S:HA-ROXY9* (LL): *35S:HA-ROXY9* plants transferred for 6 h to 15-20 µmol m^{-2} s^{-1} for 6 h.

Gene Ontology (GO) over-representation analysis supported the notion that these genes are involved in hyponastic growth. Genes grouped into the GO terms “cell “growth” were enriched. Consistent with the notion that auxin stimulates cell expansion, genes belonging to the GO term “response to auxin” were enriched as well.

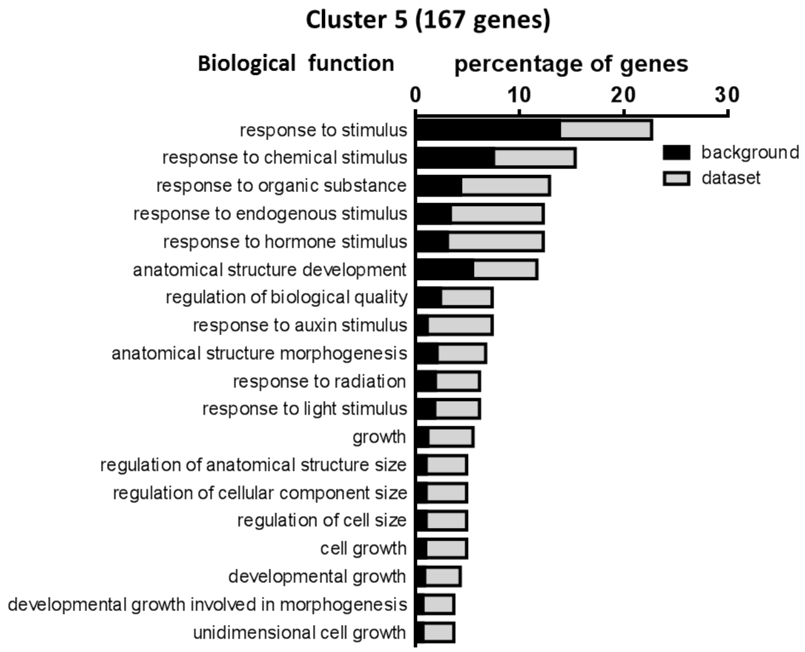

Figure 3.15 GO term analysis of genes whose expression correlates with the phenotype of wild-type, *tga1 tga4* and *35S:HA-ROXY9* plants.

167 genes which show low-light induced expression in wild-type but not in *tga1 tga4* and *35S:HA-ROXY9* plants (cluster 5) were subjected to Gene Ontology (GO) overrepresentation analysis. Black bars indicate the percentage of genes of each GO term found within the group of all annotated genes of the Arabidopsis genome. Gray bars indicate the percentage of genes of each GO term found within the group of genes that are induced by low light in Col-0 but not in *tga1 tga4* and *35S:HA-ROXY9* plants.

Next, we confirmed the expression data obtained from the four independent experiments analysed by microarray analysis. A fifth independent experiment was performed and the RNA was subjected to qRT-PCR analysis using primers detecting the transcripts of *XTH8* (xyloglucanendotransglucosylase/hydrolase 8, proposed to be related with promoting cell expansion) and *IAA19* (indole-3-acetic acid inducible 19, a primary auxin-responsive gene). The expression of both genes was induced nearly 2-fold in wild-type; in contrast, no induction was observed in the *tga1 tga4* background, which is consistent with the microarray results (Figure 3.16A). In addition, we examined whether the expression of TGA1/TGA4-regulated genes would be reduced after transfer of low light-treated plants to control conditions. As shown in Figure 3.16B, induction upon low light treatment was stronger than in the experiment shown in Figure 3.16A, which is due to the longer exposure to low light (10.5 h during the first period and 7.5 hours during the second photoperiod as opposed to 6 h). Under these conditions, *XTH8* and *IAA19* were also induced in the *tga1 tga4* mutant, although less efficiently than in wild-type plants. In both genotypes, gene expression was reverted to background levels after the transfer of plants to control light conditions. A similar pattern was observed for *XTH33*, expansin *EXPA11*, and the inodole-3-acidic acid-amido synthetase *GH3.6*.

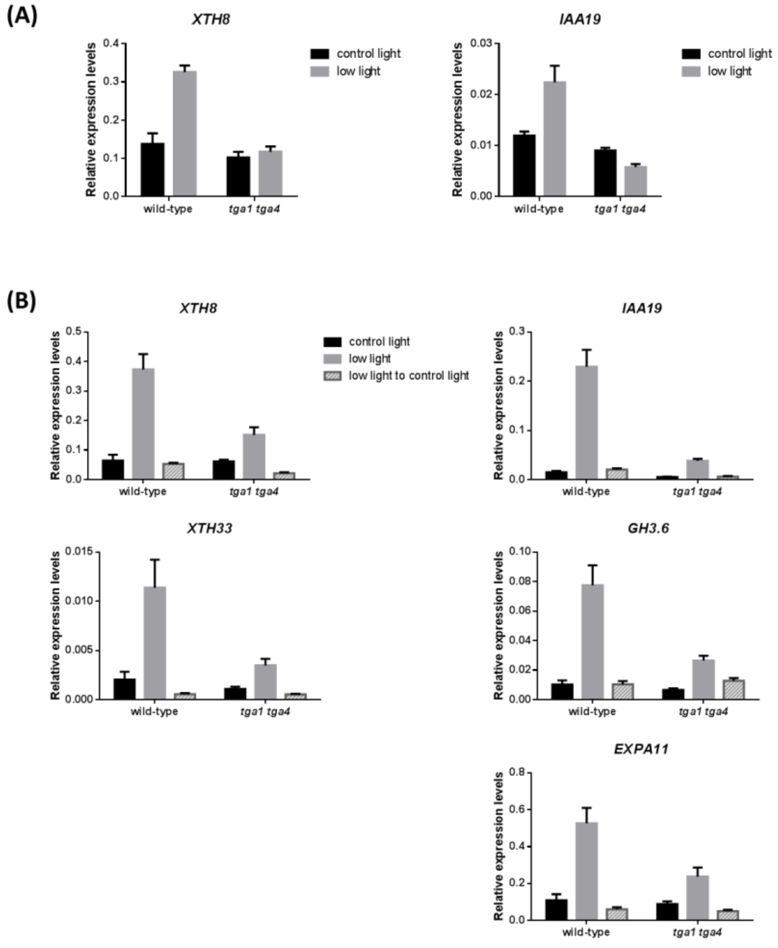

Figure 3.16 The expression of genes related to cell growth and response to auxin correlates with hyponastic growth.

(A) qRT-PCR analysis of *XTH8* and *IAA19* expression in wild-type and *tga1 tga4* after low light treatment. Four-week-old soil-grown wild-type and *tga1 tga4* were treated with low light for 6 hours (reduction in light intensity from 100-120 to 15-20 µmol m^{-2} s^{-1}). Transcript levels were normalized to the transcript level of *UBQ5*. Bars represent the average ± SEM of four biological replicates, each with dissected petioles from five independent plants.

(B) qRT-PCR analysis of light-induced genes in wild-type and *tga1 tga4* after transfer of plants from low light to control light conditions (see Figure 3.6A for the light regime). Transcript levels were normalized to the transcript level of *UBQ5*. Bars represent the average ± SEM of five biological replicates, each with dissected petioles from five independent plants.

3.13 Petioles of *tga1 tga4* and *35S:HA-ROXY9* plants are shorter than wild-type petioles

Since petioles show hyponastic growth in the dark, we assume that genes found in cluster 5 are induced during the dark period at the abaxial side of the petioles, whereas a different set of genes is induced under control light conditions on the adaxial side. This alternating growth habit would contribute to petiole length under a normal dark/light photoperiod. Since genes for hyponastic growth are less expressed in *tga1 tga4* and *35S:HA-ROXY9* plants we expected that their petioles should be shorter. Indeed, petiole length was reduced by 25% in the *tga1 tga4* mutant and by 50% in independent *35S:HA-ROXY9* plants (Figure 3.17).

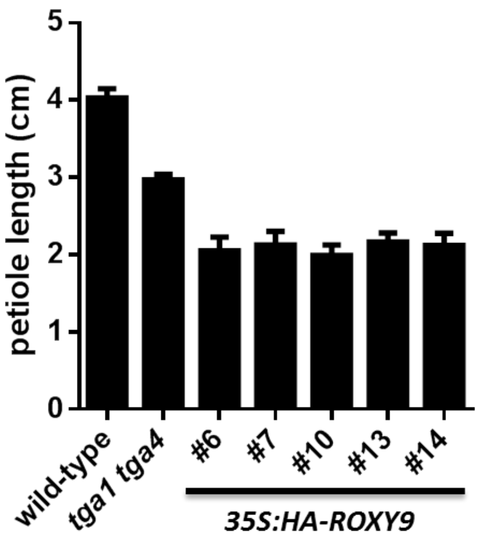

Figure 3.17 Petioles of *tga1 tga4* and *35S:HA-ROXY9* plants are shorter than wild-type petioles. Plants of the indicated genotypes were grown for four weeks under a 12/12 light/dark rhythm and the length of the petioles was measured using Image J analysis of photographs. Bars represent the average ± SEM of five biological replicates, each with a petiole of leaf number 7 to 8.

3.14 Genes with putative oxidoreductase activities are more highly expressed in *tga1 tga4* and *35S:HA-ROXY9* plants than in wild-type

Next, we focused on those genes that are differentially expressed in wild-type, *tga1 tga4* and *35S:HA-ROXY9* plants under low light, without taking into consideration whether they are regulated by light or not. Again, the relative transcript levels of all those genes that are differentially expressed in Col-0 plants depending on the light conditions (fold change (logFC) <-1 or >1, p<0.05) and those that are differentially expressed in at least one the two other genotypes as compared to Col-0 (fold change (logFC) <-0.87 or >0.87, p<0.05) were analysed with the MarVis software; but this time, only the expression data of the three low-light treated genotypes were considered (Figure 3.18).

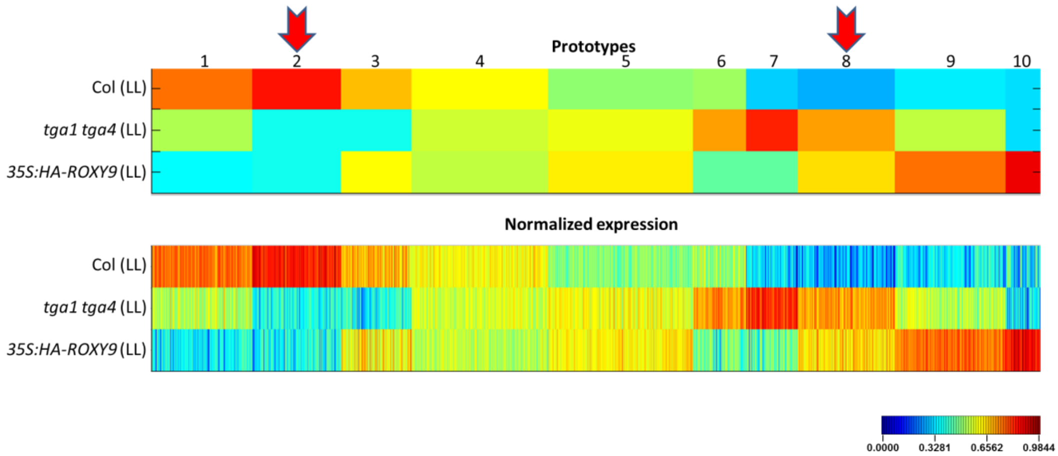

Figure 3.18 MarVis analysis leads to the identification of genes that correlate with hyponastic growth.
Clustering of 1716 genes differentially expressed in at least of the five samples analysed in Figure 3.18. Genes were clustered into 10 prototypes according to their normalized expression pattern using the MarVis software (upper panel). The width of each prototype column is proportional to the number of genes assigned to this prototype. The lower panel shows the normalized expression profiles of the individual transcripts. The program color codes the relative expression of a given prototype (upper panel) or transcript (lower panel) in the different samples. Red depicts the highest relative expression, blue the lowest (see color scale). The indicated genotypes were first grown at 100-120 µmol m^{-2} s^{-1} and subsequently transferred for 6 h to 15-20 µmol m^{-2} s^{-1}.

Cluster 2 contains genes that are less expressed in *tga1 tga4* and *35S:HA-ROXY9* plants and partially overlaps with cluster 5 discussed above (Figure 3.19B). GO term analysis (Figure 3.19A) revealed an over-representation of genes belonging to the GO term “response to auxin”.

Genes, which might represent repressors of hyponastic growth are represented in cluster 8, which partially overlaps with cluster 8 in the analysis shown in Figure 3.19B. Apparently, these genes are only slightly affected by light. Importantly, GO-term analysis revealed a strong enrichment of genes with oxidoreductase activities within the domain “molecular function” and of genes related to “response to jasmonic acid stimulus” and “cell redox homeostasis”.

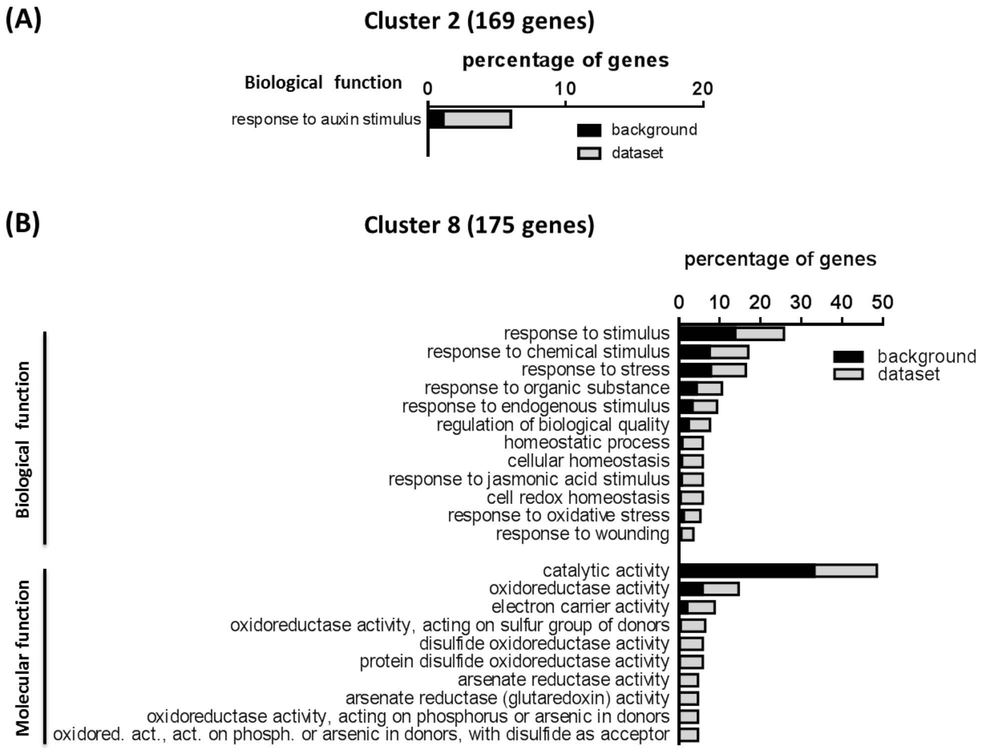

Figure 3.19 GO term analysis of genes whose expression correlates with the phenotype of wild-type, *tga1 tga4* and *35S:HA-ROXY9* plants.

(A) 169 genes which show higher expression in low light-treated wild-type than in low light-treated *tga1 tga4* and *35S:HA-ROXY9* plants were subjected to Gene Ontology (GO) overrepresentation analysis.

(B) 175 genes which show lower expression in low light-treated wild-type than in low light-treated *tga1 tga4* and *35S:HA-ROXY9* plants were subjected to Gene Ontology (GO) overrepresentation analysis.

Black bars indicate the percentage of genes of each GO term found within the group of all annotated genes of the Arabidopsis genome. Gray bars indicate the percentage of genes of each GO term found within the group of differentially regulated as indicated in (A) and (B).

Closer inspection of the list of genes that are higher expressed in *tga1 tga4* and *35S:HA-ROXY9* plants than in wild-type plants revealed that ROXY11 to ROXY15 represent the most-highly up-regulated genes (32-fold for ROXY13 to 6.4-fold for ROXY15 in *tga1 tga4*). These 5 genes are part of a gene cluster that seems to be co-regulated. In addition, *ROXY3, ROXY4, ROXY18, ROXY10* and *ROXY17* are constitutively higher expressed in in *tga1 tga4* and *35S:HA-ROXY9* plants than in wild-type plants. qRT-PCR analysis of RNA from independently grown *tga1 tga4* and *35S:HA-ROXY9* plants confirmed and extended this result (Figure 3.20).

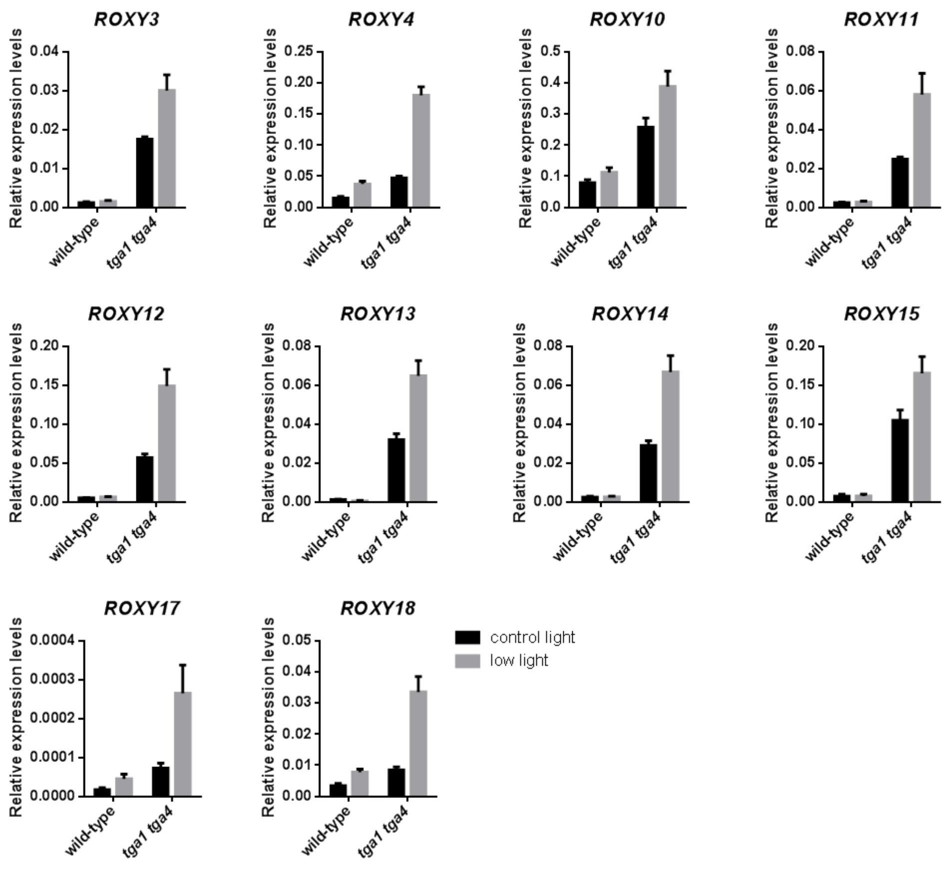

Figure 3.20 Expression of CC-type glutaredoxins in wild-type and *tga1 tga4*.
qRT-PCR analysis of CC-type glutaredoxins in wild-type and *tga1 tga4* after low light treatment. Four-week-old soil-grown wild-type and *tga1 tga4* were treated with low light for 6 hours (reduction in light intensity from 100-120 to 15-20 µmol m−2 s−1). Transcript levels were normalized to the transcript level of UBQ5. Bars represent the average ± SEM of four biological replicates, each with dissected petioles from five independent plants.

Transcription factor *SHYG* (SPEEDY HYPONASTIC GROWTH; ANAC047) is also highly expressed in *tga1 tga4* and *35S:HA-ROXY9* plants (Figure 3.21A). This result was unexpected, since overexpression of *SHYG* enhances the hyponastic response in response to waterlogging, whereas hyponastic petiole growth is clearly impaired in two *shyg* T-DNA insertion mutants *shyg-1* and *shyg-2* (Rauf et al., 2013). Although elevated expression of *SHYG* in the *tga1 tga4* mutant was not sufficient to promote hyponastic growth, we tested, whether SHYG plays a role in low light-induced hyponastic growth. However, the response was unaffected as indicated by the wild-type-like petiole angles in *35S:SHYG* and in *shyg-1* and *shyg-2* mutant plants (Figure 3.21B). It is concluded that SHYG cannot influence hyponastic growth under our experimental conditions.

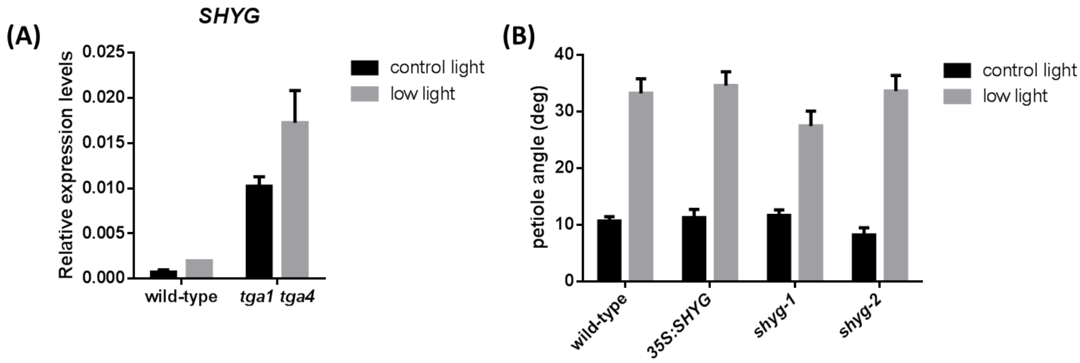

Figure 3.21 *SHYG* are not important for the regulation of hyponastic growth.

(A) qRT-PCR analysis of *SHYG* expression in wild-type and *tga1 tga4* after low light treatment. Four-week-old soil-grown wild-type and *tga1 tga4* were treated with low light for 6 hours (reduction in light intensity from 100-120 to 15-20 µmol m^{-2} s^{-1}). Transcript levels were normalized to the transcript level of *UBQ5*. Bars represent the average ± SEM of four biological replicates, each with dissected petioles from five independent plants.

(B) Effect of low light treatment (reduction in light intensity from 100-120 to 15-20 µmol m^{-2} s^{-1}) on the hyponastic growth of wild-type and *tga1 tga4*. See Figure legend 3.2 for details of plant growth and leaf angle measurements. Bars represent the average ± SEM 9 plants of each transgenic line.

3.15 Motif mapper analysis suggests that TGA1 and TGA4 are negative regulators of gene expression

To identify transcription factor binding motifs in the promoters of the different gene clusters as defined in Figure 3.14 and 3.18, we scanned 1-kb sequences upstream of the predicted transcriptional start sites using the Motif Mapper *cis* element analysis tool (Berendzen et al., 2012) (Table 3.1). The program compares the average number of specific binding sites in a given group of genes that was randomly chosen (1000 times) from the whole genome and compares this number with the actual number of binding sites within a specific group of genes. The binding site of TGA transcription factors (TGACGT) was 1.6-fold more frequent in the group of 175 genes that are higher expressed in *tga1 tga4* and *35S:HA-ROXY9* plants than in 167 randomly chosen genes from the genome. The motif TGACGTGG was even more enriched (2.1 fold). If these genes would be the direct target genes of TGA1 and TGA4, TGA1 and TGA4 would be repressors of gene expression. Target genes would repress genes involved in hyponastic growth. Promoters that control the group of 167 genes that positively correlates with hyponastic growth (cluster 5 in Figure 3.16) contain a light regulatory motif, which is plausible because these genes are induced by low light. In addition, the CACATG motif, which is recognized by bHLH transcription factor MYC2 and potentially other bHLH transcription factors as well, is enriched by a factor of 1.64. Moreover, a RY motif, which is recognized by B3 transcription factors is enriched by a factor of 1.76. These motifs might be recognized by the repressive transcription factors that are up-regulated in *tga1 tga4* and *35S:HA-ROXY9* plants.

Table 3.1 Promoter elements enriched in co-regulated genes

Cluster 5 (167 genes)

Motifs	167 genes in cluster 5 Total Motifs	Average selection Total Motifs	p-value	Ratio: total motifs
CACATG/CATGTG	135	82.585	0	1.635
CATGCATG (RY motif)	10	5.68	0.0401	1.761
CATGCA/TGCATG (RY motif, B3)	95	76.713	0.0336	1.238
ACGTGGC/GCCACGT (ABRE)	0	2.748	-0.0475	0.000
TGTATATAT/ATATATACA (light regulatory motif)	30	18.533	0.004	1.619

Cluster 2 (169 genes)

Motifs	169 genes in cluster 2 Total Motifs	Average selection Total Motifs	p-value	Ratio: total motifs
CACATG/CATGTG	138	83.95	0	1.644
CACGTA/TACGTG (G-Box, bZIP)	51	38.656	0.0329	1.319
CATGCA/TGCATG (RY motif, B3)	105	77.681	0.004	1.352
TGTATATAT/ATATATACA (light regulatory motif)	36	18.703	0.0001	1.925

Cluster 8 (175 genes)

Motif	175 genes in cluster 8 Total Motifs	Average selection Total Motifs	p-value	Ratio: total motifs
TGACGT/ACGTCA	76	47.345	0.0001	1.605
TGACG/CGTCA	203	151.601	0	1.339
TGACGTGG/CCACGTCA	12	5.591	0.0078	2.146
CACGTG	54	32.281	0.0003	1.673
CACATG/CATGTG	111	87.031	0.0113	1.275
CACGTA/TACGTG (G-Box, bZIP)	66	40.202	0.0001	1.642
CATGCATG (RY motif)	19	5.887	0	3.227
CATGCA/TGCATG (RY motif, B3)	127	80.136	0	1.585
CATGCAT/ATGCATG (RY motif)	69	34.147	0	2.021
CATGCAY/RTGCATG (RY motif)	82	45.479	0	1.803
TAACGTA/TACGTTA (GA response)	25	16.361	0.0222	1.528
TTACGT/ACGTAA (NAC)	97	69.111	0.0022	1.404
TTACGTG/CACGTAA (NAC)	23	13.692	0.0082	1.680
ACGTGGC/GCCACGT (ABRE)	25	14.816	0.0062	1.687
YACGTGGC/GCCACGTR (ABRE)	17	9.028	0.006	1.883
NGATAAGNMNN/NNKNCTTATCN (GATA)	91	46.509	0	1.957

The table depicts promoter elements enriched in the clusters resulting from MarVis analysis in Figure 3.15 (custer 5, induced by low light in wild-type but not in *tga1 tga4* and *35S:HA-ROXY9*) and Figure 3.19 (clusters 2 (higher expressed in low light-treated wild-type than in low light-treated *tga1 tga4* and *35S:HA-ROXY9*) and 8 (higher expressed in low light-treated *tga1 tga4* and *35S:HA-ROXY9* than in low light-treated wild-type). Numbers represent the total amount of motifs within the set of promoters of one cluster and within randomly chosen sets of promoters from the whole genome. The occurrence of enriched motifs was determined in the 1-kb sequences upstream of the 5' -untranslated regions using Motif Mapper (Berendzen et al., 2012).

4 Discussion

The bZIP protein TGA1a from tobacco was the first plant transcription factor to be identified by exploiting its binding activity to the *activation sequence-1* of the *Cauliflower Mosaic Virus 35S* promoter (Katagiri et al. 1989; Lam et al. 1989). Later, it was discovered that its orthologues TGA1 and TGA4 are important for defense responses against biotrophic pathogens in *Arabidopsis thaliana* (Kersawani et al., 2007, Shearer et al., 2012). Two redox-active cysteines in the coding regions of TGA1 and TGA4 might be important to control the activity of the protein by the plant defense hormone salicylic acid (SA) (Despres et al., 2003). Moreover, TGA1 and TGA4 interact with ROXY-type glutaredoxins, which might catalyze the redox modification (Dr. Martin Muthreich PhD thesis). Here, we report that TGA1 and TGA4 are not only involved in defense responses, but also in the growth response hyponasty. Moreover, we suggest that TGA1 and TGA4 activity is regulated by ROXY9 and the potentially redundant ROXYs ROXY8 and ROXY21.

4.1 TGA1 and TGA4 are connected to various signaling cascades that induce hyponastic growth

TGA1 and TGA4 are required for hyponastic growth, irrespective of whether the response is triggered by ethylene (ET), low light or heat (Figure 3.1). Under our conditions, ET is involved in low light-induced hyponastic growth, as revealed by the compromised response of the *ein2* mutant (Figure 3.2). However, the *ein2* mutants is not as stringently affected as the *tga1 tga4* mutant suggesting that other signals than ET require TGA1 and TGA4 to elicit the response. This is supported by the finding that heat-induced hyponastic growth, which is even inhibited by ET, is also diminished in the *tga1 tga4* mutant (Figure 3.1). Thus, TGA1 and TGA4 seem to be essential components of hyponastic growth that operate at a potential point of convergence of various signaling cascades.

At least three different ways on the principal function of TGA1 and TGA4 in the regulation of hyponastic growth can be envisioned. First, TGA1 and TGA4 might be unregulated amplifiers of the response. For instance, they might be expressed only at the abaxial side, where they would assist to promote induced cell expansion which would explain the asymmetry of the response.

Second, TGA1 and TGA4 might be unregulated amplifiers in terms of eliciting the hyponastic growth as outlined above, but might additionally serve as points of integration of negative signals. Such a role is postulated for TGA2/5/6 in activation of ET-mediated defense responses (Zander et al., 2014). Here, ET-mediated stabilization of ETHYLENE INSENSITIVE 3 (EIN3) is the ET-controlled process, whereas TGA2/5/6 amplify the activating effect of EIN3 to drive expression of the master regulator of the response, ORA59. The positive contribution of TGA2/5/6 on the activity of the *ORA59* promoter is counteracted by SA, possibly through ROXY19 and other redundant ROXYs. We found that the negative effect of SA on hyponastic growth is mediated by TGA2/5/6 and NPR1 (Figure 3.5). Consistent with the notion that ROXY19 interferes with the activity of TGA2/5/6, petioles of SA-treated *35S:ROXY19* plants can grow upwards under low light conditions (Figure 3.9C). This observation does not exclude that TGA1 and TGA4 are also involved in this response. However, our complementation lines which express TGA1(C260N/C266S) indicate that the redox-active cysteines are not important for the hypothetical contribution of TGA1 in mediating the inhibitory effect of SA (Figure 3.4B).

Third, TGA1 and TGA4 may be regulated at the protein level by a mechanism that is common to the diverse signaling pathways that induce hyponastic growth (Figure 4.1). We identified ROXY8, ROXY9 and ROXY20 as potential negative regulators of TGA1 and TGA4 activity as revealed by the observation that plants ectopically expressing these proteins are compromised in hyponastic growth (Figure 3.9). Moreover, microarray analyses pointed at a common set of genes that is differentially regulated in *tga1 tga4* and *35S:HA-ROXY9* plants as compared to wild-type indicating that ROXY9 and TGA1 /4 regulate the same process (Figure 3.13). Especially the expression pattern of *ROXY9* was consistent with the postulated negative role: expression was reduced upon transfer to low light potentially leading to the release of TGA1/4 activity so that hyponastic growth is promoted (Figure 3.6B; Figure 3.8). Moreover, *ROXY9* was hyper-induced after re-transfer to control light which would lead to the repression of the activity of TGA1/4 allowing reversal of the leaf angle to control conditions (Figure 3.6B; Figure 3.8). However, the *roxy9* mutant was indistinguishable from wild-type plants suggesting that other ROXYs might act in a redundant manner (Figure 3.12). Expression of the potentially redundant *ROXY8* was hyper-induced by re-transfer to control light, and *ROXY20* expression was reduced by low light (Figure 3.8). Expression of all three ROXYs depends on TGA1 and TGA4 which suggests an autoregulatory feed-back loop. A similar loop has been observed before for ROXY19, which represses the activity of TGA2, TGA5 and TGA6 at its own promoter (Ndamukong et al., 2007; Huang et al., 2016). Collectively, these data suggest that environmental cues regulating the activity of TGA1/4-inhibiting ROXYs are molecular components that regulate hyponastic growth in response to a variety of stimuli.

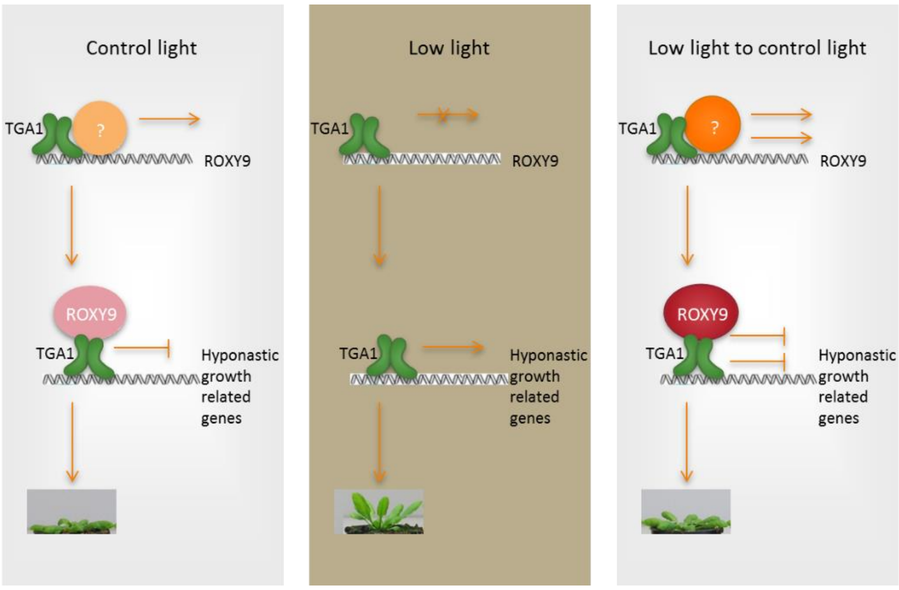

Figure 4.1 Proposed working model.

(A) Under control condition, basal levels of ROXY9 expression are controlled by TGA1/4 and yet unknown transcription factors that can respond to light conditions. ROXY9 interacts with TGA1/4 to reduce the expression of leaf movement-related genes to inhibit hyponastic growth. (B) In response to low light, the expression of ROXY9 is reduced allowing TGA1/4 to stimulate genes involved in cell elongation at the abaxial side of the petiole. (C) When plants are transferred to control light condition after low light pretreatment, ROXY9 expression is strongly re-induced, enabling ROXY9 proteins to accumulate and to repress gene expression by interacting with TGA1/4.

4.2 The CC-motif is important for the repressive activity of ROXY9

Repressive effects of ROXYs on the activity of TGA factors have been described before. Genetic analysis has shown that ROXY1 represses the activity of TGA factor PAN to regulate the initiation of floral primordia (Li et al., 2009). Likewise, ROXY19 represses TGA2/5/6-regulated target promoters (Ndamukong et al., 2007). ROXY1 and ROXY19 contain a C-terminal ALWL motif, which serves to recruit the transcriptional co-repressor TOPLESS to TGA2/5/6-regulated promoters (Uhrig et al., 2017). The ALWL motif is present in 16 of the 21 ROXYs, but not in ROXYs 6, 7, 8, 9 and 21. Interestingly, ROXY19 complements the *roxy1* mutant, but does not repress the hyponastic growth (Li et al., 2009). ROXY9 does not complement the *roxy1* mutant (Li et al., 2009) and does not repress TGA2/5/6-regulated *ORA59* (Zander et al., 2012; Zander et al., 2014). Therefore, the repressive mechanisms of ROXY19 and ROXY9 are most likely different.

The importance of the CCMC motif for ROXY function has been addressed before. As inferred from studies from canonical GRXs, the active site either contributes to oxidoreductase activity or to the binding of [Fe-S] clusters (Fernandes and Holmgren et al., 2004; Bandyopadhyay et al., 2008; Couturier et al., 2011). *In vitro* studies of a poplar CC-type GRX7.2 have revealed poor oxidoreductase activities on artificial substrates and the potential to bind [Fe-S] clusters (Couturier et al., 2010). In vivo studies with ROXY1 have led to conflicting data sets. When expressed under the *CaMV 35S* promoter, a mutated ROXY1 encoding a SCMC motif did not complement the *roxy1* phenotype (Xing et al., 2005). In contrast, when expressed under the endogenous *ROXY1* promoter, the protein was functional. Even mutating the active site into SSMS did not abolish its function (Ziemann et al., 2010; PhD thesis under the supervision of Sabine Zachgo). Plants ectopically expressing ROXY19(CPYC), in which the CCMC motif had been exchanged against the CPYC motif found in class I GRXs, showed the same phenotype as the *35S:ROXY19* control plants (Huang et al., 2016). In contrast, a ROXY19(SSMS) was not functional. This indicates that either oxidoreductase or [Fe-S] cluster binding might be important for ROXY19 function, but the relevance of the second cysteine has remained obscure. In this study, the cysteine residues of the CCLC motif of ROXY9 were individually changed into serines. If the first cysteine was mutated, the protein lost its repressive activity (Figure 3.11). In canonical GRXs, the first cysteine of the CxxC/S active site is important for the nucleophilic attack of an oxidized sulfur of a (glutathionylated) target protein (Fernandes and Holmgren, 2004). Up to now, it is not known whether ROXY9 has oxidoreductase activity. Moreover, it cannot be excluded, that TGA1 and TGA4 are redox-modulated by ROXY9 at C172 or C287. Interestingly, the second cysteine was also important for function (Figure 3.11). Given that the CC motif in the active site is so conserved, the elucidation of the molecular mechanism of ROXY9 function is extremely important.

4.3 Low light-induced expression of genes potentially involved in hyponastic growth are less expressed in *tga1 tga4* and *35S:HA-ROXY9* plants

Hyponastic growth is explained by differential expansion rates of cells at the abaxial side of the petiole. Since application of the auxin transport inhibitor TIBA did not strongly interfere with low light-induced hyponastic growth within the first six hours, it has remained unclear what growth-regulating factors create the asymmetry when the response is initiated (Millenaar et al., 2009). Our microarray analysis of RNA of petioles harvested at six after transfer to low light conditions revealed an enrichment of auxin-regulated genes in the cluster of genes that are up-regulated by low light in wild-type but not in the *tga1 tga4* and *35S:ROXY19* mutant plants (cluster 5, Figure 3.14). Since primary auxin-responsive genes were up-regulated (e.g. *IAA2*, *IAA3*, *IAA7*, *IAA19*, *IAA29*; 3 SAUR-like auxin-responsive protein family proteins) and since only two of these contain a TGACGT motif in the -1000 upstream region, it is unlikely that these genes are direct target genes of TGA1 and TGA4. Thus, TGA1 and TGA4 may be involved in earlier processes leading to increased auxin signaling. This

TGA1/TGA4-dependent process could be at any step starting from the perception of the environmental signal to the perception of the auxin in the relevant cells. Alternatively, TGA1/TGA4 might be involved in the differential sensitivity of the adaxial side and the abaxial side to the petiole for environmental cues. Therefore, the cellular expression pattern of TGA1 and TGA4 within the leaf has to be investigated. Furthermore, genes involved in cell wall loosening (e.g. *XYLOGLYGAN:XYLOGLUCOSY TRANSFERASE 33*, *XYLOGLUCAN ENDOTRANSGLUCOSYLASE/HYDROLYSES 8* and *15*, *EXPANSINS 8* and *11*) were enriched in cluster 5 (Figure 3.15). It might well be that these genes are induced by auxin. Upon reversal to control light conditions, expression of at least a selected number of these genes is reduced again (Figure 3.16B). These genes are not induced in the adaxial side upon reversal of hyponastic growth and other genes that are expressed on the upper side have to be activated to allow re-orientation of the petioles.

As stated above, we do not have a clue, which of the genes that are essential for hyponastic growth are directly regulated by TGA1 and TGA4. Motif mapper analysis indicated that TGACGT motifs are enriched in the promoters of genes that are higher expressed in *tga1 tga4* and *35S:HA-ROXY9* plants (Table 3.1). This finding points at a potential negative effect of TGA1 and TGA4 on genes that are involved in repressing hyponastic growth. However, the high expression of the positive regulator of hyponastic growth, *SHYG*, in *tga1 tga4* and *35S:ROXY19* plants is counterintuitive (Figure 3.21A). Since waterlooging-induced hyponastic growth was not reproduced in our lab, we could not test the response of the *tga1 tga4* mutant under these conditions.

Conspicuously, ten *ROXY* genes are constitutively up-regulated in the *tga1 tga4* mutant and *35S:ROXY19* plants. This effect is further enhanced by low light and exceeds by far the levels found in wild-type plants (Figure 3.7; Figure 3.20). Up to now, it cannot be excluded that the unusually high expression of these proteins in *tga1 tga4* and *35S:HA-ROXY9* plants influences yet unknown processes that lead to the inhibition of the hyponastic response.

5 Conclusion

Although we do not yet know the direct target genes of TGA1 and TGA4, the phenotype of the *tga1 tga4* mutant indicates that they are required for hyponastic growth. Moreover, we identified TGA1-interacting ROXY9 as a potential inhibitor of TGA1 and TGA4 activity. Based on the expression pattern of *ROXY9* and the potentially redundant ROXYs *ROXY8* and *ROXY20*, the corresponding promoters could be targets of the various environmental signals that initiate and terminate hyponastic growth.

6 Summary

In the rosette plant *Arabidopsis thaliana*, different environmental cues trigger upward (hyponastic) leaf movement which is evolutionary beneficial when it comes to avoid shading by neighboring plants. Hyponasty results from longitudinal cell expansion at the lower side of the leaf petiole. Here, we report that clade I TGA transcription factors TGA1 and TGA4 are required for hyponastic growth irrespective of whether it is induced by low light intensities, ethylene or heat. Expression of genes encoding cell wall-loosening or auxin-induced proteins was diminished in petioles of the *tga1 tga4* double mutant subjected to low light for six hours. Cysteines C260 and C266 of TGA1, which have been reported to be redox-modulated by the defense hormone salicylic acid (SA) in vivo, do not play a role for the function of TGA1 in hyponastic growth. Likewise, they are not important for the inhibition of hyponastic growth by SA. We identified several TGA1/4-interacting glutaredoxins (ROXY8, ROXY9, ROXY20) as potential negative regulators of TGA1/4 activity. Ectopic expression of ROXY8 and ROXY9 led to plants that show the same hyponasty-deficient phenotype as the *tga1 tga4* mutant. Expression of *ROXY9* was particularly high when hyponastic plants were transferred back to control light conditions. We therefore favour the hypothesis that the above mentioned ROXYs interfere with TGA1/4 activity in order to mediate the downward orientation of hyponastic leaves after transfer to control conditions. The repressive activity of ROXY9 depends on the integrity of the active site motif CCLC, which might be involved in oxidoreductase activity, binding of iron sulfur complexes or other yet unknown functions.

7 References

Alonso, J.M., Hirayama, T., Roman, G., Nourizadeh, S., and Ecker, J.R. (1999). EIN2, a bifunctional transducer of ethylene and stress responses in *Arabidopsis*. Science **284**: 2148–2152.

Ballaré, C.L. (2009). Illuminated behaviour: phytochrome as a key regulator of light foraging and plant anti-herbivore defence. Plant Cell Environ. **32**: 713–725.

Bandyopadhyay, S., Gama, F., Molina-Navarro, M.M., Gualberto, J.M., Claxton, R., Naik, S.G., Huynh, B.H., Herrero, E., Jacquot, J.P., Johnson, M.K., and Rouhier, N. (2008). Chloroplast monothiol glutaredoxins as scaffold proteins for the assembly and delivery of [2Fe–2S] clusters. EMBO J. **27**: 1122–1133.

Benschop, J.J., Millenaar, F.F., Smeets, M.E., Zanten, M. van, Voesenek, L.A.C.J., and Peeters, A.J.M. (2007). Abscisic acid antagonizes ethylene-induced hyponastic growth in *Arabidopsis*. Plant Physiol. **143**: 1013–1023.

Berendzen, K.W., Weiste, C., Wanke, D., Kilian, J., Harter, K., and Dröge-Laser, W. (2012). Bioinformatic cis-element analyses performed in Arabidopsis and rice disclose bZIP- and MYB-related binding sites as potential AuxRE-coupling elements in auxin-mediated transcription. BMC Plant Biol. **12**: 125.

Cao, H., Glazebrook, J., Clarke, J.D., Volko, S., and Dong, X. (1997). The Arabidopsis NPR1 gene that controls systemic acquired resistance encodes a novel protein containing ankyrin repeats. Cell **88**: 57–63.

Catalá, C., Rose, J.K.C., and Bennett, A.B. (2000). Auxin-regulated genes encoding cell wall-modifying proteins are expressed during early tomato fruit growth. Plant Physiol. **122**: 527–534.

Couturier, J. et al. (2011). Arabidopsis chloroplastic glutaredoxin C5 as a model to explore molecular determinants for iron-sulfur cluster binding into glutaredoxins. J.

Biol. Chem. **286**: 27515–27527.

Couturier, J., Didierjean, C., Jacquot, J.-P., and Rouhier, N. (2010). Engineered mutated glutaredoxins mimicking peculiar plant class III glutaredoxins bind iron–sulfur centers and possess reductase activity. Biochem. Biophys. Res. Commun. **403**: 435–441.

Cox, M.C.H., Benschop, J.J., Vreeburg, R.A.M., Wagemaker, C.A.M., Moritz, T., Peeters, A.J.M., and Voesenek, L.A.C.J. (2004). The roles of ethylene, auxin, abscisic acid, and gibberellin in the hyponastic growth of submerged Rumex palustris petioles. Plant Physiol. **136**: 2948–2960.

Cox, M.C.H., Millenaar, F.F., van Berkel, Y.E.M. de J., Peeters, A.J.M., and Voesenek, L.A.C.J. (2003). Plant movement. submergence-induced petiole elongation in Rumex palustris depends on hyponastic growth. Plant Physiol. **132**: 282–291.

Després, C., Chubak, C., Rochon, A., Clark, R., Bethune, T., Desveaux, D., and Fobert, P.R. (2003). The Arabidopsis NPR1 disease resistance protein is a novel cofactor that confers redox regulation of dna binding activity to the basic domain/leucine zipper transcription factor TGA1. Plant Cell **15**: 2181–2191.

Ecker, J.R. (1995). The ethylene signal transduction pathway in plants. Science **268**: 667–675.

Fernandes, A.P. and Holmgren, A. (2004). Glutaredoxins: glutathione-dependent redox enzymes with functions far beyond a simple thioredoxin backup system. Antioxid. Redox Signal. **6**: 63–74.

Fode, B., Siemsen, T., Thurow, C., Weigel, R., and Gatz, C. (2008). The Arabidopsis GRAS protein SCL14 interacts with class II TGA Transcription factors and is essential for the activation of stress-inducible promoters. Plant Cell **20**: 3122–3135.

Franklin, K.A. (2008). Shade avoidance. New Phytol. **179**: 930–944.

Friedman, H., Vos, J.W., Hepler, P.K., Meir, S., Halevy, A.H., and Philosoph-Hadas, S. (2003). The role of actin filaments in the gravitropic response of snapdragon flowering shoots. Planta **216**: 1034–1042.

Friml, J. and Palme, K. (2002). Polar auxin transport--old questions and new concepts? Plant Mol. Biol. **49**: 273–284.

Glaser, T., Hedman, B., Hodgson, K.O., and Solomon, E.I. (2000). Ligand K-edge X-ray absorption spectroscopy: A direct probe of ligand-metal covalency. Acc. Chem. Res. **33**.

Gutsche, N., Thurow, C., Zachgo, S., and Gatz, C. (2015). Plant-specific CC-type glutaredoxins: functions in developmental processes and stress responses. Biol. Chem. **396**: 495–509.

Huang, L.-J., Li, N., Thurow, C., Wirtz, M., Hell, R., and Gatz, C. (2016). Ectopically expressed glutaredoxin ROXY19 negatively regulates the detoxification pathway in *Arabidopsis thaliana*. BMC Plant Biol. **16**: 200.

Jakoby, M., Weisshaar, B., Dröge-Laser, W., Vicente-Carbajosa, J., Tiedemann, J., Kroj, T., Parcy, F., and bZIP Research Group (2002). bZIP transcription factors in *Arabidopsis*. Trends Plant Sci. **7**: 106–111.

Johnson, D.C., Dean, D.R., Smith, A.D., and Johnson, M.K. (2005). Structure, function, and formation of biological iron-sulfur clusters. Annu. Rev. Biochem. **74**: 247–281.

Kaever, A., Landesfeind, M., Feussner, K., Morgenstern, B., Feussner, I., and Meinicke, P. (2014). Meta-analysis of pathway enrichment: combining independent and dependent omics data sets. PloS One **9**: e89297.

Kaever, A., Landesfeind, M., Possienke, M., Feussner, K., Feussner, I., and Meinicke, P. (2012). MarVis-Filter: ranking, filtering, adduct and isotope correction of mass spectrometry data. J. Biomed. Biotechnol. **2012**: 263910.

Kaever, A., Lingner, T., Feussner, K., Göbel, C., Feussner, I., and Meinicke, P. (2009). MarVis: a tool for clustering and visualization of metabolic biomarkers. BMC Bioinformatics **10**: 92.

Kang BG (1979). Epinasty. *In* W Haupt, ME Feinleib, eds, Encyclopedia of plant physiology, New Series, Vol 7, Physiology of movements. Springer-Verlag, Berlin, pp 647–667

Katagiri F, Lam E and Chua NH. (1989). Two tobacco DNA-binding proteins with homology to the nuclear factor CREB. Nature **340**: 727-730.

Katagiri, F., Seipel, K., and Chua, N.H. (1992). Identification of a novel dimer stabilization region in a plant bZIP transcription activator. Mol. Cell. Biol. **12**: 4809–4816.

Kaufman PB, Wu LL, Brock TG, Kim D. (1995) Hormones and the orientation of growth. In PJ Davies, ed, Plant Hormones. Kluwer Academic, Dordrecht, The Netherlands, pp 547-571.

Kesarwani, M., Yoo, J., and Dong, X. (2007). genetic interactions of TGA transcription factors in the regulation of pathogenesis-related genes and disease resistance in *Arabidopsis.* Plant Physiol. **144**: 336–346.

Keuskamp, D.H., Sasidharan, R., and Pierik, R. (2010). Physiological regulation and functional significance of shade avoidance responses to neighbors. Plant Signal. Behav. **5**: 655–662.

Koini, M.A., Alvey, L., Allen, T., Tilley, C.A., Harberd, N.P., Whitelam, G.C., and Franklin, K.A. (2009). High temperature-mediated adaptations in plant architecture require the bHLH transcription factor PIF4. Curr. Biol. CB **19**: 408–413.

Koncz, C. and Schell, J. (1986). The promoter of TL-DNA gene 5 controls the tissue-specific expression of chimaeric genes carried by a novel type of Agrobacterium binary vector. Mol. Gen. Genet. MGG **204**: 383–396.

La Camera, S., L'Haridon, F., Astier, J., Zander, M., Abou-Mansour, E., Page, G., Thurow, C., Wendehenne, D., Gatz, C., Métraux, J.-P., and Lamotte, O. (2011). The glutaredoxin ATGRXS13 is required to facilitate Botrytis cinerea infection of *Arabidopsis thaliana* plants. Plant J. **68**: 507–519.

Lai, Z., Schluttenhofer, C.M., Bhide, K., Shreve, J., Thimmapuram, J., Lee, S.Y., Yun, D.-J., and Mengiste, T. (2014). MED18 interaction with distinct transcription factors regulates multiple plant functions. Nat. Commun. **5**: 3064.

Lam E, Benfey PN, Gilmartin PM, Fang R and Chua NH. (1989). Site-specific mutations alter in vitro factor binding and change promoter expression pattern in transgenic plants. Proc. Natl. Acad. Sci. **86**: 7890-7894.

Lam, E. and Lam, Y.K. (1995). Binding site requirements and differential representation of TGF factors in nuclear ASF-1 activity. Nucleic Acids Res. **23**: 3778–3785.

Lariguet, P., Schepens, I., Hodgson, D., Pedmale, U.V., Trevisan, M., Kami, C., de Carbonnel, M., Alonso, J.M., Ecker, J.R., Liscum, E., and Fankhauser, C. (2006). PHYTOCHROME KINASE SUBSTRATE 1 is a phototropin 1 binding protein required for phototropism. Proc. Natl. Acad. Sci. U. S. A. **103**: 10134–10139.

Lee, S.C., Mustroph, A., Sasidharan, R., Vashisht, D., Pedersen, O., Oosumi, T., Voesenek, L.A.C.J., and Bailey-Serres, J. (2011). Molecular characterization of the submergence response of the *Arabidopsis thaliana* ecotype Columbia. New Phytol. **190**: 457–471.

Lemaire, S.D. (2004). The glutaredoxin family in oxygenic photosynthetic organisms. Photosynth. Res. **79**: 305–318.

Li, S., Lauri, A., Ziemann, M., Busch, A., Bhave, M., and Zachgo, S. (2009). Nuclear activity of ROXY1, a glutaredoxin interacting with TGA factors, is required for petal development in *Arabidopsis thaliana*. Plant Cell **21**: 429–441.

Lillig, C.H., Berndt, C., and Holmgren, A. (2008). Glutaredoxin systems. Biochim. Biophys. Acta **1780**: 1304–1317.

Lindermayr, C., Sell, S., Müller, B., Leister, D., and Durner, J. (2010). Redox regulation of the NPR1-TGA1 system of *Arabidopsis thaliana* by nitric oxide. Plant Cell **22**: 2894–2907.

Lohse, M. et al. (2010). Robin: an intuitive wizard application for R-based expression microarray quality assessment and analysis. Plant Physiol. **153**: 642–651.

Meinicke, P., Lingner, T., Kaever, A., Feussner, K., Göbel, C., Feussner, I., Karlovsky, P., and Morgenstern, B. (2008). Metabolite-based clustering and visualization of mass spectrometry data using one-dimensional self-organizing maps. Algorithms Mol. Biol. AMB **3**: 9.

Millenaar, F.F., Cox, M.C.H., de Jong van Berkel, Y.E.M., Welschen, R.A.M., Pierik, R., Voesenek, L.A.J.C., and Peeters, A.J.M. (2005). Ethylene-induced differential growth of petioles in *Arabidopsis*. analyzing natural variation, response kinetics, and regulation. Plant Physiol. **137**: 998–1008.

Millenaar, F.F., Van Zanten, M., Cox, M.C.H., Pierik, R., Voesenek, L.A.C.J., and Peeters, A.J.M. (2009). Differential petiole growth in *Arabidopsis thaliana*: photocontrol and hormonal regulation. New Phytol. **184**: 141–152.

Mockler, T.C., Guo, H., Yang, H., Duong, H., and Lin, C. (1999). Antagonistic actions of Arabidopsis cryptochromes and phytochrome B in the regulation of floral induction. Dev. Camb. Engl. **126**: 2073–2082.

Mueller, S., Hilbert, B., Dueckershoff, K., Roitsch, T., Krischke, M., Mueller, M.J., and

Berger, S. (2008). General detoxification and stress responses are mediated by oxidized lipids through TGA transcription factors in *Arabidopsis*. Plant Cell **20**: 768–785.

Murmu, J., Bush, M.J., DeLong, C., Li, S., Xu, M., Khan, M., Malcolmson, C., Fobert, P.R., Zachgo, S., and Hepworth, S.R. (2010). Arabidopsis bZIP transcription factors TGA9 and TGA10 interact with floral glutaredoxins ROXY1 and ROXY2 and are redundantly required for anther development. Plant Physiol.: pp.110.159111.

Muthreich, M. (2014). Characterization of clade I TGA transcription factors in *Arabidopsis thaliana* with respect to biotic stress. PhD thesis. (https://ediss.uni-goettingen.de/bitstream/handle/11858/00-1735-0000-0022-5FB1-8/Thesis_MM_corrected_publish.pdf?sequence=1)

Ndamukong, I., Abdallat, A.A., Thurow, C., Fode, B., Zander, M., Weigel, R., and Gatz, C. (2007). SA-inducible Arabidopsis glutaredoxin interacts with TGA factors and suppresses JA-responsive PDF1.2 transcription. Plant J. Cell Mol. Biol. **50**: 128–139.

Ordin, L., Applewhite, T.H., and Bonner, J. (1956). Auxin-induced water uptake by avena coleoptile sections. Plant Physiol. **31**: 44–53.

Pierik, R., Millenaar, F.F., Peeters, A.J.M., and Voesenek, L. a. C.J. (2005). New perspectives in flooding research: the use of shade avoidance and *Arabidopsis thaliana*. Ann. Bot. **96**: 533–540.

Polko, J.K. et al. (2015). Ethylene-mediated regulation of A2-type CYCLINs modulates hyponastic growth in *Arabidopsis*. Plant Physiol. **169**: 194–208.

Polko, J.K., van Zanten, M., van Rooij, J.A., Marée, A.F.M., Voesenek, L.A.C.J., Peeters, A.J.M., and Pierik, R. (2012). Ethylene-induced differential petiole growth in *Arabidopsis thaliana* involves local microtubule reorientation and cell expansion. New Phytol. **193**: 339–348.

Poor, C.B., Wegner, S.V., Li, H., Dlouhy, A.C., Schuermann, J.P., Sanishvili, R., Hinshaw, J.R., Riggs-Gelasco, P.J., Outten, C.E., and He, C. (2014). Molecular mechanism and structure of the Saccharomyces cerevisiae iron regulator Aft2. Proc. Natl. Acad. Sci. U. S. A. **111**: 4043–4048.

Rauf, M., Arif, M., Fisahn, J., Xue, G.-P., Balazadeh, S., and Mueller-Roeber, B. (2013). NAC transcription factor SPEEDY HYPONASTIC GROWTH regulates flooding-induced leaf movement in *Arabidopsis*. Plant Cell **25**: 4941–4955.

Reed, J.W., Nagpal, P., Poole, D.S., Furuya, M., and Chory, J. (1993). Mutations in the gene for the red/far-red light receptor phytochrome B alter cell elongation and physiological responses throughout Arabidopsis development. Plant Cell **5**: 147–157.

Ritsema, T., van Zanten, M., Leon-Reyes, A., Voesenek, L.A.C.J., Millenaar, F.F., Pieterse, C.M.J., and Peeters, A.J.M. (2010). Kinome profiling reveals an interaction between jasmonate, salicylate and light control of hyponastic petiole growth in *Arabidopsis thaliana*. PLoS ONE **5**.

Robson, P., Whitelam, G.C., and Smith, H. (1993). Selected components of the shade-avoidance syndrome are displayed in a normal manner in mutants of *Arabidopsis thaliana* and *Brassica rapa* deficient in Phytochrome B. Plant Physiol. **102**: 1179–1184.

Roman, G., Lubarsky, B., Kieber, J.J., Rothenberg, M., and Ecker, J.R. (1995). Genetic analysis of ethylene signal transduction in *Arabidopsis thaliana*: five novel mutant loci integrated into a stress response pathway. Genetics **139**: 1393–1409.

Running, M.P. and Meyerowitz, E.M. (1996). Mutations in the PERIANTHIA gene of Arabidopsis specifically alter floral organ number and initiation pattern. Dev. Camb. Engl. **122**: 1261–1269.

Shearer, H.L., Cheng, Y.T., Wang, L., Liu, J., Boyle, P., Després, C., Zhang, Y., Li, X., and Fobert, P.R. (2012). Arabidopsis clade I TGA transcription factors regulate plant defenses in an NPR1-independent fashion. Mol. Plant-Microbe Interact. MPMI **25**: 1459–1468.

Spoel, S.H. et al. (2003). NPR1 modulates cross-talk between salicylate- and jasmonate-dependent defense pathways through a novel function in the cytosol. Plant Cell **15**: 760–770.

Taiz L. (1984). Plant cell expansion: regulation of cell wall mechanical properties. Annu Rev Plant Physiol. **35**:585–657.

Uhrig, J.F., Huang, L.-J., Barghahn, S., Willmer, M., Thurow, C., and Gatz, C. (2017). CC-type glutaredoxins recruit the transcriptional co-repressor TOPLESS to TGA-dependent target promoters in *Arabidopsis thaliana*. Biochim. Biophys. Acta **1860**: 218–226.

Vandenbussche, F., Vriezen, W.H., Smalle, J., Laarhoven, L.J.J., Harren, F.J.M., and Van Der Straeten, D. (2003). Ethylene and auxin control the arabidopsis response to decreased light intensity. Plant Physiol. **133**: 517–527.

Vreeburg, R.A.M., Benschop, J.J., Peeters, A.J.M., Colmer, T.D., Ammerlaan, A.H.M., Staal, M., Elzenga, T.M., Staals, R.H.J., Darley, C.P., McQueen-Mason, S.J., and Voesenek, L.A.C.J. (2005). Ethylene regulates fast apoplastic acidification and expansin A transcription during submergence-induced petiole elongation in *Rumex palustris*. Plant J. Cell Mol. Biol. **43**: 597–610.

Wang, L. and Fobert, P.R. (2013). Arabidopsis clade I TGA factors regulate apoplastic defences against the bacterial pathogen Pseudomonas syringae through endoplasmic reticulum-based processes. PloS One **8**: e77378.

Weiste, C., Iven, T., Fischer, U., Oñate-Sánchez, L., and Dröge-Laser, W. (2007). In planta ORFeome analysis by large-scale over-expression of GATEWAY-compatible cDNA clones: screening of ERF transcription factors involved in abiotic stress defense. Plant J. Cell Mol. Biol. **52**: 382–390.

Went, F.W., and Thimann, K.V. (1937). Phytohormones. (New York MacMillan).

Whitelam, G.C. and Johnson, C.B. (1982). Photomorphogenesis in impatiens parviflora and other plant species under simulated natural canopy radiations. New Phytol. **90**: 611–618.

Xing, S., Rosso, M.G., and Zachgo, S. (2005). ROXY1, a member of the plant glutaredoxin family, is required for petal development in *Arabidopsis thaliana*. Development **132**: 1555–1565.

Xing, S. and Zachgo, S. (2008). ROXY1 and ROXY2, two Arabidopsis glutaredoxin genes, are required for anther development. Plant J. **53**: 790–801.

Zander, M., La Camera, S., Lamotte, O., Métraux, J.-P., and Gatz, C. (2010). *Arabidopsis thaliana* class-II TGA transcription factors are essential activators of jasmonic acid/ethylene-induced defense responses. Plant J. **61**: 200–210.

Zander, M., Chen, S., Imkampe, J., Thurow, C., and Gatz, C. (2012). Repression of the *Arabidopsis thaliana* jasmonic acid/ethylene-induced defense pathway by tga-interacting glutaredoxins depends on their C-terminal ALWL motif. Mol. Plant **5**: 831–840.

Zander, M., Thurow, C., and Gatz, C. (2014). TGA transcription factors activate the salicylic acid-suppressible branch of the ethylene-induced defense program by regulating ORA59 expression. Plant Physiol. **165**: 1671–1683.

van Zanten, M., Millenaar, F.F., Cox, M.C., Pierik, R., Voesenek, L.A., and Peeters, A.J. (2009). Auxin perception and polar auxin transport are not always a prerequisite for differential growth. Plant Signal. Behav. **4**: 899–901.

van Zanten, M., Ritsema, T., Polko, J.K., Leon-Reyes, A., Voesenek, L.A.C.J., Millenaar, F.F., Pieterse, C.M.J., and Peeters, A.J.M. (2012). Modulation of ethylene-and heat-controlled hyponastic leaf movement in *Arabidopsis thaliana* by the plant defence hormones jasmonate and salicylate. Planta **235**: 677–685.

Zhang, Y., Fan, W., Kinkema, M., Li, X., and Dong, X. (1999). Interaction of NPR1 with basic leucine zipper protein transcription factors that bind sequences required for salicylic acid induction of the PR-1 gene. Proc. Natl. Acad. Sci. U. S. A. **96**: 6523–6528.

Zhang, Y., Tessaro, M.J., Lassner, M., and Li, X. (2003). Knockout analysis of arabidopsis transcription factors TGA2, TGA5, and TGA6 reveals their redundant and essential roles in systemic acquired resistance. Plant Cell **15**: 2647–2653.

Ziemann, M. (2014). Glutaredoxin family genes in plant development. PhD thesis. (https://researchbank.swinburne.edu.au/file/a43ce9b6-69a0-4011-b81b-9f129dbc4ae3/1/Mark%20Ziemann%20Thesis.pdf)

Ziemann, M., Bhave, M., and Zachgo, S. (2009). Origin and diversification of land plant CC-type glutaredoxins. Genome Biol. Evol. **1**: 265–277.

8 Abbreviations

ABA	Abscisic acid
ACC	1-aminocyclopropane-1-carboxylic acid
A. thaliana	*Arabidopsis thaliana*
A. tumefaciens	*Agrobacterium tumefaciens*
ACC	1-aminocyclopropane-1-carboxylic acid
as-1	*activation sequence-1*
bHLH	Basic helix-loop-helix
bZIP	Basic domain/leucine zipper
CL	Control light
Col-0	Columbia
CRISPR	Clustered regularly interspaced short palindromic repeats
EDTA	Ethylene di-amine tetra-acetic acid
ET	Ethylene
EtOH	Ethanol
Fe-S	Iron-sulfur
FR	Far-red light
$Gent^R$	Gentamicin
GO	Gene ontology
GR	Glutathione reductase
GRX	Glutaredoxin
GSH	Glutathione
LL	Low light
JA	Jasmonic acid
NAC	NAC (NAM, ATAF1/2, CUC2) transcription factor
NADPH	Nicotinamide adenine dinucleotide phosphate
p	*p*-value (probability of obtaining a test statistic assuming that the null hypothesis is true)
PCA	Principal components analysis
PCR	Polymerase chain reaction
qRT-PCR	Quantitative real-time PCR
R	Red light
Rif^R	Rifampicin
ROXY	CC-type glutaredoxin
SA	Salicylic acid
SD	Short day
SDS	Sodium dodecyl sulfate
SDS-PAGE	Sodium dodecyl sulfate-polyacrylamide gel electrophoresis
TF	Transcription factor
TGA	TGACG motif binding protein
WT	Wild-type

9 Supplementary data

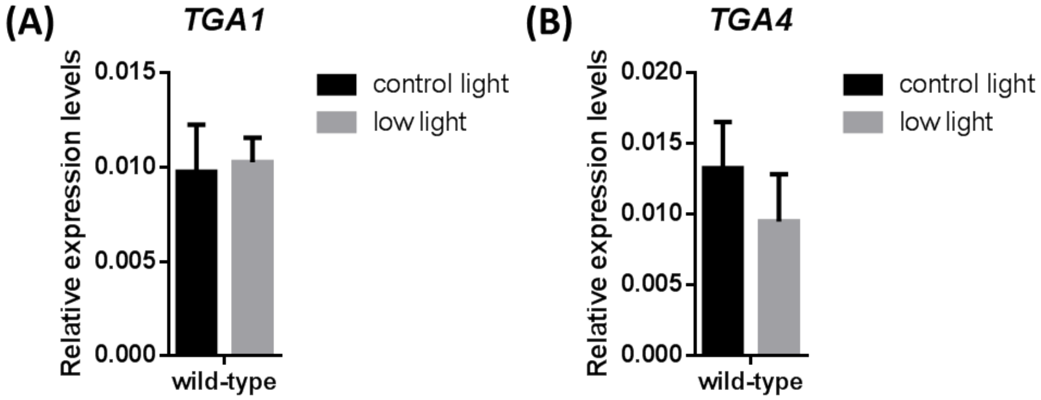

Supplementary Figure S1 Expression profiling of *TGA1 and TGA4* in wild-type after low light treatment.

(A) and (B) qRT-PCR analysis of *TGA1* and *TGA4* expression in wild-type after low light treatment. Four-week-old soil-grown wild-type were treated with low light for 6 hours (reduction in light intensity from 100-120 to 15-20 µmol m^{-2} s^{-1}). Transcript levels were normalized to the transcript level of *UBQ5*. Bars represent the average ± SEM of four biological replicates, each with dissected petioles from five independent plants.

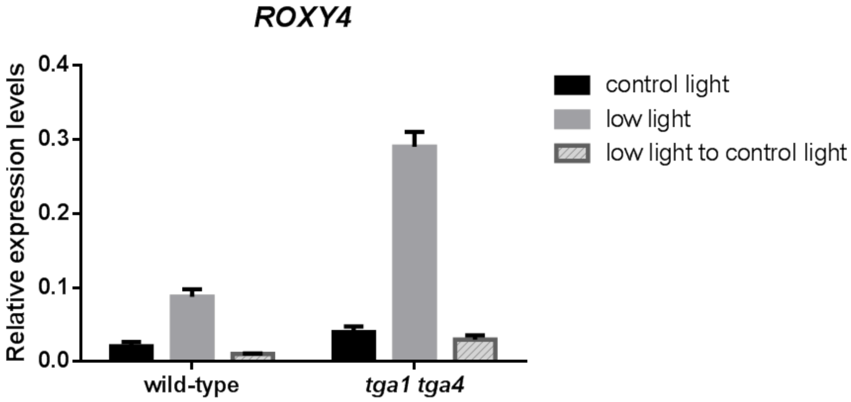

Supplementary Figure S2 Expression profiling of *ROXY4* in wild-type and *tga1 tga4* in light shifting assay.

qRT–PCR analysis of *ROXY4* expression in light shifting assay. Transcript levels were normalized to the transcript level of *UBQ5* (ubiquitin 5). Error bars represent the average ± SEM of five biological replicates, each with dissected petioles from five independent plants.

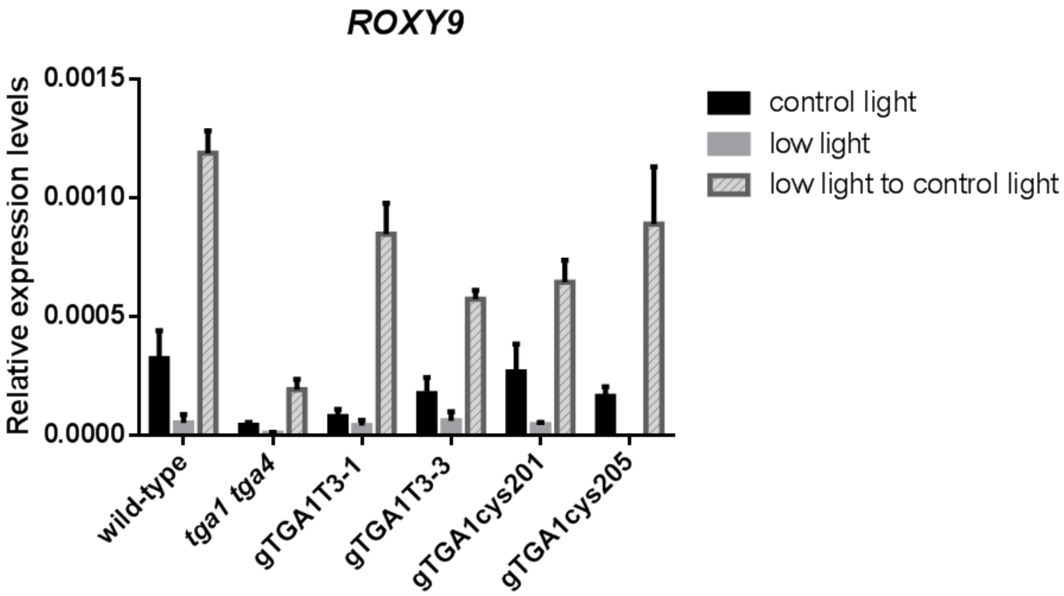

Supplementary Figure S3 Expression profiling of *ROXY9* in genomic *TGA1* complementation lines.

qRT–PCR analysis of ROXY9 expression in light shifting assay. Plants were subjected to the light regime displayed in Figure 3.6A. Four-week soil-grown wild-type, *tga1 tga4*, gTGA1(*ProTGA1:HA-TGA1* line 1 and line 3), and gTGA1cys(*ProTGA1:HA-TGA1* with mutations in the two conserved cysteines, CNLKQSC to NNLKQSS, line 1 and line 5) plants were harvested. Transcript levels were normalized to the transcript level of *UBQ5* (ubiquitin 5). Data are mean values of three biological replicates, each with dissected petioles from three independent plants. Error bars=SEM.

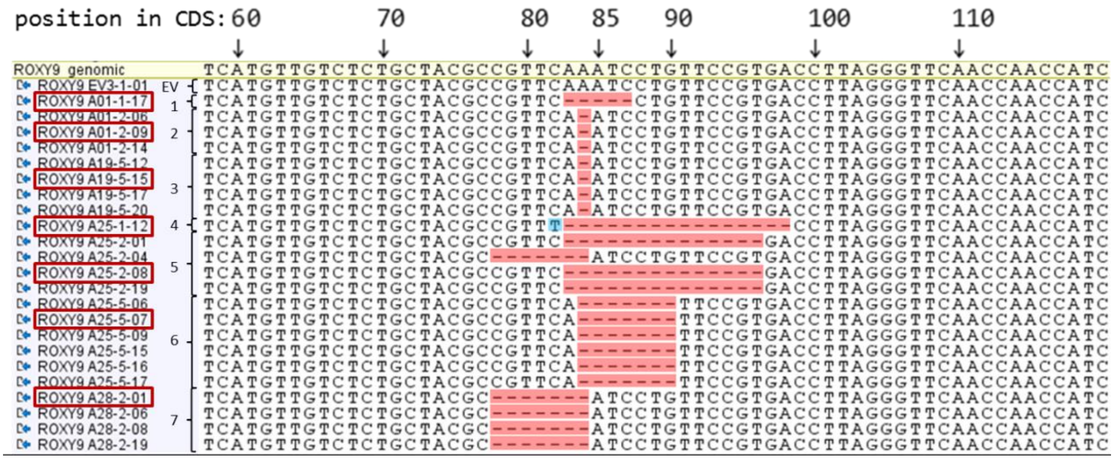

Supplementary Figure S4 *ROXY9* CRISPR-Cas9 mutant lines.

Mutant lines which were selected for light shifting assay were circled with red rectangle. Deleted nucleotides in *ROXY9* CRISPR-Cas9 mutants were indicated with short lines in red background. The mutated nucleotide was marked in blue background. DNA sequences aligned by Florian Jung (Master thesis).

Supplementary Figure S5

wild-type and *tga1 tga4* in response to 6 hours high temperature treatment

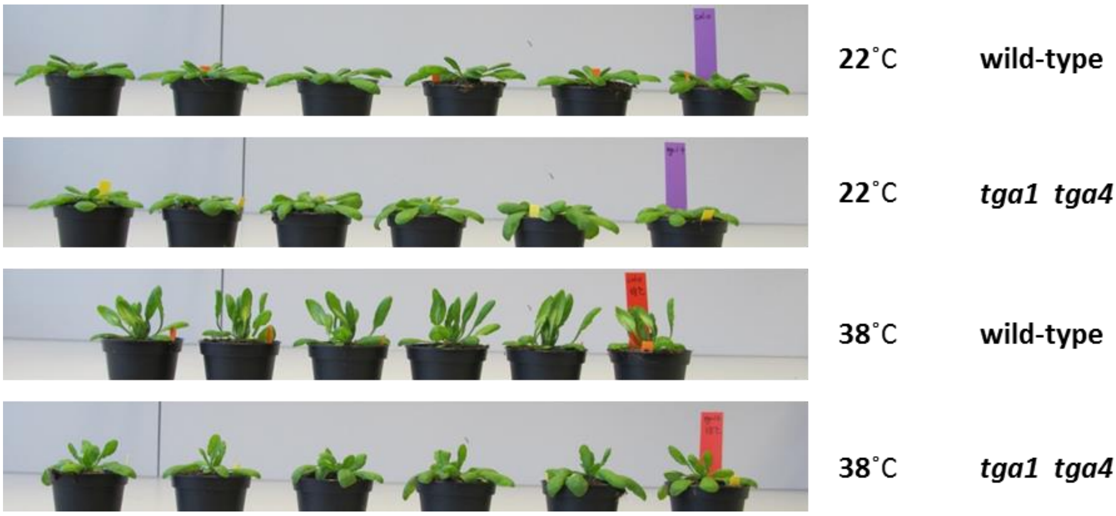

Supplementary Figure S6

wild-type, *ein2, 35S:SHYG*, *shyg-1* and *shyg-2* in response to 6 hours low light treatment. Images were used for petiole angle measurement in Figure 3.2B and Figure 3.21B.

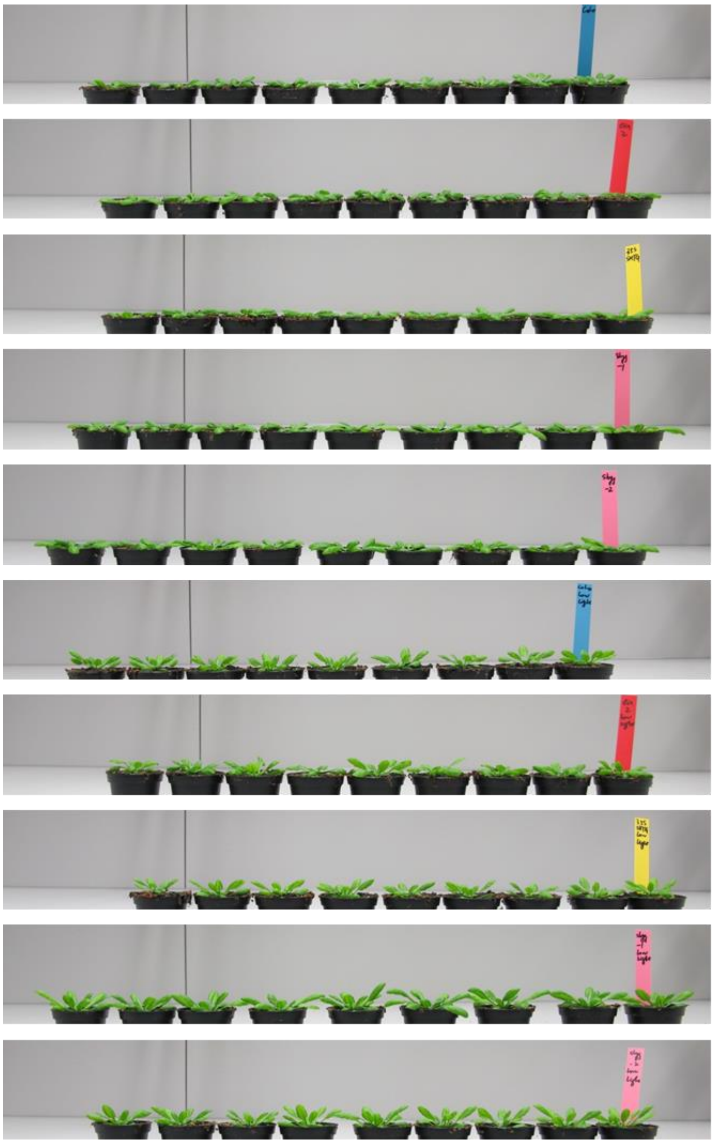

control light	**wild-type**
control light	***ein2***
control light	***35S:SHYG***
control light	***shyg-1***
control light	***shyg-2***
low light	**wild-type**
low light	***ein2***
low light	***35S:SHYG***
low light	***shyg-1***
low light	***shyg-2***

Supplementary Figure S7

wild-type, *cry1 cry2,* and *phot1 phot2* in response to 6 hours low light treatment. Images were used for petiole angle measurement in Figure 3.2C, D.

control light **wild-type**

control light ***cry1cry2***

control light ***phot1phot2***

low light **wild-type**

low light ***cry1cry2***

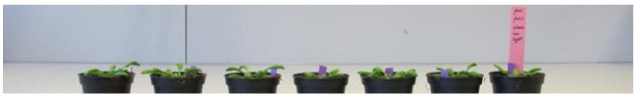

low light ***phot1phot2***

Wild-type, and *phyB* in response to 6 hours low light treatment

control light **wild-type**

control light ***phyB***

low light **wild-type**

low light ***phyB***

Supplementary Figure S8

wild-type, *tga1 tga4*, *gTGA1#1*, *gTGA1#3, gTGA1cys#1* and *gTGA1cys#3* in response to 6 hours ACC treatment. Images were used for petiole angle measurement in Figure 3.3C.

control light	**wild-type**
control light	***tga1 tga4***
control light	***gTGA1 #1***
control light	***gTGA1 #3***
control light	***gTGA1cys #1***
control light	***gTGA1cys #3***
ACC	**wild-type**
ACC	***tga1 tga4***
ACC	***gTGA1 #1***
ACC	***gTGA1 #3***
ACC	***gTGA1cys #1***
ACC	***gTGA1cys #3***

Supplementary Figure S9

wild-type, *tga1 tga4*, *gTGA1#1*, *gTGA1#3, gTGA1cys#1* and *gTGA1cys#3* in response to 6 hours low light treatment. Images were used for petiole angle measurement in Figure 3.3B.

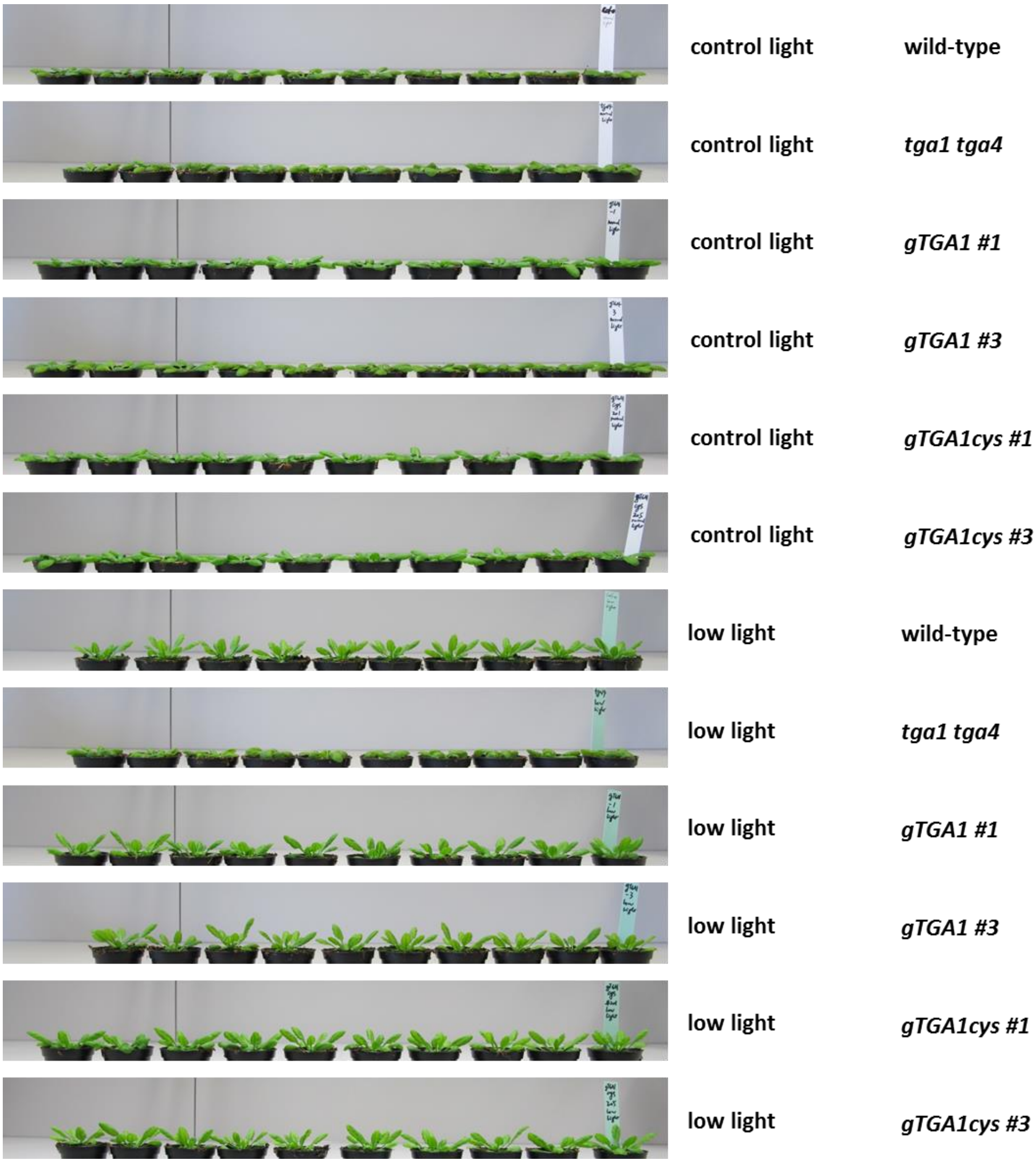

Supplementary Figure S10

wild-type, *tga1 tga4, gTGA1#1*, *gTGA1#3, gTGA1cys#1* and *gTGA1cys#3* in response to 6 hours low light , low light plus SA treatment. Images were used for petiole angle measurement in Figure 3.4B.

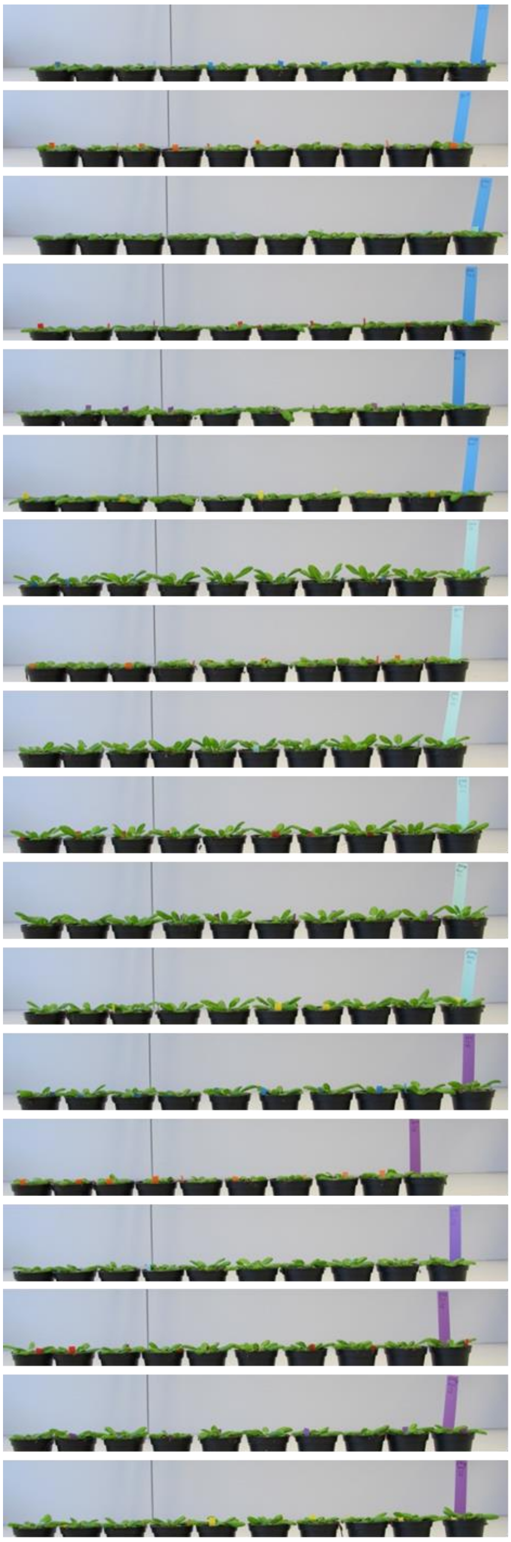

control light	**wild-type**
control light	***tga1 tga4***
control light	***gTGA1 #1***
control light	***gTGA1 #3***
control light	***gTGA1cys #1***
control light	***gTGA1cys #3***
low light	**wild-type**
low light	***tga1 tga4***
low light	***gTGA1 #1***
low light	***gTGA1 #3***
low light	***gTGA1cys #1***
low light	***gTGA1cys #3***
low light+SA	**wild-type**
low light+SA	***tga1 tga4***
low light+SA	***gTGA1 #1***
low light+SA	***gTGA1 #3***
low light+SA	***gTGA1cys #1***
low light+SA	***gTGA1cys #3***

Supplementary Figure S11

wild-type, *tga2 tga5 tga6, npr1*, and *35S:HA-ROXY19* in response to 6 hours low light, low light plus SA treatment. Images were used for petiole angle measurement in Figure 3.5.

control light **wild-type**

control light ***tga2 tga5 tga6***

control light ***npr1***

control light ***ROXY19***

low light **wild-type**

low light ***tga2 tga5 tga6***

low light ***npr1***

low light ***ROXY19***

low light+SA **wild-type**

low light+SA ***tga2 tga5 tga6***

low light+SA ***npr1***

low light+SA ***ROXY19***

Supplementary Figure S12

wild-type, *tga1 tga4, gTGA1#1*, *gTGA1#3, gTGA1cys#1* and *gTGA1cys#3* in response to low light, low light to control light treatment. Images were used for petiole angle measurement in Figure 3.6B.

control light	**wild-type**
control light	***tga1 tga4***
control light	***gTGA1 #1***
control light	***gTGA1 #3***
control light	***gTGA1cys #1***
control light	***gTGA1cys #3***
low light to control light	**wild-type**
low light to control light	***tga1 tga4***
low light to control light	***gTGA1 #1***
low light to control light	***gTGA1 #3***
low light to control light	***gTGA1cys #1***
low light to control light	***gTGA1cys #3***
low light	**wild-type**
low light	***tga1 tga4***
low light	***gTGA1 #1***
low light	***gTGA1 #3***
low light	***gTGA1cys #1***
low light	***gTGA1cys #3***

Supplementary Figure S13

wild-type, *tga1 tga4, 35S:HA-ROXY8#9,#11,#17,#22,#32* in response to 6 hours low light treatment. Images were used for petiole angle measurement in Figure 3.9A.

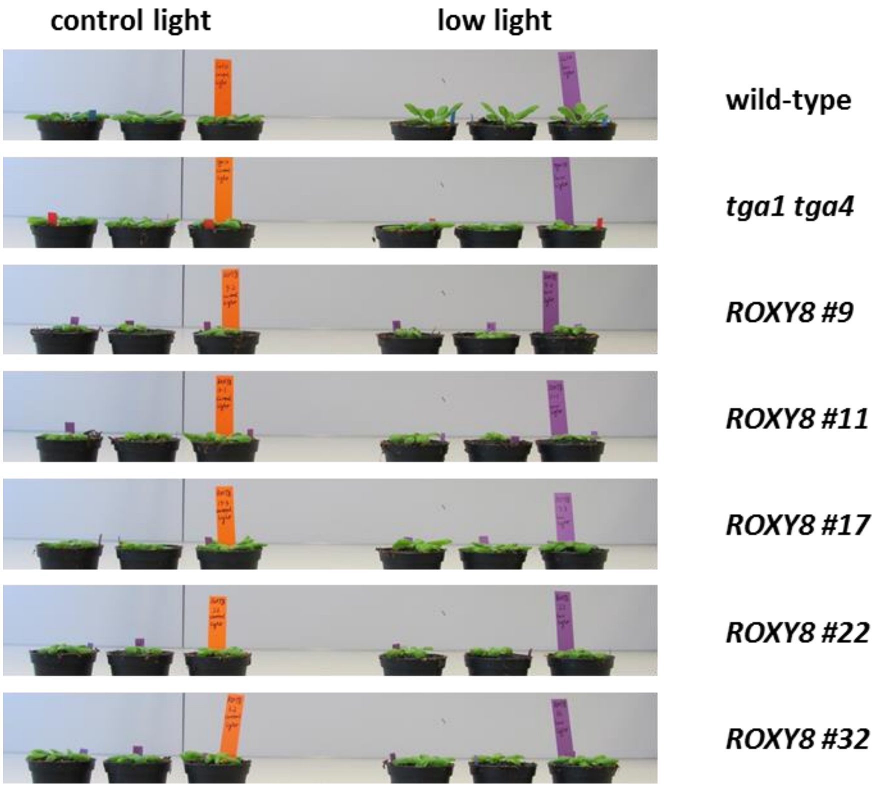

Supplementary Figure S14

wild-type, *tga1 tga4, 35S:HA-ROXY9#6,#7,#10,#13,#14* in response to 6 hours low light treatment. Images were used for petiole angle measurement in Figure 3.9B.

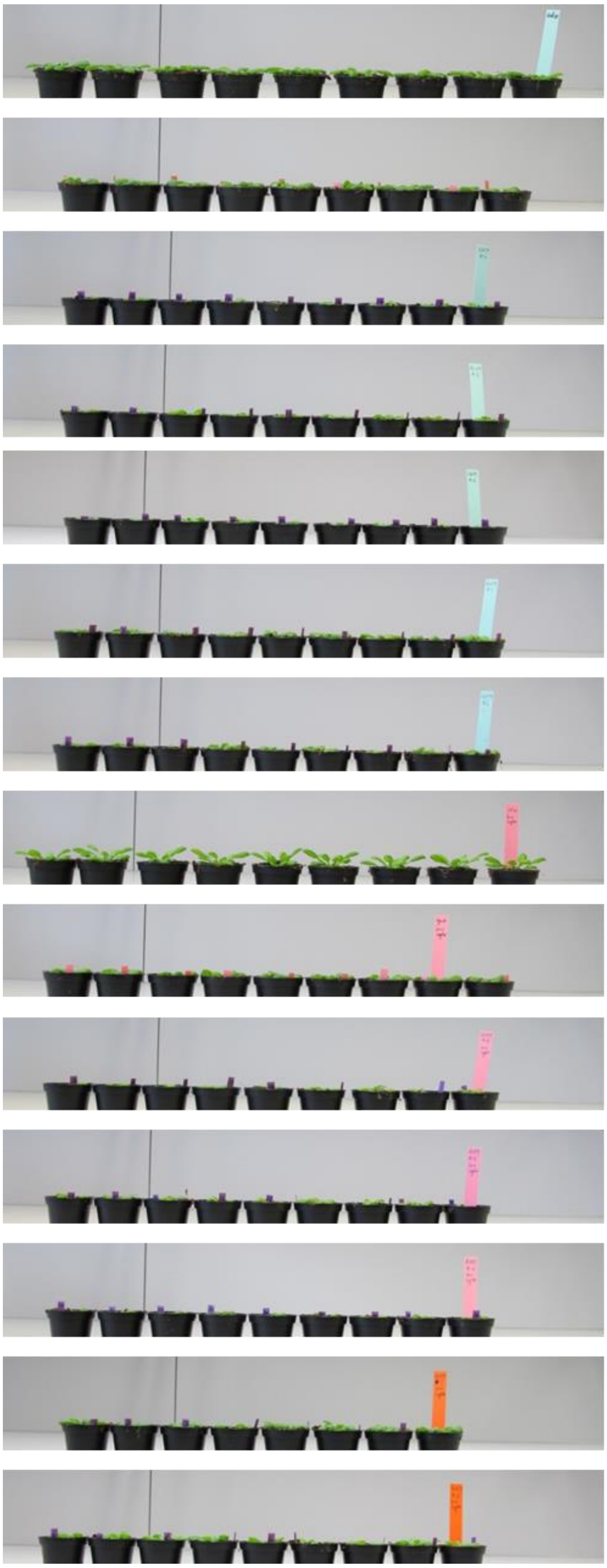

control light	**wild-type**
control light	***tga1 tga4***
control light	***ROXY9 #14***
control light	***ROXY9 #13***
control light	***ROXY9 #10***
control light	***ROXY9 #7***
control light	***ROXY9 #6***
low light	**wild-type**
low light	***tga1 tga4***
low light	***ROXY9 #14***
low light	***ROXY9 #13***
low light	***ROXY9 #10***
low light	***ROXY9 #7***
low light	***ROXY9 #6***

Table S1 List of 169 genes of cluster 2.

Identifier	Description	ColLL-tgaLL logFC	ColLL-ROXYLL logFC
AT5G25760	PEX4, UBC21 | peroxin4 | chr5:8967655-8969349 FORWARD LENGTH=745	2.06	1.78
AT1G63380	NAD(P)-binding Rossmann-fold superfamily protein | chr1:23505557-23506391 FORWARD LENGTH=709	1.99	1.52
AT3G63440	ATCKX6, CKX6, ATCKX7 | cytokinin oxidase/dehydrogenase 6 | chr3:23424157-23426536 FORWARD LENGTH=2007	1.95	2.39
AT3G49110	PRX33, PRXCA, ATPRX33, ATPCA | peroxidase CA | chr3:18200664-18203142 FORWARD LENGTH=1365	1.92	1.34
AT5G58390	Peroxidase superfamily protein | chr5:23599567-23601325 REVERSE LENGTH=1220	1.80	1.72
AT3G08840	D-alanine--D-alanine ligase family | chr3:2682453-2686224 REVERSE LENGTH=1785	1.77	1.22
AT4G23450	AIRP1, AtAIRP1 | RING/U-box superfamily protein | chr4:12240803-12242706 REVERSE LENGTH=1031	1.76	0.76
AT3G07610	IBM1 | Transcription factor jumonji (jmjC) domain-containing protein | chr3:2426148-2432876 FORWARD LENGTH=3084	1.75	0.85
AT5G66600	Protein of unknown function, DUF547 | chr5:26575000-26578826 REVERSE LENGTH=2461	1.71	1.33
AT1G75920	GDSL-like Lipase/Acylhydrolase superfamily protein | chr1:28505554-28507168 FORWARD LENGTH=1106	1.68	2.28
AT5G17920	ATCIMS, ATMETS, ATMS1 | Cobalamin-independent synthase family protein | chr5:5935038-5939487 FORWARD LENGTH=2771	1.61	1.25
AT1G37150	HCS2 | holocarboxylase synthetase 2 | chr1:14174981-14177302 REVERSE LENGTH=1101	1.56	0.59
AT5G03545	AT4, ATIPS2 | Expressed in response to phosphate starvation, this response is enhanced by the presence of IAA. | chr5:894706-895400 FORWARD LENGTH=695	1.53	1.83
AT1G56600	AtGolS2, GolS2 | galactinol synthase 2 | chr1:21207537-21209596 FORWARD LENGTH=1396	1.53	1.32
AT4G21160	ZAC | Calcium-dependent ARF-type GTPase activating protein family | chr4:11284238-11286767 FORWARD LENGTH=1404	1.53	0.47
AT1G28290	AGP31 | arabinogalactan protein 31 | chr1:9889125-9890875 REVERSE LENGTH=1186	1.52	1.49
AT1G15860	Domain of unknown function (DUF298) | chr1:5454838-5457022 FORWARD LENGTH=1182	1.52	1.95
AT3G26960	Pollen Ole e 1 allergen and extensin family protein | chr3:9944668-9945579 REVERSE LENGTH=836	1.48	1.68
AT5G66420	CONTAINS InterPro DOMAIN/s: Uncharacterised conserved protein UCP033271 (InterPro:IPR008322), TIM-barrel signal transduction protein, predicted (InterPro:IPR009215); Has 30201 Blast hits to 17322 proteins in 780 species: Archae - 12; Bacteria - 1396; Metazoa - 17338; Fungi - 3422; Plants - 5037; Viruses - 0; Other Eukaryotes - 2996 (source: NCBI BLink). | chr5:26521674-26525029 REVERSE LENGTH=2679	1.47	2.10
AT3G25010	AtRLP41, RLP41 | receptor like protein 41 | chr3:9110103-9112748 REVERSE LENGTH=2646	1.46	1.02
AT5G22820	ARM repeat superfamily protein | chr5:7623440-7626975 REVERSE LENGTH=1997	1.46	1.59
AT3G15605	nucleic acid binding | chr3:5288093-5290941 FORWARD LENGTH=1667	1.43	0.87
AT2G21540	ATSFH3, SFH3 | SEC14-like 3 | chr2:9220556-9224496 REVERSE LENGTH=2106	1.43	1.57
AT3G61880	CYP78A9 | cytochrome p450 78a9 | chr3:22905868-22907958 REVERSE LENGTH=1919	1.42	2.15
AT5G42690	Protein of unknown function, DUF547 | chr5:17116428-17119838 REVERSE LENGTH=2102	1.41	0.53
AT3G46490	2-oxoglutarate (2OG) and Fe(II)-dependent oxygenase superfamily protein | chr3:17115629-17119451 FORWARD LENGTH=993	1.39	0.74
AT4G35900	FD, FD-1, atbzip14 | Basic-leucine zipper (bZIP) transcription factor family protein | chr4:17004595-17006287 FORWARD LENGTH=1344	1.37	0.89
AT4G25090	Riboflavin synthase-like superfamily protein | chr4:12878775-12883599 REVERSE LENGTH=2705	1.37	0.69
AT2G22620	Rhamnogalacturonate lyase family protein | chr2:9604772-9610595 REVERSE LENGTH=2444	1.36	1.25
AT1G58225	unknown protein; FUNCTIONS IN: molecular_function unknown; INVOLVED IN: biological_process unknown; LOCATED IN: endomembrane system; Has 4 Blast hits to 4 proteins in 2 species: Archae - 0; Bacteria - 0; Metazoa - 0; Fungi - 0; Plants - 4; Viruses - 0; Other Eukaryotes - 0 (source: NCBI BLink). | chr1:21564111-21565171 FORWARD LENGTH=702	1.33	1.17

Identifier	Description	ColLL-tgaLL logFC	ColLL-ROXYLL logFC
AT4G18970	GDSL-like Lipase/Acylhydrolase superfamily protein | chr4:10389111-10390917 REVERSE LENGTH=1392	1.32	0.57
AT4G01680	MYB55 | myb domain protein 55 | chr4:716021-717415 REVERSE LENGTH=1248	1.31	1.21
AT2G21050	LAX2 | like AUXIN RESISTANT 2 | chr2:9034090-9036636 FORWARD LENGTH=1848	1.31	1.52
AT1G53040	Protein of unknown function (DUF616) | chr1:19764310-19767334 REVERSE LENGTH=2174	1.30	1.22
AT1G10657	Plant protein 1589 of unknown function | chr1:3530467-3531821 FORWARD LENGTH=862	1.29	0.76
AT2G34655	unknown protein; FUNCTIONS IN: molecular_function unknown; INVOLVED IN: biological_process unknown; LOCATED IN: endomembrane system; EXPRESSED IN: stem, root, inflorescence, cultured cell, leaf; Has 35333 Blast hits to 34131 proteins in 2444 species: Archae - 798; Bacteria - 22429; Metazoa - 974; Fungi - 991; Plants - 531; Viruses - 0; Other Eukaryotes - 9610 (source: NCBI BLink). | chr2:14596631-14597540 FORWARD LENGTH=910	1.26	1.45
AT4G00440	Protein of unknown function (DUF3741) | chr4:193879-198579 FORWARD LENGTH=3802	1.26	1.48
AT1G68810	basic helix-loop-helix (bHLH) DNA-binding superfamily protein | chr1:25861123-25863120 FORWARD LENGTH=1511	1.25	1.35
AT5G12880	proline-rich family protein | chr5:4068519-4068962 REVERSE LENGTH=444	1.25	0.91
AT5G09220	AAP2 | amino acid permease 2 | chr5:2866252-2869054 FORWARD LENGTH=1794	1.24	1.13
AT4G02290	AtGH9B13, GH9B13 | glycosyl hydrolase 9B13 | chr4:1002394-1005253 REVERSE LENGTH=1939	1.24	1.66
AT5G05960	Bifunctional inhibitor/lipid-transfer protein/seed storage 2S albumin superfamily protein | chr5:1790231-1790833 FORWARD LENGTH=515	1.23	1.38
AT3G20080	CYP705A15 | cytochrome P450, family 705, subfamily A, polypeptide 15 | chr3:7008774-7010677 FORWARD LENGTH=1825	1.23	1.13
AT3G20460	Major facilitator superfamily protein | chr3:7135050-7139472 FORWARD LENGTH=1470	1.23	1.30
AT5G46240	KAT1 | potassium channel in *Arabidopsis thaliana* 1 | chr5:18743566-18746730 REVERSE LENGTH=2289	1.23	1.16
AT3G06370	NHX4, ATNHX4 | sodium hydrogen exchanger 4 | chr3:1930396-1934073 REVERSE LENGTH=2207	1.22	1.43
AT5G23210	SCPL34 | serine carboxypeptidase-like 34 | chr5:7810855-7815039 FORWARD LENGTH=1848	1.22	1.44
AT3G12610	DRT100 | Leucine-rich repeat (LRR) family protein | chr3:4006399-4007807 REVERSE LENGTH=1409	1.21	1.29
AT2G40610	ATEXPA8, EXP8, ATEXP8, ATHEXP ALPHA 1.11, EXPA8 | expansin A8 | chr2:16948863-16950557 REVERSE LENGTH=1105	1.20	1.36
AT1G18710	AtMYB47, MYB47 | myb domain protein 47 | chr1:6450594-6453114 FORWARD LENGTH=1119	1.19	0.92
AT5G54510	GH3.6, DFL1 | Auxin-responsive GH3 family protein | chr5:22131093-22133678 REVERSE LENGTH=2181	1.18	1.52
AT3G28700	Protein of unknown function (DUF185) | chr3:10759559-10762114 FORWARD LENGTH=1717	1.17	1.19
AT1G23340	Protein of Unknown Function (DUF239) | chr1:8283644-8286528 REVERSE LENGTH=1289	1.17	1.15
AT1G23140	Calcium-dependent lipid-binding (CaLB domain) family protein | chr1:8202261-8203215 REVERSE LENGTH=642	1.17	0.89
AT2G14680	MEE13 | myosin heavy chain-related | chr2:6277961-6283940 FORWARD LENGTH=2359	1.16	1.06
AT3G25620	ABC-2 type transporter family protein | chr3:9316074-9319571 REVERSE LENGTH=2688	1.16	1.14
AT1G78970	LUP1, ATLUP1 | lupeol synthase 1 | chr1:29703062-29707844 FORWARD LENGTH=2642	1.15	1.85
AT4G08040	ACS11 | 1-aminocyclopropane-1-carboxylate synthase 11 | chr4:4887112-4888939 FORWARD LENGTH=1383	1.14	0.99
AT3G48900	single-stranded DNA endonuclease family protein | chr3:18131829-18136341 FORWARD LENGTH=2031	1.13	1.79
AT3G15540	IAA19, MSG2 | indole-3-acetic acid inducible 19 | chr3:5264024-5265678 FORWARD LENGTH=970	1.13	1.37
AT2G46570	LAC6 | laccase 6 | chr2:19126872-19129069 FORWARD LENGTH=1710	1.12	0.75
AT5G10430	AGP4, ATAGP4 | arabinogalactan protein 4 | chr5:3277532-3278313 REVERSE LENGTH=782	1.11	1.85
AT2G24300	Calmodulin-binding protein | chr2:10340816-10343736 FORWARD LENGTH=2214	1.10	1.02

Identifier	Description	ColLL-tgaLL logFC	ColLL-ROXYLL logFC
AT1G75780	TUB1 | tubulin beta-1 chain | chr1:28451141-28453640 REVERSE LENGTH=1619	1.09	1.21
AT2G18690	unknown protein; FUNCTIONS IN: molecular_function unknown; INVOLVED IN: biological_process unknown; LOCATED IN: membrane; EXPRESSED IN: 17 plant structures; EXPRESSED DURING: 9 growth stages; CONTAINS InterPro DOMAIN/s: Protein of unknown function DUF975 (InterPro:IPR010380); BEST *Arabidopsis thaliana* protein match is: unknown protein (TAIR:AT2G18680.1); Has 213 Blast hits to 211 proteins in 20 species: Archae - 0; Bacteria - 8; Metazoa - 0; Fungi - 0; Plants - 205; Viruses - 0; Other Eukaryotes - 0 (source: NCBI BLink). | chr2:8097420-8098827 FORWARD LENGTH=1408	1.07	1.10
AT3G54260	TBL36 | TRICHOME BIREFRINGENCE-LIKE 36 | chr3:20085010-20086763 REVERSE LENGTH=1245	1.07	0.84
AT1G80660	AHA9, HA9 | H(+)-ATPase 9 | chr1:30316227-30319948 REVERSE LENGTH=2865	1.06	1.14
AT5G06930	LOCATED IN: chloroplast; EXPRESSED IN: 15 plant structures; EXPRESSED DURING: 7 growth stages; BEST *Arabidopsis thaliana* protein match is: nucleolar protein gar2-related (TAIR:AT2G42320.2); Has 3369 Blast hits to 1526 proteins in 313 species: Archae - 2; Bacteria - 910; Metazoa - 754; Fungi - 336; Plants - 137; Viruses - 11; Other Eukaryotes - 1219 (source: NCBI BLink). | chr5:2144999-2148039 FORWARD LENGTH=2502	1.06	1.26
AT2G34300	S-adenosyl-L-methionine-dependent methyltransferases superfamily protein | chr2:14473703-14477430 REVERSE LENGTH=2700	1.05	1.93
AT1G23060	BEST *Arabidopsis thaliana* protein match is: TPX2 (targeting protein for Xklp2) protein family (TAIR:AT1G70950.1); Has 449 Blast hits to 419 proteins in 98 species: Archae - 0; Bacteria - 40; Metazoa - 139; Fungi - 21; Plants - 158; Viruses - 3; Other Eukaryotes - 88 (source: NCBI BLink). | chr1:8170755-8172992 REVERSE LENGTH=1452	1.05	1.44
AT2G46320	Mitochondrial substrate carrier family protein | chr2:19015813-19018230 FORWARD LENGTH=1497	1.05	1.31
AT5G18080	SAUR-like auxin-responsive protein family chr5:5983840-5984112 FORWARD LENGTH=273	1.05	1.49
AT1G19530	unknown protein; FUNCTIONS IN: molecular_function unknown; INVOLVED IN: N-terminal protein myristoylation, anaerobic respiration; LOCATED IN: cellular_component unknown; EXPRESSED IN: leaf apex, inflorescence meristem, hypocotyl, root, flower; EXPRESSED DURING: petal differentiation and expansion stage; Has 47 Blast hits to 47 proteins in 13 species: Archae - 0; Bacteria - 0; Metazoa - 0; Fungi - 0; Plants - 47; Viruses - 0; Other Eukaryotes - 0 (source: NCBI BLink). | chr1:6763915-6764971 FORWARD LENGTH=700	1.04	1.56
AT3G11720	Polyketide cyclase/dehydrase and lipid transport superfamily protein | chr3:3705865-3708609 REVERSE LENGTH=1947	1.04	1.23
AT2G10606	MIR396A | MIR396A; miRNA | chr2:4142323-4142473 REVERSE LENGTH=151	1.03	1.21
AT3G25710	BHLH32, ATAIG1, TMO5 | basic helix-loop-helix 32 | chr3:9369519-9371394 FORWARD LENGTH=1412	1.03	0.95
AT5G14230	CONTAINS InterPro DOMAIN/s: Ankyrin repeat-containing domain (InterPro:IPR020683), Ankyrin repeat (InterPro:IPR002110); BEST *Arabidopsis thaliana* protein match is: XB3 ortholog 2 in *Arabidopsis thaliana* (TAIR:AT5G57740.1); Has 66374 Blast hits to 25358 proteins in 1201 species: Archae - 121; Bacteria - 8133; Metazoa - 29530; Fungi - 5885; Plants - 3349; Viruses - 785; Other Eukaryotes - 18571 (source: NCBI BLink). | chr5:4591741-4595964 FORWARD LENGTH=2587	1.02	0.93
AT3G62090	PIL2, PIF6 | phytochrome interacting factor 3-like 2 | chr3:22988547-22990709 REVERSE LENGTH=1805	1.02	0.71
AT2G40130	Double Clp-N motif-containing P-loop nucleoside triphosphate hydrolases superfamily protein | chr2:16765920-16769268 FORWARD LENGTH=3037	1.02	1.37
AT1G78970	LUP1, ATLUP1 | lupeol synthase 1 | chr1:29703340-29707844 FORWARD LENGTH=2477	1.01	1.47
AT1G67750	Pectate lyase family protein | chr1:25401588-25403503 FORWARD LENGTH=1637	1.01	1.55
AT2G47000	MDR4, PGP4, ABCB4, ATPGP4 | ATP binding cassette subfamily B4 | chr2:19309868-19315241 REVERSE LENGTH=4161	1.01	0.89
AT3G23030	IAA2 | indole-3-acetic acid inducible 2 | chr3:8180768-8181800 REVERSE LENGTH=941	1.00	1.32
AT1G25530	Transmembrane amino acid transporter family protein | chr1:8964544-8967428 REVERSE LENGTH=1643	1.00	1.21
AT1G52750	alpha/beta-Hydrolases superfamily protein | chr1:19646465-19649261 REVERSE LENGTH=2275	1.00	1.55

Identifier	Description	ColLL-tgaLL logFC	ColLL-ROXYLL logFC
AT5G57150	basic helix-loop-helix (bHLH) DNA-binding superfamily protein | chr5:23152186-23154264 FORWARD LENGTH=1827	0.99	0.70
AT1G11120	unknown protein; FUNCTIONS IN: molecular_function unknown; INVOLVED IN: biological_process unknown; LOCATED IN: cellular_component unknown; EXPRESSED IN: 10 plant structures; EXPRESSED DURING: 4 anthesis, F mature embryo stage, petal differentiation and expansion stage, E expanded cotyledon stage, D bilateral stage; BEST *Arabidopsis thaliana* protein match is: unknown protein (TAIR:AT4G28170.1); Has 94 Blast hits to 94 proteins in 13 species: Archae - 0; Bacteria - 0; Metazoa - 0; Fungi - 0; Plants - 94; Viruses - 0; Other Eukaryotes - 0 (source: NCBI BLink). | chr1:3715184-3717320 FORWARD LENGTH=531	0.99	1.36
AT4G39800	MI-1-P SYNTHASE, MIPS1, ATMIPS1, ATIPS1 | myo-inositol-1-phosphate synthase 1 | chr4:18469348-18471967 REVERSE LENGTH=1921	0.99	0.91
AT1G63300	Myosin heavy chain-related protein | chr1:23482193-23486220 FORWARD LENGTH=3243	0.99	0.93
AT4G16260	Glycosyl hydrolase superfamily protein | chr4:9200010-9201552 REVERSE LENGTH=1316	0.98	0.98
AT1G52190	Major facilitator superfamily protein | chr1:19434509-19438971 FORWARD LENGTH=2284	0.98	0.97
AT1G67260	TCP1 | TCP family transcription factor chr1:25167462-25169307 REVERSE LENGTH=1307	0.98	0.98
AT1G26945	KDR | basic helix-loop-helix (bHLH) DNA-binding superfamily protein | chr1:9351454-9352761 FORWARD LENGTH=689	0.98	2.10
AT5G55550	RNA-binding (RRM/RBD/RNP motifs) family protein | chr5:22502064-22504011 REVERSE LENGTH=1640	0.97	0.67
AT3G28420	Putative membrane lipoprotein | chr3:10654470-10655388 REVERSE LENGTH=919	0.97	1.88
AT3G17185	TASIR-ARF, TAS3, ATTAS3 | TAS3/TASIR-ARF (TRANS-ACTING SIRNA3); other RNA | chr3:5861491-5862437 FORWARD LENGTH=947	0.97	0.61
AT4G32460	Protein of unknown function, DUF642 | chr4:15662266-15664948 REVERSE LENGTH=1257	0.96	1.52
AT1G76960	unknown protein; FUNCTIONS IN: molecular_function unknown; INVOLVED IN: biological_process unknown; LOCATED IN: endomembrane system; EXPRESSED IN: 9 plant structures; EXPRESSED DURING: 8 growth stages; Has 8 Blast hits to 8 proteins in 2 species: Archae - 0; Bacteria - 0; Metazoa - 0; Fungi - 0; Plants - 8; Viruses - 0; Other Eukaryotes - 0 (source: NCBI BLink). | chr1:28920457-28920956 REVERSE LENGTH=388	0.96	0.99
AT1G78040	Pollen Ole e 1 allergen and extensin family protein | chr1:29345838-29347107 FORWARD LENGTH=938	0.96	0.86
AT1G53800	unknown protein; BEST *Arabidopsis thaliana* protein match is: unknown protein (TAIR:AT1G53250.1); Has 1136 Blast hits to 882 proteins in 242 species: Archae - 2; Bacteria - 216; Metazoa - 257; Fungi - 77; Plants - 87; Viruses - 4; Other Eukaryotes - 493 (source: NCBI BLink). | chr1:20081730-20084500 FORWARD LENGTH=2045	0.96	1.23
AT5G50335	unknown protein; Has 30201 Blast hits to 17322 proteins in 780 species: Archae - 12; Bacteria - 1396; Metazoa - 17338; Fungi - 3422; Plants - 5037; Viruses - 0; Other Eukaryotes - 2996 (source: NCBI BLink). | chr5:20489094-20489727 REVERSE LENGTH=634	0.96	0.90
AT4G30180	sequence-specific DNA binding transcription factors;transcription regulators | chr4:14768936-14769648 FORWARD LENGTH=713	0.95	1.04
AT4G09890	Protein of unknown function (DUF3511) | chr4:6218396-6218927 FORWARD LENGTH=532	0.95	0.87
AT1G60960	IRT3, ATIRT3 | iron regulated transporter 3 | chr1:22445310-22447214 REVERSE LENGTH=1532	0.95	0.63
AT4G11830	PLDGAMMA2 | phospholipase D gamma 2 | chr4:7115736-7121245 REVERSE LENGTH=3820	0.95	1.41
AT4G14130	XTR7, XTH15 | xyloglucan endotransglucosylase/hydrolase 15 | chr4:8137051-8138281 REVERSE LENGTH=1065	0.95	0.72
AT1G11545	XTH8 | xyloglucan endotransglucosylase/hydrolase 8 | chr1:3878550-3880361 REVERSE LENGTH=1132	0.94	1.14
AT1G64670	BDG1 | alpha/beta-Hydrolases superfamily protein | chr1:24030820-24033556 REVERSE LENGTH=1662	0.94	0.96
AT2G44500	O-fucosyltransferase family protein | chr2:18374292-18376790 FORWARD LENGTH=2311	0.94	0.76
AT5G48900	Pectin lyase-like superfamily protein | chr5:19825137-19829092 FORWARD LENGTH=1540	0.93	1.18
AT4G33070	Thiamine pyrophosphate dependent pyruvate decarboxylase family protein | chr4:15952289-15954771 REVERSE LENGTH=2149	0.93	0.59

Identifier	Description	ColLL-tgaLL logFC	ColLL-ROXYLL logFC
AT5G18030	SAUR-like auxin-responsive protein family chr5:5968435-5968938 FORWARD LENGTH=504	0.93	1.53
AT5G67390	unknown protein; BEST *Arabidopsis thaliana* protein match is: Plant protein of unknown function (DUF863) (TAIR:AT1G69360.1); Has 186 Blast hits to 186 proteins in 18 species: Archae - 0; Bacteria - 0; Metazoa - 0; Fungi - 0; Plants - 170; Viruses - 0; Other Eukaryotes - 16 (source: NCBI BLink). | chr5:26887670-26888634 REVERSE LENGTH=866	0.93	0.72
AT5G62170	unknown protein; BEST *Arabidopsis thaliana* protein match is: unknown protein (TAIR:AT5G51850.1); Has 381 Blast hits to 359 proteins in 81 species: Archae - 0; Bacteria - 16; Metazoa - 101; Fungi - 21; Plants - 99; Viruses - 3; Other Eukaryotes - 141 (source: NCBI BLink). | chr5:24972977-24975549 REVERSE LENGTH=2324	0.92	0.98
AT4G29020	glycine-rich protein | chr4:14304921-14305721 FORWARD LENGTH=801	0.92	1.25
AT1G10820	Protein of unknown function (DUF3755) | chr1:3600910-3605076 REVERSE LENGTH=1547	0.92	1.38
AT4G24275	Identified as a screen for stress-responsive genes. | chr4:12588519-12589062 FORWARD LENGTH=544	0.92	1.30
AT4G35070	SBP (S-ribonuclease binding protein) family protein | chr4:16694170-16695698 FORWARD LENGTH=1427	0.91	1.19
AT5G61160	AACT1 | anthocyanin 5-aromatic acyltransferase 1 | chr5:24608724-24610304 FORWARD LENGTH=1581	0.91	0.70
AT1G58460	unknown protein; Has 35 Blast hits to 35 proteins in 8 species: Archae - 0; Bacteria - 0; Metazoa - 0; Fungi - 0; Plants - 35; Viruses - 0; Other Eukaryotes - 0 (source: NCBI BLink). | chr1:21721404-21722429 FORWARD LENGTH=534	0.91	0.79
AT3G26900	SKL1, ATSKL1 | shikimate kinase like 1 | chr3:9912209-9914514 REVERSE LENGTH=1038	0.91	0.78
AT5G15265	unknown protein; FUNCTIONS IN: molecular_function unknown; INVOLVED IN: biological_process unknown; LOCATED IN: endomembrane system; Has 5 Blast hits to 5 proteins in 3 species: Archae - 0; Bacteria - 0; Metazoa - 0; Fungi - 0; Plants - 5; Viruses - 0; Other Eukaryotes - 0 (source: NCBI BLink). | chr5:4956501-4957533 FORWARD LENGTH=438	0.90	0.86
AT1G10550	XTH33, XET | xyloglucan:xyloglucosyl transferase 33 | chr1:3479153-3480988 REVERSE LENGTH=1068	0.89	1.15
AT3G03820	SAUR-like auxin-responsive protein family chr3:976933-977223 REVERSE LENGTH=291	0.89	1.00
AT1G62770	Plant invertase/pectin methylesterase inhibitor superfamily protein | chr1:23245886-23246890 REVERSE LENGTH=868	0.89	0.68
AT1G01120	KCS1 | 3-ketoacyl-CoA synthase 1 | chr1:57269-59167 REVERSE LENGTH=1899	0.89	1.04
AT5G22580	Stress responsive A/B Barrel Domain | chr5:7502674-7503449 FORWARD LENGTH=683	0.89	1.00
AT2G48020	Major facilitator superfamily protein | chr2:19644100-19647178 FORWARD LENGTH=1765	0.89	1.03
AT5G12940	Leucine-rich repeat (LRR) family protein | chr5:4087712-4089004 FORWARD LENGTH=1293	0.88	1.15
AT5G07030	Eukaryotic aspartyl protease family protein | chr5:2183360-2185972 REVERSE LENGTH=1863	0.88	1.15
AT4G38825	SAUR-like auxin-responsive protein family chr4:18121526-18122010 FORWARD LENGTH=485	0.88	1.07
AT3G01472	CPuORF33 | conserved peptide upstream open reading frame 33 | chr3:182396-184403 REVERSE LENGTH=1440	0.87	0.68
AT5G48560	basic helix-loop-helix (bHLH) DNA-binding superfamily protein | chr5:19684006-19687151 FORWARD LENGTH=1931	0.87	1.05
AT5G22940	F8H | FRA8 homolog | chr5:7676938-7679179 FORWARD LENGTH=1956	0.87	0.87
AT2G43150	Proline-rich extensin-like family protein | chr2:17945893-17947022 FORWARD LENGTH=1047	0.87	0.85
AT5G56030	HSP81-2 | heat shock protein 81-2 | chr5:22686832-22689471 FORWARD LENGTH=2316	0.87	0.83
AT5G64552	CPuORF22 | conserved peptide upstream open reading frame 22 | chr5:25801528-25804980 REVERSE LENGTH=2533	0.87	0.85
AT4G00050	UNE10 | basic helix-loop-helix (bHLH) DNA-binding superfamily protein | chr4:17792-20066 FORWARD LENGTH=1489	0.86	0.94
AT1G64640	ENODL8, AtENODL8 | early nodulin-like protein 8 | chr1:24022285-24023196 REVERSE LENGTH=818	0.86	1.33
AT2G41820	Leucine-rich repeat protein kinase family protein | chr2:17446744-17450071 FORWARD LENGTH=3256	0.85	1.06

Identifier	Description	ColLL-tgaLL logFC	ColLL-ROXYLL logFC
AT5G07790	unknown protein; BEST *Arabidopsis thaliana* protein match is: unknown protein (TAIR:AT5G61300.1); Has 1807 Blast hits to 1807 proteins in 277 species: Archae - 0; Bacteria - 0; Metazoa - 736; Fungi - 347; Plants - 385; Viruses - 0; Other Eukaryotes - 339 (source: NCBI BLink). | chr5:2483311-2486361 FORWARD LENGTH=2453	0.85	0.92
AT3G59900	ARGOS | auxin-regulated gene involved in organ size | chr3:22129726-22130464 FORWARD LENGTH=739	0.85	1.39
AT3G04290	ATLTL1, LTL1 | Li-tolerant lipase 1 | chr3:1133320-1136316 REVERSE LENGTH=1494	0.84	1.30
AT4G21760	BGLU47 | beta-glucosidase 47 | chr4:11561229-11563950 FORWARD LENGTH=1687	0.84	1.10
AT5G65390	AGP7 | arabinogalactan protein 7 | chr5:26128584-26129338 REVERSE LENGTH=755	0.84	1.30
AT4G00820	iqd17 | IQ-domain 17 | chr4:349116-351550 FORWARD LENGTH=2032	0.83	0.97
AT5G59010	Protein kinase protein with tetratricopeptide repeat domain | chr5:23820368-23823265 REVERSE LENGTH=1936	0.83	0.92
AT1G18400	BEE1 | BR enhanced expression 1 | chr1:6331398-6333743 FORWARD LENGTH=1016	0.83	1.31
AT1G57590	Pectinacetylesterase family protein | chr1:21327360-21329763 REVERSE LENGTH=1489	0.82	0.63
AT4G36110	SAUR-like auxin-responsive protein family chr4:17089949-17090825 FORWARD LENGTH=877	0.82	0.96
AT3G54400	Eukaryotic aspartyl protease family protein | chr3:20140058-20142642 REVERSE LENGTH=1554	0.81	1.17
AT1G53180	unknown protein; FUNCTIONS IN: molecular_function unknown; INVOLVED IN: biological_process unknown; LOCATED IN: cellular_component unknown; EXPRESSED IN: 13 plant structures; EXPRESSED DURING: 6 growth stages; BEST *Arabidopsis thaliana* protein match is: unknown protein (TAIR:AT3G15115.1); Has 58 Blast hits to 56 proteins in 22 species: Archae - 0; Bacteria - 0; Metazoa - 6; Fungi - 4; Plants - 29; Viruses - 0; Other Eukaryotes - 19 (source: NCBI BLink). | chr1:19831441-19832895 FORWARD LENGTH=1386	0.81	0.99
AT2G39920	HAD superfamily, subfamily IIIB acid phosphatase chr2:16663017-16664539 REVERSE LENGTH=1168	0.81	0.89
AT4G13920	AtRLP50, RLP50 | receptor like protein 50 | chr4:8043803-8046559 FORWARD LENGTH=2757	0.81	0.66
AT3G15536	Unknown gene | chr3:5260723-5261322 FORWARD LENGTH=495	0.80	0.82
AT1G53070	Legume lectin family protein | chr1:19778333-19779373 FORWARD LENGTH=1041	0.80	0.91
AT1G28130	GH3.17 | Auxin-responsive GH3 family protein | chr1:9825286-9828067 FORWARD LENGTH=2159	0.79	0.94
AT2G42380	ATBZIP34, BZIP34 | Basic-leucine zipper (bZIP) transcription factor family protein | chr2:17646900-17648945 REVERSE LENGTH=1556	0.79	1.22
AT5G06440	BEST *Arabidopsis thaliana* protein match is: Polyketide cyclase/dehydrase and lipid transport superfamily protein (TAIR:AT3G11720.3); Has 157 Blast hits to 155 proteins in 41 species: Archae - 0; Bacteria - 6; Metazoa - 5; Fungi - 6; Plants - 99; Viruses - 0; Other Eukaryotes - 41 (source: NCBI BLink). | chr5:1964468-1966955 REVERSE LENGTH=1761	0.78	0.83
AT2G29130	LAC2, ATLAC2 | laccase 2 | chr2:12524889-12527747 REVERSE LENGTH=2070	0.77	1.04
AT3G43190	SUS4, ATSUS4 | sucrose synthase 4 | chr3:15179020-15183989 REVERSE LENGTH=2764	0.77	1.01
AT4G21650	Subtilase family protein | chr4:11501198-11504678 REVERSE LENGTH=2439	0.77	0.86
AT1G15550	GA4, ATGA3OX1, GA3OX1 | gibberellin 3-oxidase 1 | chr1:5344478-5346166 REVERSE LENGTH=1256	0.77	1.13
AT5G03120	unknown protein; FUNCTIONS IN: molecular_function unknown; INVOLVED IN: biological_process unknown; LOCATED IN: endomembrane system; EXPRESSED IN: 21 plant structures; EXPRESSED DURING: 13 growth stages; Has 14 Blast hits to 14 proteins in 4 species: Archae - 0; Bacteria - 0; Metazoa - 0; Fungi - 0; Plants - 14; Viruses - 0; Other Eukaryotes - 0 (source: NCBI BLink). | chr5:733979-734943 FORWARD LENGTH=574	0.76	0.84
AT3G16360	AHP4 | HPT phosphotransmitter 4 | chr3:5554474-5555393 FORWARD LENGTH=420	0.76	0.94
AT1G68600	Aluminium activated malate transporter family protein | chr1:25759842-25762934 FORWARD LENGTH=1875	0.75	0.91
AT1G10970	ZIP4, ATZIP4 | zinc transporter 4 precursor | chr1:3665087-3667139 REVERSE LENGTH=1547	0.75	0.60
AT3G12500	ATHCHIB, PR3, PR-3, CHI-B, B-CHI, HCHIB | basic chitinase | chr3:3962382-3963984 REVERSE LENGTH=1127	0.74	0.98

Identifier	Description	ColLL-tgaLL logFC	ColLL-ROXYLL logFC
AT5G04160	Nucleotide-sugar transporter family protein | chr5:1142782-1144912 REVERSE LENGTH=1316	0.74	0.92
AT3G62090	PIL2 | phytochrome interacting factor 3-like 2 | chr3:22988547-22990709 REVERSE LENGTH=1614	0.74	1.20
AT3G18210	2-oxoglutarate (2OG) and Fe(II)-dependent oxygenase superfamily protein | chr3:6237930-6240605 REVERSE LENGTH=1728	0.71	1.00

Table S2 List of 167 genes of cluster 5.

Identifier	Description	Col-ColLL logFC	ColLL-tgaLL logFC	ColLL-ROXYLL logFC
AT4G31430	unknown protein; LOCATED IN: plasma membrane; EXPRESSED IN: 25 plant structures; EXPRESSED DURING: 15 growth stages; Has 35333 Blast hits to 34131 proteins in 2444 species: Archae - 798; Bacteria - 22429; Metazoa - 974; Fungi - 991; Plants - 531; Viruses - 0; Other Eukaryotes - 9610 (source: NCBI BLink). | chr4:15248456-15252529 FORWARD LENGTH=2104	-2.29	0.65	1.84
AT1G19530	unknown protein; FUNCTIONS IN: molecular_function unknown; INVOLVED IN: N-terminal protein myristoylation, anaerobic respiration; LOCATED IN: cellular_component unknown; EXPRESSED IN: leaf apex, inflorescence meristem, hypocotyl, root, flower; EXPRESSED DURING: petal differentiation and expansion stage; Has 47 Blast hits to 47 proteins in 13 species: Archae - 0; Bacteria - 0; Metazoa - 0; Fungi - 0; Plants - 47; Viruses - 0; Other Eukaryotes - 0 (source: NCBI BLink). | chr1:6763915-6764971 FORWARD LENGTH=700	-2.21	1.04	1.56
AT1G75920	GDSL-like Lipase/Acylhydrolase superfamily protein | chr1:28505554-28507168 FORWARD LENGTH=1106	-2.04	1.68	2.28
AT4G08040	ACS11 | 1-aminocyclopropane-1-carboxylate synthase 11 | chr4:4887112-4888939 FORWARD LENGTH=1383	-1.54	1.14	0.99
AT2G18480	Major facilitator superfamily protein | chr2:8009323-8011255 REVERSE LENGTH=1798	-1.53	0.61	1.38
AT4G04570	CRK40 | cysteine-rich RLK (RECEPTOR-like protein kinase) 40 | chr4:2289959-2292755 FORWARD LENGTH=2089	-1.53	0.37	1.84
AT5G10430	AGP4, ATAGP4 | arabinogalactan protein 4 | chr5:3277532-3278313 REVERSE LENGTH=782	-1.52	1.11	1.85
AT2G21540	ATSFH3, SFH3 | SEC14-like 3 | chr2:9220556-9224496 REVERSE LENGTH=2106	-1.52	1.43	1.57
AT4G01680	MYB55 | myb domain protein 55 | chr4:716021-717415 REVERSE LENGTH=1248	-1.51	1.31	1.21
AT5G22940	F8H | FRA8 homolog | chr5:7676938-7679179 FORWARD LENGTH=1956	-1.47	0.87	0.87
AT5G22820	ARM repeat superfamily protein | chr5:7623440-7626975 REVERSE LENGTH=1997	-1.47	1.46	1.59
AT1G67265	DVL3, RTFL21 | ROTUNDIFOLIA like 21 | chr1:25175558-25176202 REVERSE LENGTH=645	-1.43	0.42	1.17
AT2G46320	Mitochondrial substrate carrier family protein | chr2:19015813-19018230 FORWARD LENGTH=1497	-1.40	1.05	1.31
AT5G25760	PEX4, UBC21 | peroxin4 | chr5:8967655-8969349 FORWARD LENGTH=745	-1.39	2.06	1.78
AT1G10820	Protein of unknown function (DUF3755) | chr1:3600910-3605076 REVERSE LENGTH=1547	-1.38	0.92	1.38
AT2G14900	Gibberellin-regulated family protein | chr2:6404175-6405330 FORWARD LENGTH=649	-1.33	0.69	1.04
AT1G10550	XTH33, XET | xyloglucan:xyloglucosyl transferase 33 | chr1:3479153-3480988 REVERSE LENGTH=1068	-1.33	0.89	1.15
AT3G07610	IBM1 | Transcription factor jumonji (jmjC) domain-containing protein | chr3:2426148-2432876 FORWARD LENGTH=3084	-1.32	1.75	0.85
AT5G66600	Protein of unknown function, DUF547 | chr5:26575000-26578826 REVERSE LENGTH=2461	-1.31	1.71	1.33
AT5G17920	ATCIMS, ATMETS, ATMS1 | Cobalamin-independent synthase family protein | chr5:5935038-5939487 FORWARD LENGTH=2771	-1.26	1.61	1.25
AT1G74670	Gibberellin-regulated family protein | chr1:28053286-28054149 FORWARD LENGTH=654	-1.25	0.63	1.29

Identifier	Description	Col-ColLL logFC	ColLL-tgaLL logFC	ColLL-ROXYLL logFC
AT1G11120	unknown protein; FUNCTIONS IN: molecular_function unknown; INVOLVED IN: biological_process unknown; LOCATED IN: cellular_component unknown; EXPRESSED IN: 10 plant structures; EXPRESSED DURING: 4 anthesis, F mature embryo stage, petal differentiation and expansion stage, E expanded cotyledon stage, D bilateral stage; BEST *Arabidopsis thaliana* protein match is: unknown protein (TAIR:AT4G28170.1); Has 94 Blast hits to 94 proteins in 13 species: Archae - 0; Bacteria - 0; Metazoa - 0; Fungi - 0; Plants - 94; Viruses - 0; Other Eukaryotes - 0 (source: NCBI BLink). | chr1:3715184-3717320 FORWARD LENGTH=531	-1.20	0.99	1.36
AT5G19210	P-loop containing nucleoside triphosphate hydrolases superfamily protein | chr5:6461391-6463866 FORWARD LENGTH=1647	-1.18	0.64	2.23
AT4G30180	sequence-specific DNA binding transcription factors;transcription regulators | chr4:14768936-14769648 FORWARD LENGTH=713	-1.17	0.95	1.04
AT4G14130	XTR7, XTH15 | xyloglucan endotransglucosylase/hydrolase 15 | chr4:8137051-8138281 REVERSE LENGTH=1065	-1.14	0.95	0.72
AT2G23760	BLH4, SAW2 | BEL1-like homeodomain 4 | chr2:10107709-10113213 REVERSE LENGTH=2386	-1.13	0.28	1.81
AT4G32280	IAA29 | indole-3-acetic acid inducible 29 | chr4:15583387-15584769 FORWARD LENGTH=989	-1.13	0.60	1.44
AT3G53350	RIP4 | ROP interactive partner 4 | chr3:19780091-19782680 REVERSE LENGTH=1496	-1.13	0.41	1.20
AT2G37550	ASP1, AGD7 | ARF-GAP domain 7 | chr2:15755097-15757601 REVERSE LENGTH=1882	-1.11	0.84	1.13
AT4G16260	Glycosyl hydrolase superfamily protein | chr4:9200010-9201552 REVERSE LENGTH=1316	-1.11	0.98	0.98
AT4G10160	RING/U-box superfamily protein | chr4:6336023-6337332 FORWARD LENGTH=709	-1.10	0.58	1.04
AT5G15265	unknown protein; FUNCTIONS IN: molecular_function unknown; INVOLVED IN: biological_process unknown; LOCATED IN: endomembrane system; Has 5 Blast hits to 5 proteins in 3 species: Archae - 0; Bacteria - 0; Metazoa - 0; Fungi - 0; Plants - 5; Viruses - 0; Other Eukaryotes - 0 (source: NCBI BLink). | chr5:4956501-4957533 FORWARD LENGTH=438	-1.09	0.90	0.86
AT5G59780	MYB59, ATMYB59, ATMYB59-1 | myb domain protein 59 | chr5:24082197-24083431 REVERSE LENGTH=1128	-1.09	0.53	0.92
AT3G29370	unknown protein; BEST *Arabidopsis thaliana* protein match is: unknown protein (TAIR:AT5G39240.1); Has 16 Blast hits to 16 proteins in 5 species: Archae - 0; Bacteria - 0; Metazoa - 0; Fungi - 0; Plants - 16; Viruses - 0; Other Eukaryotes - 0 (source: NCBI BLink). | chr3:11278589-11279108 FORWARD LENGTH=520	-1.09	0.29	1.01
AT5G57150	basic helix-loop-helix (bHLH) DNA-binding superfamily protein | chr5:23152186-23154264 FORWARD LENGTH=1827	-1.07	0.99	0.70
AT2G44500	O-fucosyltransferase family protein | chr2:18374292-18376790 FORWARD LENGTH=2311	-1.06	0.94	0.76
AT2G22122	unknown protein; Has 35333 Blast hits to 34131 proteins in 2444 species: Archae - 798; Bacteria - 22429; Metazoa - 974; Fungi - 991; Plants - 531; Viruses - 0; Other Eukaryotes - 9610 (source: NCBI BLink). | chr2:9403264-9403808 FORWARD LENGTH=545	-1.06	0.58	1.09
AT1G26208	other RNA | chr1:9066636-9068432 REVERSE LENGTH=1499	-1.06	0.66	0.63
AT3G61880	CYP78A9 | cytochrome p450 78a9 | chr3:22905868-22907958 REVERSE LENGTH=1919	-1.03	1.42	2.15
AT4G06701	other RNA | chr4:3939600-3940720 REVERSE LENGTH=511	-1.03	0.49	1.13
AT3G58620	TTL4 | tetratricopetide-repeat thioredoxin-like 4 | chr3:21680326-21683135 FORWARD LENGTH=2296	-1.03	0.39	0.86
AT3G58120	ATBZIP61, BZIP61 | Basic-leucine zipper (bZIP) transcription factor family protein | chr3:21520974-21523327 REVERSE LENGTH=1554	-1.03	0.63	0.85

Identifier	Description	Col-ColLL logFC	ColLL-tgaLL logFC	ColLL-ROXYLL logFC
AT5G03120	unknown protein; FUNCTIONS IN: molecular_function unknown; INVOLVED IN: biological_process unknown; LOCATED IN: endomembrane system; EXPRESSED IN: 21 plant structures; EXPRESSED DURING: 13 growth stages; Has 14 Blast hits to 14 proteins in 4 species: Archae - 0; Bacteria - 0; Metazoa - 0; Fungi - 0; Plants - 14; Viruses - 0; Other Eukaryotes - 0 (source: NCBI BLink). | chr5:733979-734943 FORWARD LENGTH=574	-1.02	0.76	0.84
AT3G23050	IAA7, AXR2 | indole-3-acetic acid 7 | chr3:8194711-8196514 FORWARD LENGTH=990	-1.02	0.51	0.68
AT4G20910	HEN1, CRM2 | double-stranded RNA binding protein-related / DsRBD protein-related | chr4:11186084-11190691 REVERSE LENGTH=3125	-0.99	1.60	0.83
AT5G02760	Protein phosphatase 2C family protein | chr5:625254-627124 FORWARD LENGTH=1543	-0.97	0.40	1.57
AT5G50335	unknown protein; Has 30201 Blast hits to 17322 proteins in 780 species: Archae - 12; Bacteria - 1396; Metazoa - 17338; Fungi - 3422; Plants - 5037; Viruses - 0; Other Eukaryotes - 2996 (source: NCBI BLink). | chr5:20489094-20489727 REVERSE LENGTH=634	-0.96	0.96	0.90
AT5G19810	Proline-rich extensin-like family protein | chr5:6693052-6693801 FORWARD LENGTH=750	-0.95	0.62	0.92
AT1G51690	ATB ALPHA, B ALPHA | protein phosphatase 2A 55 kDa regulatory subunit B alpha isoform | chr1:19164063-19170446 FORWARD LENGTH=3741	-0.95	0.44	1.37
AT5G59010	Protein kinase protein with tetratricopeptide repeat domain | chr5:23820368-23823265 REVERSE LENGTH=1936	-0.93	0.83	0.92
AT5G24570	unknown protein; Has 30201 Blast hits to 17322 proteins in 780 species: Archae - 12; Bacteria - 1396; Metazoa - 17338; Fungi - 3422; Plants - 5037; Viruses - 0; Other Eukaryotes - 2996 (source: NCBI BLink). | chr5:8405681-8406132 REVERSE LENGTH=452	-0.93	0.46	0.87
AT2G48020	Major facilitator superfamily protein | chr2:19644100-19647178 FORWARD LENGTH=1765	-0.92	0.89	1.03
AT1G09270	IMPA-4 | importin alpha isoform 4 | chr1:2994369-2998222 FORWARD LENGTH=2062	-0.92	0.71	1.38
AT4G23450	AIRP1, AtAIRP1 | RING/U-box superfamily protein | chr4:12240803-12242706 REVERSE LENGTH=1031	-0.91	1.76	0.76
AT5G65430	GRF8, GF14 KAPPA | general regulatory factor 8 | chr5:26148201-26150342 REVERSE LENGTH=1173	-0.90	0.85	1.26
AT4G24275	Identified as a screen for stress-responsive genes. | chr4:12588519-12589062 FORWARD LENGTH=544	-0.90	0.92	1.30
AT1G47820	unknown protein; BEST *Arabidopsis thaliana* protein match is: unknown protein (TAIR:AT1G47813.1); Has 29 Blast hits to 29 proteins in 9 species: Archae - 0; Bacteria - 0; Metazoa - 0; Fungi - 0; Plants - 29; Viruses - 0; Other Eukaryotes - 0 (source: NCBI BLink). | chr1:17612038-17612548 FORWARD LENGTH=511	-0.90	0.26	1.28
AT3G23030	IAA2 | indole-3-acetic acid inducible 2 | chr3:8180768-8181800 REVERSE LENGTH=941	-0.87	1.00	1.32
AT5G65390	AGP7 | arabinogalactan protein 7 | chr5:26128584-26129338 REVERSE LENGTH=755	-0.87	0.84	1.30
AT1G15550	GA4, ATGA3OX1, GA3OX1 | gibberellin 3-oxidase 1 | chr1:5344478-5346166 REVERSE LENGTH=1256	-0.87	0.77	1.13
AT3G12500	ATHCHIB, PR3, PR-3, CHI-B, B-CHI, HCHIB | basic chitinase | chr3:3962382-3963984 REVERSE LENGTH=1127	-0.87	0.74	0.98
AT3G02410	ICME-LIKE2 | alpha/beta-Hydrolases superfamily protein | chr3:492118-494948 REVERSE LENGTH=1335	-0.86	0.45	1.08
AT4G21160	ZAC | Calcium-dependent ARF-type GTPase activating protein family | chr4:11284238-11286767 FORWARD LENGTH=1404	-0.86	1.53	0.47
AT4G35070	SBP (S-ribonuclease binding protein) family protein | chr4:16694170-16695698 FORWARD LENGTH=1427	-0.85	0.91	1.19
AT5G61160	AACT1 | anthocyanin 5-aromatic acyltransferase 1 | chr5:24608724-24610304 FORWARD LENGTH=1581	-0.85	0.91	0.70
AT2G24300	Calmodulin-binding protein | chr2:10340816-10343736 FORWARD LENGTH=2214	-0.84	1.10	1.02
AT2G15130	Plant basic secretory protein (BSP) family protein | chr2:6564945-6566004 FORWARD LENGTH=1060	-0.84	0.39	0.96
AT2G28085	SAUR-like auxin-responsive protein family chr2:11968120-11968620 REVERSE LENGTH=501	-0.84	0.87	0.41

Identifier	Description	Col-ColLL logFC	ColLL-tgaLL logFC	ColLL-ROXYLL logFC
AT3G50970	LTI30, XERO2 | dehydrin family protein | chr3:18940777-18941554 FORWARD LENGTH=778	-0.83	0.65	0.79
AT1G62770	Plant invertase/pectin methylesterase inhibitor superfamily protein | chr1:23245886-23246890 REVERSE LENGTH=868	-0.83	0.89	0.68
AT1G53180	unknown protein; FUNCTIONS IN: molecular_function unknown; INVOLVED IN: biological_process unknown; LOCATED IN: cellular_component unknown; EXPRESSED IN: 13 plant structures; EXPRESSED DURING: 6 growth stages; BEST *Arabidopsis thaliana* protein match is: unknown protein (TAIR:AT3G15115.1); Has 58 Blast hits to 56 proteins in 22 species: Archae - 0; Bacteria - 0; Metazoa - 6; Fungi - 4; Plants - 29; Viruses - 0; Other Eukaryotes - 19 (source: NCBI BLink). | chr1:19831441-19832895 FORWARD LENGTH=1386	-0.83	0.81	0.99
AT1G52750	alpha/beta-Hydrolases superfamily protein | chr1:19646465-19649261 REVERSE LENGTH=2275	-0.83	1.00	1.55
AT1G78970	LUP1, ATLUP1 | lupeol synthase 1 | chr1:29703062-29707844 FORWARD LENGTH=2642	-0.80	1.15	1.85
AT1G63380	NAD(P)-binding Rossmann-fold superfamily protein | chr1:23505557-23506391 FORWARD LENGTH=709	-0.79	1.99	1.52
AT1G28130	GH3.17 | Auxin-responsive GH3 family protein | chr1:9825286-9828067 FORWARD LENGTH=2159	-0.78	0.79	0.94
AT5G06930	LOCATED IN: chloroplast; EXPRESSED IN: 15 plant structures; EXPRESSED DURING: 7 growth stages; BEST *Arabidopsis thaliana* protein match is: nucleolar protein gar2-related (TAIR:AT2G42320.2); Has 3369 Blast hits to 1526 proteins in 313 species: Archae - 2; Bacteria - 910; Metazoa - 754; Fungi - 336; Plants - 137; Viruses - 11; Other Eukaryotes - 1219 (source: NCBI BLink). | chr5:2144999-2148039 FORWARD LENGTH=2502	-0.77	1.06	1.26
AT4G32460	Protein of unknown function, DUF642 | chr4:15662266-15664948 REVERSE LENGTH=1257	-0.77	0.96	1.52
AT3G62090	PIL2 | phytochrome interacting factor 3-like 2 | chr3:22988547-22990709 REVERSE LENGTH=1614	-0.77	0.74	1.20
AT1G26440	ATUPS5, UPS5 | ureide permease 5 | chr1:9143967-9145987 REVERSE LENGTH=1698	-0.76	0.77	1.38
AT3G54030	Protein kinase protein with tetratricopeptide repeat domain | chr3:20010927-20013693 FORWARD LENGTH=1911	-0.76	0.58	1.23
AT4G03415	Protein phosphatase 2C family protein | chr4:1503708-1506500 REVERSE LENGTH=1732	-0.76	1.20	0.38
AT4G38825	SAUR-like auxin-responsive protein family chr4:18121526-18122010 FORWARD LENGTH=485	-0.75	0.88	1.07
AT5G23210	SCPL34 | serine carboxypeptidase-like 34 | chr5:7810855-7815039 FORWARD LENGTH=1848	-0.75	1.22	1.44
AT4G04745	unknown protein; BEST *Arabidopsis thaliana* protein match is: unknown protein (TAIR:AT4G21902.1); Has 32 Blast hits to 32 proteins in 9 species: Archae - 0; Bacteria - 0; Metazoa - 0; Fungi - 0; Plants - 32; Viruses - 0; Other Eukaryotes - 0 (source: NCBI BLink). | chr4:2412754-2413328 REVERSE LENGTH=575	-0.73	0.52	0.94
AT4G11830	PLDGAMMA2 | phospholipase D gamma 2 | chr4:7115736-7121245 REVERSE LENGTH=3820	-0.72	0.95	1.41
AT5G12880	proline-rich family protein | chr5:4068519-4068962 REVERSE LENGTH=444	-0.72	1.25	0.91
AT1G58460	unknown protein; Has 35 Blast hits to 35 proteins in 8 species: Archae - 0; Bacteria - 0; Metazoa - 0; Fungi - 0; Plants - 35; Viruses - 0; Other Eukaryotes - 0 (source: NCBI BLink). | chr1:21721404-21722429 FORWARD LENGTH=534	-0.70	0.91	0.79
AT2G10606	MIR396A | MIR396A; miRNA | chr2:4142323-4142473 REVERSE LENGTH=151	-0.70	1.03	1.21
AT2G29130	LAC2, ATLAC2 | laccase 2 | chr2:12524889-12527747 REVERSE LENGTH=2070	-0.69	0.77	1.04
AT1G19070	F-box family protein | chr1:6584454-6584705 FORWARD LENGTH=252	-0.66	0.08	1.17
AT1G52190	Major facilitator superfamily protein | chr1:19434509-19438971 FORWARD LENGTH=2284	-0.66	0.98	0.97
AT1G18400	BEE1 | BR enhanced expression 1 | chr1:6331398-6333743 FORWARD LENGTH=1016	-0.65	0.83	1.31
AT5G19530	ACL5 | S-adenosyl-L-methionine-dependent methyltransferases superfamily protein | chr5:6588958-6591211 REVERSE LENGTH=1358	-0.65	0.27	0.96

Identifier	Description	Col-ColLL logFC	ColLL-tgaLL logFC	ColLL-ROXYLL logFC
AT2G17500	Auxin efflux carrier family protein | chr2:7606784-7609278 FORWARD LENGTH=1638	-0.65	1.46	0.22
AT1G33700	Beta-glucosidase, GBA2 type family protein | chr1:12208308-12214182 REVERSE LENGTH=3482	-0.64	0.87	0.55
AT2G34410	O-acetyltransferase family protein | chr2:14518406-14522622 FORWARD LENGTH=2391	-0.64	0.11	1.03
AT3G43740	Leucine-rich repeat (LRR) family protein | chr3:15644054-15645662 FORWARD LENGTH=946	-0.64	0.34	0.91
AT2G42380	ATBZIP34, BZIP34 | Basic-leucine zipper (bZIP) transcription factor family protein | chr2:17646900-17648945 REVERSE LENGTH=1556	-0.64	0.79	1.22
AT1G67340	HCP-like superfamily protein with MYND-type zinc finger | chr1:25230265-25231840 FORWARD LENGTH=1416	-0.63	0.87	0.57
AT1G01060	LHY, LHY1 | Homeodomain-like superfamily protein | chr1:33379-37757 REVERSE LENGTH=2517	-0.63	0.80	1.55
AT1G78970	LUP1, ATLUP1 | lupeol synthase 1 | chr1:29703340-29707844 FORWARD LENGTH=2477	-0.61	1.01	1.47
AT3G16360	AHP4 | HPT phosphotransmitter 4 | chr3:5554474-5555393 FORWARD LENGTH=420	-0.61	0.76	0.94
AT3G62720	ATXT1, XT1, XXT1 | xylosyltransferase 1 | chr3:23201156-23202913 FORWARD LENGTH=1660	-0.60	0.44	0.93
AT3G63440	ATCKX6, CKX6, ATCKX7 | cytokinin oxidase/dehydrogenase 6 | chr3:23424157-23426536 FORWARD LENGTH=2007	-0.60	1.95	2.39
AT1G04240	SHY2, IAA3 | AUX/IAA transcriptional regulator family protein | chr1:1128188-1129551 REVERSE LENGTH=1178	-0.59	0.70	0.98
AT3G18210	2-oxoglutarate (2OG) and Fe(II)-dependent oxygenase superfamily protein | chr3:6237930-6240605 REVERSE LENGTH=1728	-0.59	0.71	1.00
AT5G20730	NPH4, MSG1, IAA21, ARF7, TIR5, BIP | Transcriptional factor B3 family protein / auxin-responsive factor AUX/IAA-related | chr5:7016445-7022042 REVERSE LENGTH=4292	-0.59	1.85	0.69
AT1G26945	KDR | basic helix-loop-helix (bHLH) DNA-binding superfamily protein | chr1:9351454-9352761 FORWARD LENGTH=689	-0.58	0.98	2.10
AT3G01472	CPuORF33 | conserved peptide upstream open reading frame 33 | chr3:182396-184403 REVERSE LENGTH=1440	-0.57	0.87	0.68
AT1G63300	Myosin heavy chain-related protein | chr1:23482193-23486220 FORWARD LENGTH=3243	-0.56	0.99	0.93
AT5G54510	GH3.6, DFL1 | Auxin-responsive GH3 family protein | chr5:22131093-22133678 REVERSE LENGTH=2181	-0.56	1.18	1.52
AT3G12710	DNA glycosylase superfamily protein | chr3:4040324-4041982 REVERSE LENGTH=1341	-0.56	0.72	0.95
AT3G28700	Protein of unknown function (DUF185) | chr3:10759559-10762114 FORWARD LENGTH=1717	-0.55	1.17	1.19
AT2G14890	AGP9 | arabinogalactan protein 9 | chr2:6399621-6401059 FORWARD LENGTH=938	-0.55	0.39	0.97
AT4G09890	Protein of unknown function (DUF3511) | chr4:6218396-6218927 FORWARD LENGTH=532	-0.55	0.95	0.87
AT1G20190	ATEXPA11, EXP11, ATEXP11, ATHEXP ALPHA 1.14, EXPA11 | expansin 11 | chr1:6998489-6999817 REVERSE LENGTH=1139	-0.55	0.68	0.97
AT1G37150	HCS2 | holocarboxylase synthetase 2 | chr1:14174981-14177302 REVERSE LENGTH=1101	-0.55	1.56	0.59
AT5G48560	basic helix-loop-helix (bHLH) DNA-binding superfamily protein | chr5:19684006-19687151 FORWARD LENGTH=1931	-0.54	0.87	1.05
AT3G45050	unknown protein; FUNCTIONS IN: molecular_function unknown; INVOLVED IN: biological_process unknown; LOCATED IN: chloroplast; EXPRESSED IN: 22 plant structures; EXPRESSED DURING: 13 growth stages; Has 28 Blast hits to 28 proteins in 12 species: Archae - 0; Bacteria - 2; Metazoa - 0; Fungi - 0; Plants - 26; Viruses - 0; Other Eukaryotes - 0 (source: NCBI BLink). | chr3:16475966-16477524 FORWARD LENGTH=951	-0.53	0.65	1.50
AT5G42690	Protein of unknown function, DUF547 | chr5:17116428-17119838 REVERSE LENGTH=2102	-0.53	1.41	0.53
AT2G45315	other RNA | chr2:18682108-18683810 REVERSE LENGTH=1448	-0.50	0.91	0.33

Identifier	Description	Col-ColLL logFC	ColLL-tgaLL logFC	ColLL-ROXYLL logFC
AT3G06770	Pectin lyase-like superfamily protein | chr3:2134800-2137228 REVERSE LENGTH=1855	-0.49	0.34	1.05
AT3G62720	ATXT1, XT1, XXT1 | xylosyltransferase 1 | chr3:23201117-23202907 FORWARD LENGTH=1791	-0.49	0.50	0.87
AT4G31000	Calmodulin-binding protein | chr4:15103159-15105979 FORWARD LENGTH=2112	-0.49	0.37	0.95
AT4G02330	ATPMEPCRB | Plant invertase/pectin methylesterase inhibitor superfamily | chr4:1032413-1035037 FORWARD LENGTH=1897	-0.48	0.62	0.89
AT4G38400	ATEXLA2, EXPL2, ATEXPL2, ATHEXP BETA 2.2, EXLA2 | expansin-like A2 | chr4:17978443-17979740 REVERSE LENGTH=1105	-0.47	0.60	0.90
AT1G19840	SAUR-like auxin-responsive protein family chr1:6872794-6873255 REVERSE LENGTH=462	-0.46	0.68	0.90
AT3G15540	IAA19, MSG2 | indole-3-acetic acid inducible 19 | chr3:5264024-5265678 FORWARD LENGTH=970	-0.46	1.13	1.37
AT1G61240	Protein of unknown function (DUF707) | chr1:22582024-22585203 FORWARD LENGTH=1674	-0.46	0.25	1.05
AT5G61910	DCD (Development and Cell Death) domain protein | chr5:24859878-24864120 REVERSE LENGTH=2899	-0.46	1.23	0.31
AT2G38325	MIR390A, MIR390 | MIR390A; miRNA | chr2:16061954-16062060 FORWARD LENGTH=107	-0.46	0.59	0.92
AT3G25620	ABC-2 type transporter family protein | chr3:9316074-9319571 REVERSE LENGTH=2688	-0.45	1.16	1.14
AT1G72880	Survival protein SurE-like phosphatase/nucleotidase | chr1:27423385-27426140 REVERSE LENGTH=1663	-0.45	1.24	0.30
AT5G48900	Pectin lyase-like superfamily protein | chr5:19825137-19829092 FORWARD LENGTH=1540	-0.44	0.93	1.18
AT4G35900	FD, FD-1, atbzip14 | Basic-leucine zipper (bZIP) transcription factor family protein | chr4:17004595-17006287 FORWARD LENGTH=1344	-0.44	1.37	0.89
AT2G14890	AGP9 | arabinogalactan protein 9 | chr2:6399621-6400982 FORWARD LENGTH=1362	-0.44	0.56	0.87
AT4G19880	Glutathione S-transferase family protein | chr4:10784391-10786423 REVERSE LENGTH=1496	-0.44	0.67	1.22
AT5G62170	unknown protein; BEST *Arabidopsis thaliana* protein match is: unknown protein (TAIR:AT5G51850.1); Has 381 Blast hits to 359 proteins in 81 species: Archae - 0; Bacteria - 16; Metazoa - 101; Fungi - 21; Plants - 99; Viruses - 3; Other Eukaryotes - 141 (source: NCBI BLink). | chr5:24972977-24975549 REVERSE LENGTH=2324	-0.43	0.92	0.98
AT1G27580	Protein of unknown function (DUF295) | chr1:9589933-9591075 REVERSE LENGTH=1095	-0.43	0.56	0.90
AT3G45160	Putative membrane lipoprotein | chr3:16533451-16534082 REVERSE LENGTH=549	-0.43	0.88	0.52
AT1G64640	ENODL8, AtENODL8 | early nodulin-like protein 8 | chr1:24022285-24023196 REVERSE LENGTH=818	-0.42	0.86	1.33
AT1G02920	ATGSTF7, GST11, ATGSTF8, GSTF7, ATGST11 | glutathione S-transferase 7 | chr1:658657-659771 REVERSE LENGTH=925	-0.41	0.99	0.01
AT3G28420	Putative membrane lipoprotein | chr3:10654470-10655388 REVERSE LENGTH=919	-0.41	0.97	1.88
AT2G40610	ATEXPA8, EXP8, ATEXP8, ATHEXP ALPHA 1.11, EXPA8 | expansin A8 | chr2:16948863-16950557 REVERSE LENGTH=1105	-0.41	1.20	1.36
AT1G01120	KCS1 | 3-ketoacyl-CoA synthase 1 | chr1:57269-59167 REVERSE LENGTH=1899	-0.41	0.89	1.04
AT1G11545	XTH8 | xyloglucan endotransglucosylase/hydrolase 8 | chr1:3878550-3880361 REVERSE LENGTH=1132	-0.40	0.94	1.14
AT4G16745	Exostosin family protein | chr4:9411840-9414897 FORWARD LENGTH=2173	-0.40	1.00	0.30
AT2G03140	alpha/beta-Hydrolases superfamily protein | chr2:941912-950034 FORWARD LENGTH=6056	-0.39	1.03	1.13
AT1G78040	Pollen Ole e 1 allergen and extensin family protein | chr1:29345838-29347107 FORWARD LENGTH=938	-0.38	0.96	0.86
AT3G15605	nucleic acid binding | chr3:5288093-5290941 FORWARD LENGTH=1667	-0.37	1.43	0.87
AT4G00820	iqd17 | IQ-domain 17 | chr4:349116-351550 FORWARD LENGTH=2032	-0.34	0.83	0.97
AT3G49110	PRX33, PRXCA, ATPRX33, ATPCA | peroxidase CA | chr3:18200664-18203142 FORWARD LENGTH=1365	-0.31	1.92	1.34

Identifier	Description	Col-ColLL logFC	ColLL-tgaLL logFC	ColLL-ROXYLL logFC
AT5G09220	AAP2 | amino acid permease 2 | chr5:2866252-2869054 FORWARD LENGTH=1794	-0.31	1.24	1.13
AT3G10580	Homeodomain-like superfamily protein | chr3:3307051-3308233 REVERSE LENGTH=899	-0.30	0.49	0.91
AT5G55230	ATMAP65-1, MAP65-1 | microtubule-associated proteins 65-1 | chr5:22402028-22405492 FORWARD LENGTH=2217	-0.27	1.04	0.38
AT1G78500	Terpenoid cyclases family protein | chr1:29531646-29535177 FORWARD LENGTH=2304	-0.27	0.72	0.38
AT3G61160	Protein kinase superfamily protein | chr3:22635881-22638817 FORWARD LENGTH=1848	-0.26	-0.26	0.95
AT3G27430	PBB1 | N-terminal nucleophile aminohydrolases (Ntn hydrolases) superfamily protein | chr3:10152517-10155342 FORWARD LENGTH=1230	-0.24	0.19	1.29
AT2G31370	Basic-leucine zipper (bZIP) transcription factor family protein | chr2:13378944-13381523 FORWARD LENGTH=1694	-0.24	1.02	0.35
AT3G58810	MTPA2, ATMTPA2, MTP3, ATMTP3 | metal tolerance protein A2 | chr3:21749966-21752006 FORWARD LENGTH=2041	-0.23	-0.01	1.44
AT3G24900	AtRLP39, RLP39 | receptor like protein 39 | chr3:9099183-9101837 REVERSE LENGTH=2655	-0.17	0.74	0.51
AT3G25710	BHLH32, ATAIG1, TMO5 | basic helix-loop-helix 32 | chr3:9369519-9371394 FORWARD LENGTH=1412	-0.17	1.03	0.95
AT1G14400	UBC1, ATUBC1 | ubiquitin carrier protein 1 | chr1:4927011-4928690 REVERSE LENGTH=995	-0.14	0.20	1.30
AT4G34660	SH3 domain-containing protein | chr4:16545197-16548453 REVERSE LENGTH=1595	-0.10	0.73	0.35
AT1G70730	PGM2 | Phosphoglucomutase/phosphomannomutase family protein | chr1:26668865-26672779 REVERSE LENGTH=1966	-0.10	0.81	0.24
AT2G28840	XBAT31 | XB3 ortholog 1 in *Arabidopsis thaliana* | chr2:12378337-12380742 FORWARD LENGTH=1844	-0.09	0.63	0.26
AT3G04720	PR4, HEL, PR-4 | pathogenesis-related 4 | chr3:1285524-1286562 REVERSE LENGTH=837	-0.03	0.78	0.34
AT5G55390	EDM2 | ENHANCED DOWNY MILDEW 2 | chr5:22447966-22454802 REVERSE LENGTH=4258	0.04	0.26	0.58
AT3G26900	SKL1, ATSKL1 | shikimate kinase like 1 | chr3:9912209-9914514 REVERSE LENGTH=1038	0.06	0.91	0.78
AT2G29452	unknown protein; Has 30201 Blast hits to 17322 proteins in 780 species: Archae - 12; Bacteria - 1396; Metazoa - 17338; Fungi - 3422; Plants - 5037; Viruses - 0; Other Eukaryotes - 2996 (source: NCBI BLink). | chr2:12625854-12625985 REVERSE LENGTH=132	0.14	-0.22	0.21

Table S3 List of 175 genes of cluster 8.

Identifier	Description	ColLL-tgaLL logFC	ColLL-ROXYLL logFC
AT4G15680	Thioredoxin superfamily protein | chr4:8931652-8932295 FORWARD LENGTH=644	-4.98	-4.89
AT1G14250	GDA1/CD39 nucleoside phosphatase family protein | chr1:4868452-4871488 FORWARD LENGTH=1846	-3.89	-3.65
AT4G15670	Thioredoxin superfamily protein | chr4:8929179-8929765 FORWARD LENGTH=587	-3.88	-3.87
AT4G15700	Thioredoxin superfamily protein | chr4:8937393-8937892 FORWARD LENGTH=500	-3.60	-3.79
AT4G01430	nodulin MtN21 /EamA-like transporter family protein | chr4:585598-588029 FORWARD LENGTH=1390	-3.46	-3.80
AT4G15690	Thioredoxin superfamily protein | chr4:8934324-8934921 FORWARD LENGTH=598	-3.28	-3.24
AT3G14075	Mono-/di-acylglycerol lipase, N-terminal;Lipase, class 3 | chr3:4663602-4666968 REVERSE LENGTH=2305	-3.25	-2.51
AT4G15660	Thioredoxin superfamily protein | chr4:8925806-8926310 FORWARD LENGTH=505	-3.21	-3.16
AT4G23600	CORI3, JR2 | Tyrosine transaminase family protein | chr4:12310619-12313212 FORWARD LENGTH=1660	-2.98	-2.64
AT1G15380	Lactoylglutathione lyase / glyoxalase I family protein | chr1:5290745-5292535 FORWARD LENGTH=983	-2.86	-2.55
AT1G10070	ATBCAT-2, BCAT-2 | branched-chain amino acid transaminase 2 | chr1:3288087-3290471 FORWARD LENGTH=1668	-2.39	-2.14

Identifier	Description	ColLL-tgaLL logFC	ColLL-ROXYLL logFC
AT4G09510	CINV2 | cytosolic invertase 2 | chr4:6021164-6023873 REVERSE LENGTH=2032	-2.33	-2.18
AT1G66100	Plant thionin | chr1:24605671-24606537 REVERSE LENGTH=674	-2.32	-1.75
AT1G71880	SUC1, ATSUC1 | sucrose-proton symporter 1 | chr1:27054180-27056341 FORWARD LENGTH=1937	-2.31	-2.55
AT4G11320	Papain family cysteine protease | chr4:6887254-6889059 FORWARD LENGTH=1430	-2.31	-2.50
AT5G13220	JAZ10, TIFY9, JAS1 | jasmonate-zim-domain protein 10 | chr5:4218888-4220700 FORWARD LENGTH=1375	-2.22	-1.48
AT4G28040	nodulin MtN21 /EamA-like transporter family protein | chr4:13940601-13942436 FORWARD LENGTH=1462	-2.18	-1.69
AT3G62950	Thioredoxin superfamily protein | chr3:23266249-23266934 FORWARD LENGTH=686	-2.14	-2.22
AT2G36080	AP2/B3-like transcriptional factor family protein | chr2:15150551-15151575 REVERSE LENGTH=1025	-2.11	-1.76
AT2G36080	AP2/B3-like transcriptional factor family protein | chr2:15148259-15151575 REVERSE LENGTH=1252	-2.05	-1.54
AT4G26260	MIOX4 | myo-inositol oxygenase 4 | chr4:13297803-13300319 FORWARD LENGTH=1266	-2.04	-1.70
AT3G09260	PYK10, PSR3.1, BGLU23, LEB | Glycosyl hydrolase superfamily protein | chr3:2840477-2843781 REVERSE LENGTH=1806	-1.99	-1.57
AT4G17190	FPS2 | farnesyl diphosphate synthase 2 | chr4:9648527-9650912 REVERSE LENGTH=1292	-1.93	-1.51
AT5G24780	VSP1, ATVSP1 | vegetative storage protein 1 | chr5:8507590-8508957 REVERSE LENGTH=1094	-1.84	-2.04
AT3G18280	Bifunctional inhibitor/lipid-transfer protein/seed storage 2S albumin superfamily protein | chr3:6267049-6267643 FORWARD LENGTH=595	-1.82	-1.76
AT5G44572	unknown protein; FUNCTIONS IN: molecular_function unknown; INVOLVED IN: biological_process unknown; LOCATED IN: endomembrane system; Has 7 Blast hits to 7 proteins in 2 species: Archae - 0; Bacteria - 0; Metazoa - 0; Fungi - 0; Plants - 7; Viruses - 0; Other Eukaryotes - 0 (source: NCBI BLink). | chr5:17968152-17969563 FORWARD LENGTH=537	-1.78	-1.98
AT5G21960	Integrase-type DNA-binding superfamily protein | chr5:7258363-7259308 REVERSE LENGTH=946	-1.76	-1.55
AT3G15950	NAI2 | DNA topoisomerase-related | chr3:5397569-5402652 REVERSE LENGTH=2461	-1.75	-1.46
AT3G30775	ERD5, PRODH, AT-POX, ATPOX, ATPDH, PRO1 | Methylenetetrahydrofolate reductase family protein | chr3:12448636-12451248 REVERSE LENGTH=1866	-1.75	-1.76
AT4G21450	PapD-like superfamily protein | chr4:11426023-11428343 FORWARD LENGTH=1480	-1.74	-1.42
AT2G47750	GH3.9 | putative indole-3-acetic acid-amido synthetase GH3.9 | chr2:19560127-19563191 REVERSE LENGTH=2155	-1.73	-1.72
AT5G18600	Thioredoxin superfamily protein | chr5:6183258-6183954 REVERSE LENGTH=697	-1.72	-1.53
AT5G02260	ATEXPA9, EXP9, ATEXP9, ATHEXP ALPHA 1.10, EXPA9 | expansin A9 | chr5:463158-465246 FORWARD LENGTH=1249	-1.72	-1.24
AT4G15530	PPDK | pyruvate orthophosphate dikinase | chr4:8864828-8870861 REVERSE LENGTH=2908	-1.70	-1.71
AT5G60100	PRR3 | pseudo-response regulator 3 | chr5:24197998-24201364 REVERSE LENGTH=2182	-1.69	-1.08
AT3G47340	ASN1, DIN6, AT-ASN1 | glutamine-dependent asparagine synthase 1 | chr3:17437884-17441242 REVERSE LENGTH=2299	-1.68	-0.78
AT1G33440	Major facilitator superfamily protein | chr1:12127389-12130407 REVERSE LENGTH=2209	-1.65	-1.78
AT3G15950	NAI2 | DNA topoisomerase-related | chr3:5397569-5402652 REVERSE LENGTH=2575	-1.64	-1.74
AT3G44990	XTR8, ATXTR8, XTH31 | xyloglucan endo-transglycosylase-related 8 | chr3:16446975-16448764 REVERSE LENGTH=1273	-1.63	-1.52
AT5G23810	AAP7 | amino acid permease 7 | chr5:8028378-8030163 FORWARD LENGTH=1194	-1.63	-1.32
AT3G62930	Thioredoxin superfamily protein | chr3:23261442-23261927 REVERSE LENGTH=486	-1.61	-1.49
AT4G24050	NAD(P)-binding Rossmann-fold superfamily protein | chr4:12497055-12500128 FORWARD LENGTH=1698	-1.59	-1.56
AT5G11870	Alkaline phytoceramidase (aPHC) | chr5:3825532-3827306 FORWARD LENGTH=1042	-1.59	-1.37
AT1G43910	P-loop containing nucleoside triphosphate hydrolases superfamily protein | chr1:16655884-16657658 REVERSE LENGTH=1624	-1.56	-1.80
AT1G15380	Lactoylglutathione lyase / glyoxalase I family protein | chr1:5290747-5292535 FORWARD LENGTH=864	-1.55	-1.97

Identifier	Description	ColLL-tgaLL logFC	ColLL-ROXYLL logFC
AT2G43820	GT, UGT74F2, ATSAGT1, SGT1, SAGT1 | UDP-glucosyltransferase 74F2 | chr2:18152227-18153908 FORWARD LENGTH=1595	-1.50	-1.44
AT4G32920	glycine-rich protein | chr4:15887270-15896006 REVERSE LENGTH=4889	-1.50	-1.34
AT4G36850	PQ-loop repeat family protein / transmembrane family protein | chr4:17353291-17355891 REVERSE LENGTH=1372	-1.49	-1.55
AT4G17470	alpha/beta-Hydrolases superfamily protein | chr4:9742759-9744860 REVERSE LENGTH=1212	-1.49	-0.86
AT5G19110	Eukaryotic aspartyl protease family protein | chr5:6411561-6413170 REVERSE LENGTH=1377	-1.48	-1.38
AT5G41080	PLC-like phosphodiesterases superfamily protein | chr5:16441808-16443985 FORWARD LENGTH=1408	-1.46	-1.13
AT1G24575	unknown protein; Has 7 Blast hits to 7 proteins in 2 species: Archae - 0; Bacteria - 0; Metazoa - 0; Fungi - 0; Plants - 7; Viruses - 0; Other Eukaryotes - 0 (source: NCBI BLink). | chr1:8711036-8711528 REVERSE LENGTH=493	-1.45	-1.25
AT3G26818	MIR169M | MIR169M; miRNA | chr3:9878168-9878379 REVERSE LENGTH=212	-1.45	-1.26
AT5G50330	Protein kinase superfamily protein | chr5:20485223-20488684 REVERSE LENGTH=1744	-1.44	-1.11
AT5G14420	RGLG2 | RING domain ligase2 | chr5:4648111-4651309 REVERSE LENGTH=1882	-1.44	-1.12
AT3G18560	unknown protein; BEST *Arabidopsis thaliana* protein match is: unknown protein (TAIR:AT1G49000.1); Has 95 Blast hits to 95 proteins in 13 species: Archae - 0; Bacteria - 0; Metazoa - 0; Fungi - 0; Plants - 95; Viruses - 0; Other Eukaryotes - 0 (source: NCBI BLink). | chr3:6393910-6394785 FORWARD LENGTH=876	-1.42	-1.68
AT3G22550	Protein of unknown function (DUF581) | chr3:7991646-7993454 REVERSE LENGTH=1483	-1.40	-1.59
AT4G19810	Glycosyl hydrolase family protein with chitinase insertion domain | chr4:10763934-10765753 REVERSE LENGTH=1357	-1.40	-1.64
AT3G60160	ATMRP9, MRP9, ABCC9 | multidrug resistance-associated protein 9 | chr3:22223803-22229204 REVERSE LENGTH=4556	-1.38	-1.17
AT2G29670	Tetratricopeptide repeat (TPR)-like superfamily protein | chr2:12681958-12685087 REVERSE LENGTH=2149	-1.37	-1.12
AT5G20250	DIN10 | Raffinose synthase family protein | chr5:6833659-6836782 FORWARD LENGTH=2836	-1.36	-1.52
AT2G40200	basic helix-loop-helix (bHLH) DNA-binding superfamily protein | chr2:16791098-16792090 FORWARD LENGTH=828	-1.36	-1.06
AT1G53160	SPL4 | squamosa promoter binding protein-like 4 | chr1:19806419-19807608 FORWARD LENGTH=857	-1.35	-1.62
AT1G70700	JAZ9, TIFY7 | TIFY domain/Divergent CCT motif family protein | chr1:26654768-26657064 FORWARD LENGTH=1247	-1.34	-1.46
AT1G03020	Thioredoxin superfamily protein | chr1:698207-698515 REVERSE LENGTH=309	-1.33	-1.37
AT1G50000	methyltransferases | chr1:18515059-18517249 REVERSE LENGTH=1020	-1.32	-0.83
AT4G36410	UBC17 | ubiquitin-conjugating enzyme 17 | chr4:17201922-17202988 FORWARD LENGTH=631	-1.31	-1.30
AT1G20160	ATSBT5.2 | Subtilisin-like serine endopeptidase family protein | chr1:6990784-6993972 REVERSE LENGTH=2383	-1.30	-1.34
AT1G19180	TIFY10A | jasmonate-zim-domain protein 1 | chr1:6622114-6623620 FORWARD LENGTH=1507	-1.29	-1.13
AT4G30450	glycine-rich protein | chr4:14886027-14886675 REVERSE LENGTH=649	-1.29	-1.24
AT3G22410	Sec14p-like phosphatidylinositol transfer family protein | chr3:7933167-7935808 REVERSE LENGTH=1508	-1.28	-1.07
AT1G11080	scpl31 | serine carboxypeptidase-like 31 | chr1:3694672-3697808 REVERSE LENGTH=1674	-1.27	-0.95
AT4G37520	Peroxidase superfamily protein | chr4:17631657-17633235 FORWARD LENGTH=1203	-1.27	-1.11
AT3G32980	Peroxidase superfamily protein | chr3:13526097-13529997 REVERSE LENGTH=1414	-1.26	-0.78
AT1G48140	dolichol-phosphate mannosyltransferase-related | chr1:17782042-17784211 FORWARD LENGTH=689	-1.26	-0.98
AT1G70700	TIFY7 | TIFY domain/Divergent CCT motif family protein | chr1:26654768-26657064 FORWARD LENGTH=1175	-1.25	-1.43
AT4G33150	lysine-ketoglutarate reductase/saccharopine dehydrogenase bifunctional enzyme | chr4:15985189-15991538 REVERSE LENGTH=3602	-1.24	-0.69
AT5G20250	DIN10 | Raffinose synthase family protein | chr5:6833659-6836782 FORWARD LENGTH=2846	-1.22	-1.14

Identifier	Description	ColLL-tgaLL logFC	ColLL-ROXYLL logFC
AT3G49620	DIN11 | 2-oxoglutarate (2OG) and Fe(II)-dependent oxygenase superfamily protein | chr3:18393747-18396816 FORWARD LENGTH=1304	-1.22	-1.17
AT3G02140	TMAC2, AFP4 | AFP2 (ABI five-binding protein 2) family protein | chr3:385317-386538 REVERSE LENGTH=1222	-1.22	-1.26
AT2G34600	JAZ7, TIFY5B | jasmonate-zim-domain protein 7 | chr2:14573080-14573856 FORWARD LENGTH=677	-1.22	-0.78
AT5G06870	PGIP2, ATPGIP2 | polygalacturonase inhibiting protein 2 | chr5:2133918-2135166 FORWARD LENGTH=1166	-1.21	-1.14
AT4G38240	CGL1, CGL, GNTI | alpha-1,3-mannosyl-glycoprotein beta-1,2-N-acetylglucosaminyltransferase, putative | chr4:17931570-17935325 REVERSE LENGTH=1887	-1.21	-0.97
AT5G02230	Haloacid dehalogenase-like hydrolase (HAD) superfamily protein | chr5:448105-450654 FORWARD LENGTH=1103	-1.20	-0.46
AT3G57520	AtSIP2, SIP2 | seed imbibition 2 | chr3:21288765-21293158 REVERSE LENGTH=2699	-1.20	-1.28
AT2G24960	unknown protein; BEST *Arabidopsis thaliana* protein match is: unknown protein (TAIR:AT4G02210.2); Has 1453 Blast hits to 509 proteins in 26 species: Archae - 0; Bacteria - 0; Metazoa - 1; Fungi - 39; Plants - 1363; Viruses - 0; Other Eukaryotes - 50 (source: NCBI BLink). | chr2:10617263-10620034 FORWARD LENGTH=2394	-1.20	-0.89
AT5G62890	Xanthine/uracil permease family protein | chr5:25243417-25247377 FORWARD LENGTH=2207	-1.18	-0.82
AT5G04770	ATCAT6, CAT6 | cationic amino acid transporter 6 | chr5:1379068-1382419 FORWARD LENGTH=1917	-1.17	-0.84
AT5G54080	HGO | homogentisate 1,2-dioxygenase | chr5:21945869-21948285 FORWARD LENGTH=1652	-1.17	-0.89
AT1G61810	BGLU45 | beta-glucosidase 45 | chr1:22830015-22834728 FORWARD LENGTH=1696	-1.17	-0.84
AT3G26815	MIR169K | MIR169K; miRNA | chr3:9875525-9875737 REVERSE LENGTH=213	-1.16	-0.95
AT5G59080	unknown protein; FUNCTIONS IN: molecular_function unknown; INVOLVED IN: response to oxidative stress; LOCATED IN: chloroplast; EXPRESSED IN: 18 plant structures; EXPRESSED DURING: 9 growth stages; BEST *Arabidopsis thaliana* protein match is: unknown protein (TAIR:AT3G46880.1); Has 1807 Blast hits to 1807 proteins in 277 species: Archae - 0; Bacteria - 0; Metazoa - 736; Fungi - 347; Plants - 385; Viruses - 0; Other Eukaryotes - 339 (source: NCBI BLink). | chr5:23847405-23848557 REVERSE LENGTH=848	-1.16	-0.88
AT4G24230	ACBP3 | acyl-CoA-binding domain 3 | chr4:12566861-12568770 REVERSE LENGTH=1372	-1.16	-0.83
AT3G57520	AtSIP2, SIP2 | seed imbibition 2 | chr3:21288765-21293158 REVERSE LENGTH=2727	-1.15	-1.19
AT4G35770	SEN1, ATSEN1, DIN1 | Rhodanese/Cell cycle control phosphatase superfamily protein | chr4:16944941-16946192 FORWARD LENGTH=894	-1.14	-1.05
AT2G15880	Leucine-rich repeat (LRR) family protein | chr2:6918039-6920319 REVERSE LENGTH=2184	-1.14	-1.08
AT1G80050	APT2, ATAPT2, PHT1.1 | adenine phosphoribosyl transferase 2 | chr1:30111514-30113324 REVERSE LENGTH=836	-1.14	-1.26
AT5G05600	2-oxoglutarate (2OG) and Fe(II)-dependent oxygenase superfamily protein | chr5:1672120-1674739 FORWARD LENGTH=1399	-1.13	-1.10
AT2G47180	AtGolS1, GolS1 | galactinol synthase 1 | chr2:19368798-19370441 REVERSE LENGTH=1355	-1.13	-0.96
AT3G28220	TRAF-like family protein | chr3:10524404-10526728 FORWARD LENGTH=1360	-1.13	-0.87
AT1G02610	RING/FYVE/PHD zinc finger superfamily protein | chr1:553050-555994 REVERSE LENGTH=937	-1.12	-1.15
AT3G18780	ACT2, DER1, LSR2, ENL2 | actin 2 | chr3:6474871-6477204 FORWARD LENGTH=1813	-1.11	-0.72
AT4G37530	Peroxidase superfamily protein | chr4:17634784-17636288 FORWARD LENGTH=1131	-1.11	-0.98
AT3G47340	ASN1, DIN6, AT-ASN1 | glutamine-dependent asparagine synthase 1 | chr3:17437884-17441242 REVERSE LENGTH=2380	-1.11	-0.98
AT3G25780	AOC3 | allene oxide cyclase 3 | chr3:9409290-9410567 FORWARD LENGTH=1007	-1.10	-0.92
AT3G15270	SPL5 | squamosa promoter binding protein-like 5 | chr3:5140365-5141348 REVERSE LENGTH=897	-1.10	-0.75
AT1G49320	ATUSPL1, USPL1 | unknown seed protein like 1 | chr1:18246305-18247992 FORWARD LENGTH=1154	-1.10	-0.97
AT1G31770	ABCG14 | ATP-binding cassette 14 | chr1:11374893-11377794 REVERSE LENGTH=2456	-1.09	-1.12

Identifier	Description	ColLL-tgaLL logFC	ColLL-ROXYLL logFC
AT4G19820	Glycosyl hydrolase family protein with chitinase insertion domain | chr4:10767436-10768614 REVERSE LENGTH=1101	-1.09	-0.92
AT3G16470	JR1 | Mannose-binding lectin superfamily protein | chr3:5595929-5598027 REVERSE LENGTH=1593	-1.08	-0.99
AT5G05860	UGT76C2 | UDP-glucosyl transferase 76C2 | chr5:1765507-1767455 FORWARD LENGTH=1498	-1.08	-0.98
AT5G22000	RHF2A | RING-H2 group F2A | chr5:7277322-7280255 FORWARD LENGTH=1729	-1.08	-0.66
AT1G17380	JAZ5, TIFY11A | jasmonate-zim-domain protein 5 | chr1:5955488-5957212 REVERSE LENGTH=1133	-1.07	-0.86
AT5G23350	GRAM domain-containing protein / ABA-responsive protein-related | chr5:7858253-7859387 REVERSE LENGTH=1135	-1.07	-0.94
AT1G30110	NUDX25 | nudix hydrolase homolog 25 | chr1:10581735-10583949 FORWARD LENGTH=847	-1.07	-1.09
AT5G23820	MD-2-related lipid recognition domain-containing protein | chr5:8031268-8033020 FORWARD LENGTH=824	-1.05	-1.16
AT2G28120	Major facilitator superfamily protein | chr2:11985687-11987738 FORWARD LENGTH=2052	-1.04	-0.99
AT1G51620	Protein kinase superfamily protein | chr1:19140130-19141787 FORWARD LENGTH=1344	-1.03	-1.15
AT4G20860	FAD-binding Berberine family protein | chr4:11172622-11174467 FORWARD LENGTH=1846	-1.03	-0.61
AT2G29995	unknown protein; FUNCTIONS IN: molecular_function unknown; INVOLVED IN: biological_process unknown; LOCATED IN: endomembrane system; EXPRESSED IN: 15 plant structures; EXPRESSED DURING: 6 growth stages; BEST *Arabidopsis thaliana* protein match is: unknown protein (TAIR:AT1G07175.1); Has 14 Blast hits to 14 proteins in 3 species: Archae - 0; Bacteria - 0; Metazoa - 0; Fungi - 0; Plants - 14; Viruses - 0; Other Eukaryotes - 0 (source: NCBI BLink). | chr2:12796907-12799419 REVERSE LENGTH=522	-1.03	-0.63
AT3G27110	Peptidase family M48 family protein | chr3:9997895-10000230 FORWARD LENGTH=1395	-1.01	-0.59
AT2G34930	disease resistance family protein / LRR family protein | chr2:14737066-14739904 REVERSE LENGTH=2839	-1.01	-0.66
AT5G49830	EXO84B | exocyst complex component 84B | chr5:20250486-20255039 REVERSE LENGTH=3035	-1.01	-1.05
AT5G25770	alpha/beta-Hydrolases superfamily protein | chr5:8969215-8972125 REVERSE LENGTH=1597	-1.00	-0.82
AT2G22860	ATPSK2, PSK2 | phytosulfokine 2 precursor | chr2:9737607-9738298 FORWARD LENGTH=544	-1.00	-0.81
AT2G29450	ATGSTU5, ATGSTU1, AT103-1A, GSTU5 | glutathione S-transferase tau 5 | chr2:12624586-12625637 REVERSE LENGTH=934	-0.99	-0.99
AT1G35910	TPPD | Haloacid dehalogenase-like hydrolase (HAD) superfamily protein | chr1:13363003-13365060 REVERSE LENGTH=1402	-0.98	-0.78
AT1G53160	SPL4 | squamosa promoter binding protein-like 4 | chr1:19806421-19807301 FORWARD LENGTH=803	-0.98	-0.51
AT1G21050	Protein of unknown function, DUF617 | chr1:7366775-7367678 FORWARD LENGTH=904	-0.98	-0.84
AT5G20250	DIN10 | Raffinose synthase family protein | chr5:6833659-6836782 FORWARD LENGTH=2753	-0.98	-0.60
AT1G33055	unknown protein; FUNCTIONS IN: molecular_function unknown; INVOLVED IN: anaerobic respiration; LOCATED IN: endomembrane system; EXPRESSED IN: 13 plant structures; EXPRESSED DURING: 6 growth stages; Has 20 Blast hits to 20 proteins in 8 species: Archae - 0; Bacteria - 0; Metazoa - 0; Fungi - 0; Plants - 20; Viruses - 0; Other Eukaryotes - 0 (source: NCBI BLink). | chr1:11971308-11972578 REVERSE LENGTH=1271	-0.97	-0.64
AT1G07175	unknown protein; FUNCTIONS IN: molecular_function unknown; INVOLVED IN: biological_process unknown; LOCATED IN: endomembrane system; BEST *Arabidopsis thaliana* protein match is: unknown protein (TAIR:AT2G29995.1); Has 30201 Blast hits to 17322 proteins in 780 species: Archae - 12; Bacteria - 1396; Metazoa - 17338; Fungi - 3422; Plants - 5037; Viruses - 0; Other Eukaryotes - 2996 (source: NCBI BLink). | chr1:2202330-2202774 FORWARD LENGTH=268	-0.97	-1.09
AT4G02550	unknown protein; BEST *Arabidopsis thaliana* protein match is: unknown protein (TAIR:AT4G02210.2); Has 35333 Blast hits to 34131 proteins in 2444 species: Archae - 798; Bacteria - 22429; Metazoa - 974; Fungi - 991; Plants - 531; Viruses - 0; Other Eukaryotes - 9610 (source: NCBI BLink). | chr4:1120421-1121725 REVERSE LENGTH=1221	-0.97	-0.66
AT3G14850	TBL41 | TRICHOME BIREFRINGENCE-LIKE 41 | chr3:4996448-4997693 FORWARD LENGTH=988	-0.96	-0.80

Identifier	Description	ColLL-tgaLL logFC	ColLL-ROXYLL logFC
AT4G24120	YSL1, ATYSL1 | YELLOW STRIPE like 1 | chr4:12524491-12527341 FORWARD LENGTH=2430	-0.95	-0.61
AT1G61610	S-locus lectin protein kinase family protein | chr1:22733472-22736509 FORWARD LENGTH=2529	-0.95	-0.95
AT2G21500	RING/U-box superfamily protein | chr2:9207549-9210231 REVERSE LENGTH=1817	-0.95	-0.92
AT1G45145	ATTRX5, ATH5, LIV1, TRX5 | thioredoxin H-type 5 | chr1:17074942-17076330 REVERSE LENGTH=753	-0.94	-0.89
AT5G05440	PYL5, RCAR8 | Polyketide cyclase/dehydrase and lipid transport superfamily protein | chr5:1609250-1610446 FORWARD LENGTH=1197	-0.93	-0.71
AT4G18440	L-Aspartase-like family protein | chr4:10186131-10188909 REVERSE LENGTH=1942	-0.93	-0.95
AT5G60410	ATSIZ1, SIZ1 | DNA-binding protein with MIZ/SP-RING zinc finger, PHD-finger and SAP domain | chr5:24294890-24301091 FORWARD LENGTH=3154	-0.93	-0.74
AT2G06050	OPR3 | oxophytodienoate-reductase 3 | chr2:2359240-2362118 REVERSE LENGTH=1233	-0.93	-0.96
AT1G03090	MCCA | methylcrotonyl-CoA carboxylase alpha chain, mitochondrial / 3-methylcrotonyl-CoA carboxylase 1 (MCCA) | chr1:739679-744184 FORWARD LENGTH=2606	-0.93	-0.70
AT5G65140	TPPJ | Haloacid dehalogenase-like hydrolase (HAD) superfamily protein | chr5:26020410-26022222 REVERSE LENGTH=1124	-0.92	-0.81
AT5G56870	BGAL4 | beta-galactosidase 4 | chr5:23004196-23008649 FORWARD LENGTH=2502	-0.92	-0.65
AT3G10915	Reticulon family protein | chr3:3415975-3417788 REVERSE LENGTH=1201	-0.92	-0.70
AT5G55100	SWAP (Suppressor-of-White-APricot)/surp domain-containing protein | chr5:22361102-22364759 REVERSE LENGTH=2806	-0.92	-0.60
AT1G63530	BEST *Arabidopsis thaliana* protein match is: hydroxyproline-rich glycoprotein family protein (TAIR:AT1G63540.1); Has 10212 Blast hits to 4024 proteins in 434 species: Archae - 1; Bacteria - 1259; Metazoa - 3608; Fungi - 2247; Plants - 291; Viruses - 90; Other Eukaryotes - 2716 (source: NCBI BLink). | chr1:23563315-23565555 FORWARD LENGTH=1925	-0.92	-0.79
AT3G21510	AHP1 | histidine-containing phosphotransmitter 1 | chr3:7578175-7579599 REVERSE LENGTH=784	-0.91	-0.84
AT3G17712	unknown protein; FUNCTIONS IN: molecular_function unknown; INVOLVED IN: biological_process unknown; LOCATED IN: cellular_component unknown; CONTAINS InterPro DOMAIN/s: Protein of unknown function DUF1740 (InterPro:IPR013633); BEST *Arabidopsis thaliana* protein match is: unknown protein (TAIR:AT3G17740.1). | chr3:6056870-6060287 FORWARD LENGTH=2653	-0.91	-0.61
AT1G11925	Stigma-specific Stig1 family protein | chr1:4025930-4026732 REVERSE LENGTH=803	-0.91	-1.09
AT2G19800	MIOX2 | myo-inositol oxygenase 2 | chr2:8530896-8533508 REVERSE LENGTH=1318	-0.90	-0.90
AT5G17650	glycine/proline-rich protein | chr5:5816698-5818347 REVERSE LENGTH=993	-0.90	-0.71
AT3G48390	MA3 domain-containing protein | chr3:17920815-17923496 FORWARD LENGTH=2344	-0.90	-0.92
AT1G19230	Riboflavin synthase-like superfamily protein | chr1:6644189-6649375 FORWARD LENGTH=3007	-0.90	-0.54
AT3G47490	HNH endonuclease | chr3:17498337-17499301 FORWARD LENGTH=965	-0.89	-1.05
AT3G22640	PAP85 | cupin family protein | chr3:8011724-8013902 REVERSE LENGTH=1658	-0.89	-0.77
AT5G49520	WRKY48, ATWRKY48 | WRKY DNA-binding protein 48 | chr5:20090776-20093346 FORWARD LENGTH=1793	-0.89	-0.48
AT1G21140	Vacuolar iron transporter (VIT) family protein | chr1:7404383-7405281 FORWARD LENGTH=899	-0.89	-0.82
AT2G07680	ATMRP11, MRP11, ABCC13 | multidrug resistance-associated protein 11 | chr2:3514745-3522491 FORWARD LENGTH=4244	-0.89	-0.85
AT4G08300	nodulin MtN21 /EamA-like transporter family protein | chr4:5244891-5248342 FORWARD LENGTH=1444	-0.89	-0.97
AT4G27450	Aluminium induced protein with YGL and LRDR motifs | chr4:13727484-13728886 REVERSE LENGTH=1137	-0.89	-1.00
AT1G65120	Ubiquitin carboxyl-terminal hydrolase-related protein | chr1:24191348-24196073 REVERSE LENGTH=3719	-0.89	-0.57
AT1G64500	Glutaredoxin family protein | chr1:23953233-23954492 FORWARD LENGTH=1260	-0.88	-0.53

Identifier	Description	ColLL-tgaLL logFC	ColLL-ROXYLL logFC
AT1G61120	TPS04, GES, TPS4 | terpene synthase 04 | chr1:22523637-22528811 FORWARD LENGTH=2899	-0.88	-0.67
AT5G56100	glycine-rich protein / oleosin | chr5:22717115-22717751 FORWARD LENGTH=637	-0.88	-1.00
AT4G33770	Inositol 1,3,4-trisphosphate 5/6-kinase family protein | chr4:16193422-16195357 REVERSE LENGTH=1183	-0.87	-0.70
AT3G26816	MIR169L | MIR169L; miRNA | chr3:9875893-9876103 REVERSE LENGTH=211	-0.84	-1.05
AT5G13220	JAZ10, TIFY9, JAS1 | jasmonate-zim-domain protein 10 | chr5:4218888-4220767 FORWARD LENGTH=1025	-0.84	-0.69
AT2G41640	Glycosyltransferase family 61 protein | chr2:17360486-17363788 FORWARD LENGTH=2496	-0.84	-0.60
AT5G18170	GDH1 | glutamate dehydrogenase 1 | chr5:6006039-6008472 FORWARD LENGTH=1593	-0.83	-0.86
AT5G16370	AAE5 | acyl activating enzyme 5 | chr5:5356605-5358511 REVERSE LENGTH=1907	-0.82	-0.88
AT4G39780	Integrase-type DNA-binding superfamily protein | chr4:18457957-18459180 REVERSE LENGTH=1224	-0.81	-0.89
AT1G66783	MIR157A | MIR157A; miRNA | chr1:24913206-24913296 REVERSE LENGTH=91	-0.81	-1.11
AT4G33770	Inositol 1,3,4-trisphosphate 5/6-kinase family protein | chr4:16193422-16196428 REVERSE LENGTH=1529	-0.79	-0.84
AT4G38470	ACT-like protein tyrosine kinase family protein | chr4:17999432-18003681 FORWARD LENGTH=1858	-0.79	-0.65
AT1G12780	UGE1, ATUGE1 | UDP-D-glucose/UDP-D-galactose 4-epimerase 1 | chr1:4355926-4358328 REVERSE LENGTH=1462	-0.77	-0.76
AT3G06125	other RNA | chr3:1848883-1850596 FORWARD LENGTH=513	-0.76	-0.89
AT3G06125	other RNA | chr3:1848848-1849332 FORWARD LENGTH=485	-0.76	-0.76
AT5G26200	Mitochondrial substrate carrier family protein | chr5:9157142-9158404 FORWARD LENGTH=1263	-0.76	-0.72
AT2G39570	ACT domain-containing protein | chr2:16507896-16510198 FORWARD LENGTH=1760	-0.75	-0.59
AT3G01850	Aldolase-type TIM barrel family protein | chr3:299987-302038 REVERSE LENGTH=1056	-0.74	-0.63
AT1G49130	B-box type zinc finger protein with CCT domain | chr1:18174741-18176022 REVERSE LENGTH=1171	-0.74	-0.70
AT1G62480	Vacuolar calcium-binding protein-related | chr1:23128705-23129759 FORWARD LENGTH=764	-0.73	-0.50
AT5G57655	xylose isomerase family protein | chr5:23346760-23350039 FORWARD LENGTH=1938	-0.73	-0.63
AT5G10030	TGA4, OBF4 | TGACG motif-binding factor 4 | chr5:3137323-3140252 REVERSE LENGTH=1675	-0.73	-0.65
AT5G30490	CONTAINS InterPro DOMAIN/s: Craniofacial development protein 1/Bucentaur (InterPro:IPR011421); Has 333 Blast hits to 324 proteins in 149 species: Archae - 0; Bacteria - 18; Metazoa - 117; Fungi - 96; Plants - 49; Viruses - 0; Other Eukaryotes - 53 (source: NCBI BLink). | chr5:11611983-11614530 FORWARD LENGTH=1050	-0.72	-0.55

Acknowledgements

All the work was done in the Department of Plant Molecular Biology and Physiology, Georg-August-University. This is the last part of my thesis and I would like to say thanks to all the people who helped me during my study.

First and foremost, I would like to offer my sincere gratitude to my doctoral advisor Prof. Dr. Christiane Gatz for giving me the opportunity to work in her laboratory under her guidance. Her immense knowledge and criticism served as a resource to frequently promote this project. I would also like to thank for giving advice in countless revisions of this thesis.

I wish to express my sincere thanks to my thesis committee members: Prof. Ivo Feussner, Prof. Volker Lipka, PD Dr. Thomas Teichman, Dr. Marcel Wiermer and Dr. Martin Fulda for their constructive suggestion concerning my research. I would also like to acknowledge Dr. Corinna Thurow for helping to analyze the microarray data and offering valuable suggestions throughout the course of my research.

Especially, I would like to thank Dr. Martin Muthreich for initiating the research on clade I TGA factors and ROXY9 and Florian Jung for generating *roxy9* CRISPR-Cas9 lines.

I am deeply grateful to Ronald Scholz, Anna Hermann, Katharina Dworak, and Larissa Kunz for their excellent technical support. I am also thankful to Dr. Guido Kriete for managing laboratory-related issues. I also greatly appreciate the help from all my past and current lab colleagues. Sina Barghahn, Jelena Budimir, Ronja Hacke, Dr. Nathannon Leelarasamee, Dr. Li-Jun Huang, Dr. Alexander Meier, Aswin Nair, Jan Oberdiek, Dr. Frederik Polzin, Dr. Neena Ratnakaran, Dr. Johanna Schmitz, Julia Schröder, Dr. Armin Töller, Katrin Treffon, PD Dr. Joachim Uhrig. I have really enjoyed working with them.

Last but not least, I would like to thank all of my friends in Goettingen. We have spent a wonderful time together.

Curriculum Vitae

1. Personal data:

Name: Ning Li

Date of Birth: 10.10.1985

Place of Birth: Zibo city, Shandong province, China

E-mail: nli@gwdg.de

2. Education:

Ph.D. (Plant Molecular Biology), University of Goettingen, Germany 2012.10-present

M.Sc. (Environmental Biotechnology), Gyeongsang National University, Korea 2009.09-2012.08

B.Sc. (Biological Science), Northeast Forestry University, Harbin, China 2005.09-2009.07

3. Research Projects

- Plant-specific glutaredoxin ROXY9 regulates hyponastic growth by inhibiting TGA1 function. (2012- present)
- Characterization of GIGANTEA-mediated ABA signaling in *Arabidopsis thaliana.* (2011-2012)
- Arabidopsis Yucca6 plays as a thioredoxin reductase and reactive oxygen species scavenger. (2009-2011)

4. Publications

Huang LJ, **Li N**, Thurow C, Wirtz M, Hell R, and Gatz C (2016). Ectopically expressed glutaredoxin ROXY19 negatively regulates the detoxification pathway in *Arabidopsis thaliana*. ***BMC Plant Biology*** 16: 200.

Cha JY, Kim WY, Kang SB, Kim JI, Baek D, Jung IJ, Kim MR, **Li N**, Kim HJ, Nakajima M, Asami T, Sabir JS, Park HC, Lee SY, Bohnert HJ, Bressan RA, Pardo JM, Yun DJ (2015). A novel thiol-reductase activity of Arabidopsis YUC6 confers drought tolerance independently of auxin biosynthesis. ***Nature Communications*** 6: 8041-8054.

Kim WY, Ali Z, Park HJ, Park SJ, Cha JY, Perez-Hormaeche J, Quintero FJ, Shin G, Kim MR, Zhang Q, **Li N**, Park HC, Lee SY, Bressan RA, Pardo JM, Bohnert HJ, Yun DJ (2013). Release of SOS2 kinase from sequestration with GIGANTEA determines salt tolerance in *Arabidopsis*. ***Nature Communications*** 4: 1352–1364.